IMPACT OF STORAGE CONDITIONS ON THERMAL ANALYSIS AND BIODIESEL PROPERTIES DERIVED FROM USED COOKING OIL

A THESIS SUBMITTED TO THE GRADUATE
SCHOOL OF APPLIED SCIENCES
OF
NEAR EAST UNIVERSITY

By
TAMUSATHI NIGEL BABVU

In Partial Fulfillment of the Requirements for
The Degree of Master of Science
in
Mechanical Engineering

NICOSIA, 2018

TAMUSATHI NIGEL
BABVU

IMPACT OF STORAGE CONDITIONS ON THERMAL
ANALYSIS AND BIODIESEL PROPERTIES DERIVED
FROM USED COOKING OIL

NEU
2018

IMPACT OF STORAGE CONDITIONS ON THERMAL ANALYSIS AND BIODIESEL PROPERTIES DERIVED FROM USED COOKING OIL

A THESIS SUBMITTED TO THE GRADUATE
SCHOOL OF APPLIED SCIENCES
OF
NEAR EAST UNIVERSITY

By
TAMUSATHI NIGEL BABVU

In Partial Fulfillment of the Requirements for
The Degree of Master of Science
in
Mechanical Engineering

NICOSIA, 2018

Tamusathi Nigel BABVU: IMPACT OF STORAGE CONDITIONS ON THERMAL ANALYSIS AND BIODIESEL PROPERTIES DERIVED FROM USED COOKING OIL

Approval of Director of Graduate School of
Applied Sciences

Prof. Dr. Nadire ÇAVUŞ

We certify this thesis is satisfactory for the award of the degree of Master of Science in Mechanical Engineering

Examining Committee in Charge:

Prof. Dr. Cavit ATALAR	Committee Chairman, Department of Petroleum and Natural Gas Engineering, NEU
Assist. Prof. Dr. Ali EVCİL	Department of Mechanical Engineering, NEU
Assist. Prof. Dr. Hüseyin ÇAMUR	Supervisor, Department of Mechanical Engineering, NEU

I hereby declare that, all the information in this document has been obtained and presented in accordance with academic rules and ethical conduct. I also declare that, as required by these rules and conduct, I have fully cited and referenced all materials and results that are not original to this work.

Name, Last Name:
Signature:
Date:

ACKNOWLEDGEMENTS

This thesis wouldn’t have been possible without the patience of my principal supervisor, Assist. Prof. Dr. Hüseyin ÇAMUR. I am very thankful and indebted to Dr. Youssef KASSEM, for constant guidance and encouragement. A big shout out to Abdelrahman ALGHAZALI and Berk AKTUĞ for constant assistance throughout the whole thesis. The continued support from Nornubari Barituka BORNU is highly appreciated. Also to mention Dr. Ali ŞEFIK for his willingness to provide assistance in whichever way possible.

My unlimited thanks and heartfelt love is dedicated to the one that provides for me, protects me and gives me all the unconditional love that is more than earthly.

To my Mother, Family
and all my loved ones…

ABSTRACT

Biodiesel is a renewable source of energy that comes from organic feedstocks. These feedstocks can either be waste cooking oil or seed oils. They are converted to methyl esters through a transesterification process. Biodiesel can be blended with kerosene to improve the quality of the fuel. This study focuses on used cooking oil methyl ester (UCOME) biodiesel blended with kerosene. The blend ratios are from 100% Biodiesel (B100) to 80% biodiesel 20% kerosene (B80K20) by volume in steps of 5%. Therefore, 5 samples were prepared. The purpose of the research is to establish the effects of storage period, method and conditions on the samples. Kinematic viscosity was measured at 40 ^{O}C and density at 15 ^{O}C over a period of 90 days, and it was established that these properties increase with time progression. The samples were stored at ambient conditions and in an oven set to 40 ^{O}C. The samples in the oven had a steady growth of the properties as compared to identical samples that were stored in ambient conditions. The cold flow properties were established via a thermal analysis. These were affected by the amount of kerosene in the respective samples. The fraction of solid composition for the B90K10 and B80K20 samples, at a time, during solidification was determined through the thermal analysis designed with Newtonian principles. This was aided by a Computer Assisted Cooling Curve Analysis (CA-CCA).

Keywords: Ambient Conditions; Biodiesel; Density; Thermal Analysis; Used Cooking Oil

ÖZET

Biyodizel, organik hammaddeden gelen yenilenebilir bir enerji kaynağıdır. Bu hammaddeler atık yemek pişirme yağı veya tohum yağları olabilir. Hammadeler transesterifikasyon işlemiyle metil esterlere dönüştürülürler. Yakıtın kalitesini artırmak için biyodizel gazyağı ile karıştırılabilir. Bu çalışma, kerosenle karıştırılmış atık pişirme yağı metil ester biyodizeline odaklanmaktadır. Karışım oranları % 5 Biyodizel (B100) ile % 80 biyodizel ve % 20 kerosen (B80 K20)% 5'lik adımlarla elde edilmiştir. Bu nedenle beş numune hazırlanmıştır. Araştırmanın amacı, depolama süresinin, yöntem ve koşulların numuneler üzerindeki etkilerini tespit etmektir. Kinematik vikozite ve yoğunluk sırasıyla at 40 ^{O}C ve 15 ^{O}C’lik sıcaklıklarda doksani günlük bir zaman diliminde ölçülmüştür. Bu özelliklerin zaman ilerledikçe ile arttığı tespit edilmiştir. Numuneler uygun ortam koşullarında ve 40°C'ye ayarlanmış bir fırında depolanmıştır. Fırındaki numuneler, ortam koşullarında depolanan özdeş numunelere kıyasla, özelliklerin sabit bir şekilde büyümesini sağlamıştır. Soğuk akış özellikleri termal analiz yöntemi ile oluşturulmuştur. Soğuk akış özellikleri biyodizel içerisindeki gazyağı miktarından etkilenmiştir. Katı bileşim yüzdesi, katılaşma sırasında, termal analiz olarak adlandırılan bir analiz ile belirlenmiştir. Bu işlem bilgisayar destekli soğutma eğrisi analizi ile desteklenmiştir.

Anahtar kelimeler: Çevre koşulları; Isı analizi; Yoğunluk; Kullanılmış Pişirme Yağı; Biyodizel

TABLE OF CONTENTS

LIST OF TABLES

LIST OF FIGURES

LIST OF ABBREVIATIONS

ASTM:	American Society for Testing Materials
BxKy:	x Percent Biodiesel, y Percent Kerosene
B100:	100 Percent Biodiesel
CA-CCA	Computer Aided Cooling Curve Analysis
CCA	Cooling Curve Analysis
CFPP	Cold Filter Plugging Point
CP	Cloud Point
EXP:	Experiment
FAME:	Fatty Acid Methyl Ester
HHV	Higher Heating Value
KV	Kinematic Viscosity
LHV	Lower Heating Value
NTA	Newtonian Thermal Analysis
PP	Pour Point
UCOME	Used Cooking Oil Methyl Ester
Z_n	Newtonian Zero Curve

LIST OF SYMBOLS

A	Area (m^2)
cc	Cooling Curve First Derivative
C_p	Specific Heat (J/g°C)
g	Gravity (ms^{-2})
K	Kinematic Viscosity constant (mm^2/s^2)
L	Latent heat (J/kg)
m_e	Mass of the empty pycnometer (g)
m_f	Completely filled pycnometer mass (g)
m	Mass (g)
T_o	Cooling Bath Temperature (°C)
T	Thermocouple Temperature (°C)
T_i	Temperature at point i
t	Time (sec)
t_e	End of Solidification (sec)
t_s	Start of Solidification (sec)
u	Velocity (m/s)
V	Volume (m^3)
V_{bd}	Volume of biodiesel (m^3)
V_k	Volume of kerosene (m^3)
v_θ	Velocity in Angular Direction (rad/s)
v_r	Velocity in Radian Direction (rad/s)
v_z	Velocity in Flow Direction (m/s)
y	Kinetic energy correction
z	Length in Flow Time (m)

Greek Symbols

μ	Dynamic viscosity (N.s/m^2)
ν	Kinematic viscosity (mm^2/s)
ρ	Density (kg/m^3)
τ	Shear Stress (N/m^2)
γ	Strain
$\dot{\gamma}$	Strain rate (s^{-1})
θ	Angle (^{O})

CHAPTER 1
INTRODUCTION

This chapter looks into the general aspects of energy, in particular the renewable energy in the form of biodiesel. The definition of the topic is explained and the aims and objectives are outlined. The general forms of energy are mentioned and the distribution in terms of usage is also stated. This was done to identify the sector in which biodiesel may be used or in which sector it will substitute the non-renewable energy. In general, the chapter introduces the topic of biodiesel and its intended role in the energy sector.

1.1 Energy

Energy is divided into two main groups, which are non- renewable and renewable energy. Non-renewable is the energy group existing in finite quantities and it cannot ever be replenished (Oxford, 2018). They are typically found in the earth's crust and need to be mined. Millions of years pass for them to be formed from dead matter such as trees and dead animals. The types of energy sources which fall under this definition are; Coal, Oil, Natural Gas, Peat, Uranium, Plutonium. The last three examples belong to a special type of non-renewable energy called nuclear energy. Nuclear Energy is a non-renewable source of energy which comes from unstable atoms of an element.

Renewable sources of energy include, but are not limited to; Biofuels, Biomass, Hydro, Wind, Solar and Geothermal energies.

These, however, are energy sources which are replenished with time naturally. They conform to the principal of sustainability.

The engineers are currently researching ways of reducing the use of fossil fuels and other non-renewable sources of energy. Many methods have been applied such as, hybrid vehicles which use petrochemical fuel and electric energy, electric cars from Tesla Inc. which they are rechargeable, solar powered cars and ethanol blended vehicles. Solar and wind energy have been on the rise as a possible long term solutions. The reason for the replacement is not only depletion, but a drive towards a more environmentally friendly means of energy. Energy which conforms to the idea of sustainability. A major alternative is biodiesel and its blends.

1.2 Biodiesel in General.

Biodiesel is mono-alkyl ester (National Biodiesel Board, 2018) renewable fuel which is produced via the transesterification of oils and fat from vegetables and animals respectively. These oils and fat maybe used/waste frying oils from the restaurants and homes. The process of transesterification includes, reacting the raw materials, vegetable oil, seed oil or animal fat, with methanol, being influenced by a catalyst to have the biodiesel, Fatty Acid Methyl Esters (FAME) (Evcil et al., 2018). Different catalysts may be used with the different raw materials or feedstocks to be used. Typically, base/alkaline catalysts are used, mainly sodium and potassium hydroxides, because they produce the end product quicker. In single stage biodiesel production via either, a bath of water or microwave heating, a sodium hydroxide catalyst is used (Loong & Idris, 2017).

Other catalysts include acid catalysts. These are used in the pre esterification step and are 4000 times slower than the base catalysts. However, a more affordable environmentally friendly catalyst is the cement waste catalyst. The cement, concrete and mortar from demolished construction sites is used. The used concrete or mortar is said to be calcined and it is comparable to the calcium oxide, (CaO) of commercial cement (Kumar et al., 2018).

Biodiesel is rapidly being used in engines, cars and trucks all over the world. It is by far a sustainable energy source, controlled by legislature such as ASTMD6751. For quality parameters, it can be used in different forms (Pratas, et al., 2010). Biodiesel used in its purest form is denoted as B100. The letter “B” representing the biodiesel proportion. The numerical represents the percentage of the biodiesel in the fuel. Common biodiesel blends involve mixtures with petrochemical fuels. Blends of up to B20 are being used in engines with no special modifications at all. Blending of biodiesel can be done at different stages. These can be; blending in tanks at production point before transporting to fuel carrier trucks. Splash blending in the fuel carrier trucks i.e. pouring a specified percent of biodiesel and petroleum diesel. Pipe-line fuel blending. The two fuels reach the fuel carrier trucks at all at once. Metered pump blending. Petrochemical diesel and biofuel meters are programmed to Y overall volume, a pump pulls from both points and blend is made on leaving pump.

When dealing with biodiesel, there are certain characteristics that should be put into consideration. These include, the kinematic viscosity, density, acid number, cetane number and oxidation stability. These are affected during storage and the storage conditions contribute to the changes.

The uses of biodiesel vary across the energy field. From the name, the major use is in diesel engines. However, due to its clean way of burning, uses have expanded to, heating and cooking.

1.3 Research Statement

A biodiesel sample was prepared from a feedstock of Used Cooking Oil to form a sample named Used Cooking Oil Methyl Ester (UCOME). It was blended with kerosene from 0-20 percent, in 5% intervals, to make 5 samples. Equal amounts of each sample were poured into identical glass bottles. One set of the biodiesel blended samples were stored in ambient temperatures in the dark and the other set in an oven at 40 ^{O}C.

1.4 Aims

This study focuses on the blends of UCOME and kerosene from B100 to B80K20. “B” denotes the biodiesel percentage in the sample and “K” denotes the kerosene percentage of the fuel. The feedstock is a mixture of different cooking oils collected after use in homes.

The aims of this study are; To measure the kinematic viscosity of each sample at 40 ^{O}C over 90 days every 10 days; To measure the density of each sample at 15 ^{O}C over 90 days every 10 days; To study the thermos-physical properties of B90K10 and B80K20; To measure the kinematic viscosity and density before and after cooling of the samples which will be studied for cooling rate; To analyse the storage effect of the biodiesel on the cold flow properties, acid number and Oxidation Stability.

1.5 Objectives

These are the steps which will lead to the successful achievement of the above aims. To set up a kinematic viscosity test according to ASTM D44-06 and measure every ten days. To set up a density test according to ASTM 941-88 and measure every ten days. To set up an alcohol bath to -20^{O}C for cooling the sample from a temperature of 65 ^{O}C. To perform a cooling curve analysis (CCA), so as to derive the cooling rate. To determine, through ASTM standards, the Cold Flow Properties, Point of pouring and Cloud Point, of the biodiesels. To determine the solid fraction by performing the Newtonian thermal analysis procedure.

1.6 Research Layout

Chapter 2 will focus on the literature of the biodiesel covered before. It will also look into the new theories that are intended by the researcher to use in analysing the data.

Chapter 3 will focus on the methodologies and experimental set ups.

Chapter 4 will detail the results of the experiments conducted in an abstract and graphical manner.

Chapter 5 is for the concise explanation of the results, conclusions and then briefly state recommendations.

CHAPTER 2
LITERATURE REVIEW AND THEORIES

This chapter describes the work that was done by other researchers. It will be used as a comparison and a benchmark for the work to be studied in this research. The main properties of biodiesel are explained in detail. These are, kinematic viscosity, density and the cold flow properties. Equations used and other derivations of the theories such as the Newtonian Thermal Analysis, are explained in detail. The theory of the viscometer is described more so as to understand the concept in measuring kinematic viscosity. It is a quantity dependant on flow rate and this is shown mathematically. This chapter will guide the research work by further defining the aims and objects mentioned in Chapter 1. This will be done through the analysis of similar literature and information done by other researchers.

2.1 Biodiesel Properties

There basic properties of biodiesel that need to be considered before completely replacing the fossil fuels. These include density, kinematic viscosity, cetane and acid number, oxidation stability, emission value, cold flow properties, high heating values and so on. Other factors that should be considered are the functionality of the biodiesel with respect to the point of usage. Modifications may need to be done if using biodiesel in diesel engines, however, B80K20 (BK20) is said to be useable in diesel engines with very little to no modifications or adjustments to the engine because it exhibits characteristics of petrochemical diesel (Aydin et al., 2010).

The biodiesel feedstock mentioned in Table 2.1 is waste oil. It clearly shows that the parameters stated decrease with the increment of the blend. B85K15 exhibits qualities that are similar to petrochemical diesel. A similar table, table 2.2 shows, (Hasan et al., 2016), B80K20 having the better qualities as compared to that of B85K15. This is in line with Aydin et al., 2010 that B80K20 is a good blend and which can be used in engines without much adjustments.

Table 2.1: Biodiesel Blend with Kerosene (Hasan et al., 2016)

Property	Blend Range (%Biodiesel: %Kerosene)							Limits
	100:0	95:5	85:15	75:25	65:35	50:50	0:100	
Density kgm^{-3}	875	868	861	855	849	837	807	815-870
Viscosity cSt	4.92	4.84	4.25	3.95	3.45	2.76	1.38	2-5
Flash Point ^{O}C	176	135	105	70	66	62	45	Min60diesel Min100 BD
Cloud Point ^{O}C	4	3	3	1	-2	-4	-	Max 18
Pour Point ^{O}C	2	0	-1	-2	-4	-5	-7	Max 18
Cetane Index	67.4	67.1	65.3	62.1	59.2	52.5	-	48-60

Table 2.2 compares Biodiesel, diesel fuel (DF), kerosene, 80% diesel 20% biodiesel (D80B20), B80K20. The aim for the study was to determine the possibility of blending with a higher kerosene percentage and to compare the characteristics of the fuel with other blends. (Aydin et al., 2010).

Table 2.2: Comparison of Different Diesel Fuels and their Blends (Aydin et al., 2010)

Fuel	**Heating Value. Kj.kg^{-1}**	**Density g.cm^{-3} at 15^{O}C**	**Flash Point ^{O}C**	**Viscosity mm^{2}s^{-1} at 40^{O}C**	**Flow point ^{O}C**	**Cloud Point ^{O}C**	**Cetane Index**
ASTM Test No	D2015	D1298	D93	D445	D97	D2500	D613
B100	41 303	0.874	132	3.76	-21	-11	54
DF	42 900	0.848	75	2.0-3.5	-33	-16	46-55
Kerosene	43 500	0.780	39	1.4	-35	-18	39
D80B20	41 708	0.862	97	3.15	-28	-14	53.1
B80K20	42 850	0.850	68	2.63	-32	-16	50

Table 2.2 shows the properties of different types of fuels that were compared. From the table, it can be seen that the properties of the blends are not so different from the petrochemical diesel fuel, especially B80K20. For example, the density, there is a difference of 0.002 g/cm^3. This difference is highly insignificant and both values are within the ASTM D44 standard for kinematic viscosity. The feedstock of the biodiesel blends in Table 2.2 was cotton seed oil. Kerosene is used as a solvent additive in blending with biodiesel.

The research work done by (Hasan et al., 2016) and (Aydin et al., 2010) is almost similar. The work focused on measuring the quantities without, however, stating the storage conditions. This study will analyse the effect of storage conditions on biodiesel blends. These conditions are explained in more detail in chapter 3. It involves hold constant the temperature of the storage facility and compare with that is stored in a non-controlled environment, which are the ambient conditions at room temperature. The latter conditions fluctuate as the weather changes.

2.2 Density

This is the mass of any substance per unit volume of the substance (Giakoumis & Sarakatsanis, 2018). This is the Archimedes Principle and it is expressed in a formula as

$$\rho = \ m/V \tag{2.1}$$

Where ρ (kg/m^3) = density (kg/ml)

m (kg) = mass of the biodiesel (kg)

V (m^3) = volume of the biodiesel (m^3)

Methyl esters possess a greater value of density as compared to the petrochemical diesel. This will lead to diesel engine fuel pumps which are mainly based only on volumetric operations (Agarwal., 2007), to spray a larger weight of biodiesel as compared to the petrochemical diesel into the engine (Gabrowski & McCormick, 1998). This will have a direct impact on the air to fuel ratio (Demirbas., 2005 and Giakoumis et al., 2012).

Density rises proportionally with the number of double bonds, meaning that the greater the unsaturated the feedstock oil is, the greater the density of the produced methyl ester, and the higher the biodiesel mass that will be sprayed if a diesel-tuned engine is used with biodiesel (Giakoumis., 2013).

Equation 2.2 (Giakoumis, 2013), can be used to determine the density of a biodiesel. This will require the researcher to understand the chemical composition of the biodiesel under research.

$$\rho = 869.25 + 9.17n_{DB} \tag{2.2}$$

The equation was derived by (Giakoumis, 2013) after observing 158 samples of biodiesel from 26 feedstocks. The density was measured in kg/m^3 and the constant 9.17n$_{DB}$ is the average number of double bonds in the unsaturated FAME. This formula can only provide for an empirical value that one can use within the absence of the proper equipment.

A pycnometer is the standard apparatus that is used to measure the density of biodiesel. It is charged with the fuel and it is measured on a sensitive scale. The mass of the empty pycnometer is also recoded and is used in the calculation of the density.

2.3 Viscosity

This is a measure of the inside friction recorded against motion of flow. If there is an increment on temperature of the oil, there will be a decrease in viscosity and it will be much more ready to flow easily. It is a key parameter in the discussion biodiesel since it affects the operation of fuel injection equipment, especially at low temperatures where viscosity is high and affects the fluidity of the fuel. High viscosity brings about bad atomization of the fuel injection and this causes less accurate function of the fuel injectors (Demirbas., 2008).

Viscosity is considered as the integral of all forces affecting the fluid from molecular forces, to surface tension. Its variance affects the quality of the atomization. When the particles are exposed to oxygen and heat, the surface of the droplets burns out releasing large amounts of heat. This influences the other competitive reactions such as charring, choking and polymerization (Krisnangkura et al., 2006).

There are two types of viscosities.

2.3.1 Dynamic viscosity

This is the ratio of the shear stress to the velocity gradient of a fluid. It is also called absolute viscosity (The Physics hyper textbook., 2018). When a material deforms sideways through a force called shear, acting in the same plane and vector, a shear stress is resultant in the middle of the two layers and a strain of shear is made. This is expressed as;

$$\gamma = \frac{dx}{dy} \tag{2.3}$$

The strain/time is therefore expressed as follows;

$$\dot{\gamma} = \frac{\gamma}{dt} \tag{2.4}$$

Therefore, the formula for dynamic Viscosity is expressed as;

$$\mu = \frac{\tau}{\dot{\gamma}} = \tau \frac{dy}{du} \tag{2.5}$$

Pascal second, (Pa s), is major unit for dynamic viscosity.

2.3.2 Kinematic viscosity

Kinematic viscosity is a measure of the resistive flow of a fluid under the influence of gravity. It is basically dynamic viscosity divided by its density. This statement can be mathematically expressed as;

$$v = \frac{\mu}{\rho} \tag{2.6}$$

The units of kinematic viscosity are mm^2/s or cSt

The kinematic viscosity of diesel fuel and biodiesel blends strongly depends on temperature and composition. There are several numerical models that attempt to describe the viscosity of blends of known composition as a function of temperature are found in the literature (Corach et al., 2017).

2.3.3 Measurement of viscosity

Measuring depends with the conformance to the Newtonian fluid. Rheometers are used when the liquid is not defined with one value of viscosity. Temperature control is key as some viscosities double with a $5^{O}C$ variation in temperature. Some viscosities are constant with a wide range of shear rates, these are Newtonian fluids. These are fluids with a linear proportion to the local strain rate, that is, the rate of change of its deformation. Those without a constant cannot be described with a single number. These are called non Newtonian fluids. These require a finite amount of stress to effect the deformation of the fluid. These include the Bingham Plastic and the Bingham Psuedoplastic. Basically these are fluids whose shear stress is not directly proportional to deformation (Fox et al., 2012). Biodiesel is hence, a Newtonian fluid because its deformation under shear stress is directly proportional to the local strain rate.

Viscometers are some of the instruments available to measure viscosity and these are in the following types

- Capillary Viscometers (glass capillary being the most common)
- Orifice viscometer
- High temperature low shear rate viscometer
- Vibrational Viscometer
- Falling Sphere Viscometer
- Ultrasonic Viscometer
- Rotational Viscometer
- Rheometers
- Bubble Viscometers

2.3.3.1 Capillary viscometers and theory

These are best used when measuring the fluids which conform to the Newtonian Fluid theory. They are widely used due to their precise calibration. These measure the time taken by a fluid to flow through a capillary. Alternatively referred to as U-tube viscometers, these instruments include in their range the Ubbelohde and Ostwald varieties. These are easy and simple to use, with a U-like shaped glass tube with two bulbs, a top and a bottom. Fluid goes through from the top bulb down to the bottom bulb through a capillary, and viscosity is recorded by recording the time it taken by the fluid to go through the tube (Saint Clair Systems Norcross., 2018). Figure 2.1 shows an idealized viscometer.

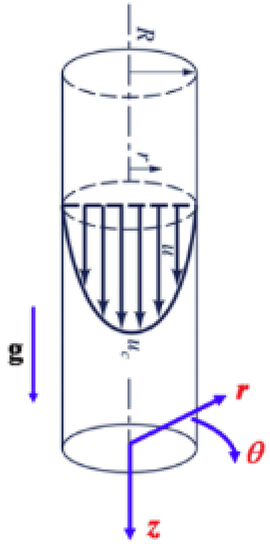

Figure 2.1: Hagen-Poiseuilles Fluid Flow through a Vertical Pipe (Fox et al., 2012)

The viscosity calculation from data of a capillary viscometer follows the Newtonian Fluid equation by Poiseuilles.

The particles travel through the Z axis.

$$v_r = 0, \qquad v_z \neq 0, \qquad v_\theta = 0 \tag{2.7}$$

From the equation of continuity

$$\frac{v_r}{\underbrace{r}_{0}} + \frac{\partial v_z}{\partial z} + \frac{\partial v_r}{\underbrace{\partial_r}_{0}} = 0 \tag{2.8}$$

Symmetry of Rotation

$$\frac{\partial v_\theta}{\partial \theta}\frac{1}{r} = 0; \quad v_z\,(r,t) \ = v_z \quad or \quad \frac{\partial}{\partial \theta} = 0 \tag{2.9}$$

Taking Equations 2.7, 2.8 with 2.9 into the Navier Stoke's Equation in cylindrical coordinates, the expression becomes;

$$\frac{\partial v_z}{\partial t} = v\left(\frac{\partial^3 v_z}{\partial r^3} + \frac{1}{r}\frac{\partial v_z}{\partial r}\right) - \frac{1}{\rho}\,.\frac{\partial p}{\partial z}\ follows\ z\ direction \tag{2.10}$$

For Flow which is steady, the equation will be expressed as

$$\frac{1}{\mu}\frac{\partial p}{\partial z} = \frac{1}{r}\frac{\partial v_z}{\partial r} + \frac{\partial^2 v_z}{\partial r^2} \tag{2.11}$$

Using the following boundary conditions to solve the differential equation 2.11

$$v_z\ is\ finite\ ; \quad r = 0 \tag{2.12}$$

$$v_z = 0;\ R = r \tag{2.13}$$

Gives

$$\left(-\frac{\partial p}{\partial z}\right).\frac{R^3}{4\mu}.\left(1-\frac{r^3}{R^3}\right) = v_z \tag{2.14}$$

While

$$-\frac{\Delta p}{L} = \frac{\partial p}{\partial z} \tag{2.15}$$

Volume flow rate discharge is

$$Q = \int_0^R \pi 2 v_z r dr \tag{2.16}$$

Putting 2.14 with 2.15 in 2.16

$$Q = \left(\frac{\Delta p}{L}\right)\frac{R^3}{8\mu}\pi \tag{2.17}$$

And

$$\frac{V}{t} = Q \tag{2.18}$$

Overall flow rate is Q, volume is V and time is t.

$$\frac{\mu}{\rho} = \ v \tag{2.19}$$

$$\Delta p = \rho g h \tag{2.20}$$

Therefore

$$v = \frac{\pi g H R^4}{(2 \times 4) L V} \ .t \tag{2.21}$$

Calibration constant K

$$K = \frac{\pi g H R^4}{8 V L} \tag{2.22}$$

Therefore, the equation will simply look like

$$v = K t \tag{2.23}$$

Equation 2.23 is almost identical to ASTM 446-07 kinematic viscosity equation, but only excluding the factor for correction.

$$v = \frac{10\pi g D^4 t H}{138LV} - \frac{E}{t^3} \tag{2.24}$$

E being the factor of correction.

2.4 Oxidation Stability

Oxidation Stability (OS) is a chemical reaction that occurs with a combination of oxygen and the lubricating oil. The rate of oxidation is increased by high temperatures, water, acids and catalysts such as copper.

The disadvantage with biodiesel is in its oxidation instability. Oxidation may change the chemical and physical properties of biofuels, for instance, it may lead to acidic characteristics and rising viscosities due to making of insoluble waxes that may clog the filters of fuel. This makes it, biodiesel, unsuitable for use in engines since the end resultant oxidation products may cause malfunction of the motors of vehicles (Meiraa, et al., 2011).

Oxidative rancidity is associated with the degradation by oxygen in the air. The Rancimat method, which is outlined in EN 14112, has been a part of the European biodiesel standards. The method is similar to the Oil Stability Index method (OSI) Cd12b-92. These methods are highly automatic and include heating the sample to a specific temperature, which is 110°C and passing air through the sample, which in will sweep volatiles from the sample into water. Water conductivity is monitored as it changes when the volatile acids are contained inside it (Knothe, 2006).

2.5 Acid Number

Acid Number (AN) or Total Acid Number (TAN) can be defined as the weight of potassium hydroxide, in mg, needed to neutralize the acidic species, such as fatty acids, contained in per weight, in g, of biodiesel (Xiea, et al., 2017).

It is also referred to as the neutralization number. The ASTM D664 and EN14104 state that the maximum is 0.5mg KOH/g. The presence of free fatty acids can lead to wear in the fuel line system.

2.6 Cold Flow Properties

Operability is defined as the lowest temperature a vehicle will operate without loss of power due to waxing of the fuel delivery system. The cold temperature properties of diesel fuel vary across the globe depending on the time of year the fuel is produced and the climate. Diesel fuels used in cold areas have better cold flow characteristics than diesel fuels used in warmer places (National Biodiesel Board, 2014).

The cold flow properties of biodiesel fuels are dependent on the feedstock from which they are made and are a strong function of the level of saturated fat. Animal fats, palm and coconut oils are more highly saturated, traditionally higher Cetane Number, higher cloud point.

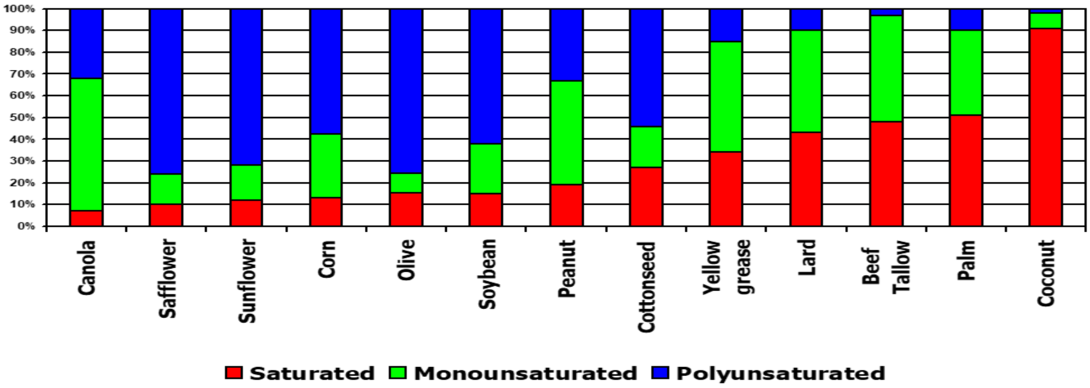

Figure 2.2: CN stability of different feedstocks (National Biodiesel Board, 2014)

Figure 2.2 shows thirteen different biodiesel feedstocks. The data demonstrate the variability in three main fats and the impact on cetane number and fuel stability. As the amount of saturation increases, the cetane and stability increases, but the cloud point increases as well (McCormick, et al 2001).

The important cold climate parameters that define operability for diesel fuels & biodiesel are;

2.6.1 Cloud point

This is the temperature where wax crystals become visible. The fuel starts to look cloudy or translucent. Biodiesel has a higher cloud point as compared to the petrochemical diesel. When measuring the Cloud Point, ASTM D2500 is the standard to follow.

2.6.2 Pour point

The lowest temperature at which a fuel is observed to flow. Again, this temperature is lower in petrochemical diesel as compare to biodiesel. This is due to the gel formation of the fuel. Viscosity will be high and the fuel will be opaque. The pour point is usually lower than the cloud point. The standard to follow when determining the pour point is the ASTM D 97-05.

2.6.3 Cold filter plugging point

The lowest temperature at which a vehicle will seize to operate. At this temperature, the wax particles begin to clog the fuel filters. Operability of the vehicle will become nearly obsolete. The measurement of this point is difficult for a naked eye. It is however outlined in the ASTM D 6371-05. It is found usually to be in between the cloud and pour points.

2.7 Thermal Analysis

Thermal analysis is a concept of materials science where the properties of materials are studied as they vary with temperature. Several methods are normally used, which are differentiated from one another by the property which is measured (Paulik, et al., 1966).

2.7.1 Newtonian thermal analysis

Can be abbreviated as NTA. The heat flow produced during solidification of the sample is expressed from a balance of heat equation as (Kierkus & J. H. Sokolowski, 1999)

$$-\mathrm{MC_p}\frac{\mathrm{dT}}{\mathrm{dt}}+\frac{\mathrm{dQ}}{\mathrm{dt}}=(\mathrm{T}-\mathrm{T_0})UA \qquad (2.25)$$

With; *M* being sample mass, $C_p$sample specific heat, *T* is the temperature of sample, *t* the time taken, *U* is the overall heat transfer coefficient, *A* is the sample surface area, T_0 is temperature of the cooling bath and *Q*, latent heat of solidification.

The assumption on the course of cooling is there no phase change that happens. $\frac{dQ}{dt} = 0$. The biodiesel sample cooling rate can be written thus,

$$\frac{dT}{dt} = -\frac{UA(T-T_0)}{MC_p} = Z_N \tag{2.26}$$

Z_N Being termed the Zero Curve of Newtonian or simply, the baseline

Therefore, the total latent heat L is calculated as

$$L = \frac{Q}{M} = C_P \int_{t_s}^{t_e} \left[\left(\frac{dT}{dt} \right)_{cc} - Z_N \right] dt \tag{2.27}$$

With t_e and t_s being the times for end and start of solidification, $\left(\frac{dT}{dt}\right)_{cc}$ showing the first derivative of the cooling curve.

The solidification latent heat of the biofuel sample can be expressed as,

$$L = C_p \times \text{(Area in-between cooling curve and baseline)} \tag{2.28}$$

Equation 2.28 is useful when the C_p of the biofuel is known. The total area inside the rate curve and the Newtonian baseline, as a fraction of total area between these two curves, the solid fraction at time *t* during freezing can be obtained (Evcil, et al., 2018).

CHAPTER 3

EXPERIMENTAL PROCEDURES AND METHODS

The methods and set up ups of the experiments are detailed in this chapter. Strict adherence to the standards was followed. These standards include ASTM D 445 for kinematic viscosity, ASTM D 1298 for density, ASTM D 97 and D2500 for the cold flow properties. Initially, the blend preparation and storage methods are outlined. This is the followed by the setup of experiments of the basic properties. The cooling curve setup is outlined and all material used in the process are pictured.

3.1 Biodiesel Blend Sample Preparation

The following instruments and equipment were used in the preparation of the biodiesel sample;

- Measuring cylinder, 1000 ml
- Pipette, 1 ml and 10 ml
- Funnel
- Beaker, 2000 ml and 5000 ml
- Storage Bottles, 1000 ml
- Stirrer/Spatula.

Step 1

Clean the instruments with the locally prepared detergent. The detergent should contain 70% distilled water, 15% muriatic acid and 15% hydrogen peroxide. To finish the process, rinse with acetone.

Step 2

Measure the volume required. The ratios are determined by the percentage volume. The following equation were used to determine the various volumes of kerosene, $V_{k,}$ to be used;

$$V_k = \frac{x}{100} \times 2000 \qquad (3.1)$$

Where x = (0, 5, 10, 15, 20)

The calculated volume, in ml, is then measured in a measuring cylinder, Figure 3.1 and poured into 5000ml beaker. This beaker is used so as to allow proper stirring at a later stage.

Figure 3.1: Measuring Cylinder

Step 3

Repeat step 1 on the measuring cylinder or any other instrument you would have used to measure the kerosene.

Step 4

Measure the biodiesel. The volume of biodiesel, V_{bd}, to be used is determined by the following equation;

$$V_{bd} = 2000 - V_k \tag{3.2}$$

The volume is in millilitres, ml.

Step 5

The total volume, V_t, is given by

$$V_t = V_{bd} + V_k \tag{3.3}$$

Mix the two measured quantities of biodiesel and kerosene in a 5000 ml beaker, Figure 3.2, making sure they are of corresponding percentages and use a stirrer or spatula to stir.

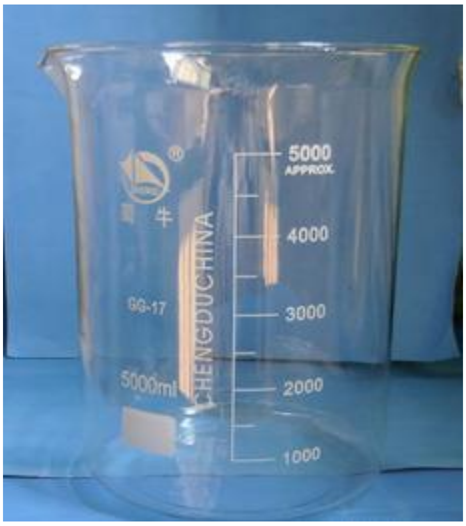

Figure 3.2: 5000 ml Beaker

Step 6

Pour some of the blended fuel into a 2000 ml beaker, then use this to fill up the 1000 ml storage containers. Label the containers and store them. Repeat the same steps until the required samples have been achieved.

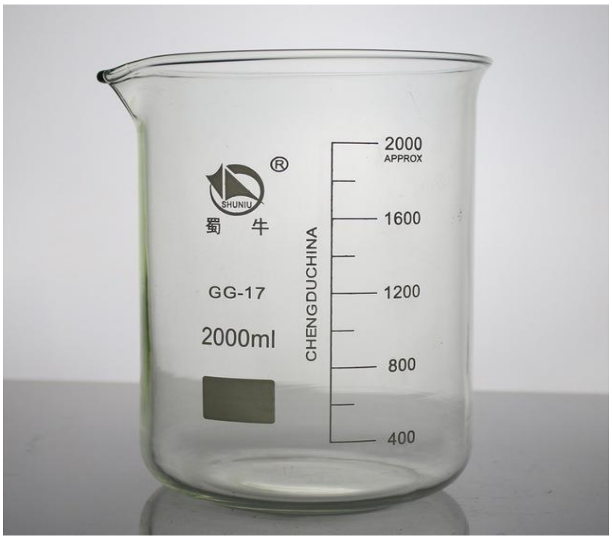

Figure 3.3: 2000 ml Beaker

Table 3.1 shows the samples prepared by volume.

Table 3.1: Biodiesel Kerosene Blends by Volume

Sample	B100	B95K5	B90K10	B85K15	B80K20
BD Volume (ml)	2000	1900	1800	1700	1600
Kerosene Volume (ml)	0	100	200	300	400

Figure 3.4: B90K10 after Blending Ready for Storage

3.2 Storage

The samples were poured in identical bottles and in equal amounts as shown in Fig 3.4. They were kept in two different places with different conditions. Figure 3.5 shows the first set of samples in ambient conditions in a cabinet.

Figure 3.5: Biodiesel Samples in a Cabinet

Figure 3.6: Oven with Digital Thermometer Set at 40^{O}C

Figure 3.6 shows an oven set at 40 ^{O}C were the second set of identical samples were stored.

3.3 Kinematic Viscosity

As defined in Chapter 2, this shows the resistance to flow. This is a major component of biodiesel as it influences the quality of the fuel. It is highly sensitive to temperature and great care must be taken when measuring the kinematic viscosity. Many methods and instruments can be used for the purpose, however, the capillary viscometer was selected for this purpose. An Ubbelohde viscometer was used for the purpose of this experiment. The total volume of the fluid under test does not affect the result measured by this type of viscometer. Table 3.2 shows the Kinematic Energy corrections of the Ubbelohde Viscometer ISO 3105/DIN51 562/Part1/BS188/NFT 60-100, Ref.No.501, 530, 532.

The 525-10/I was used in the experiment. Figure 3.7 shows the viscometer and its parts.

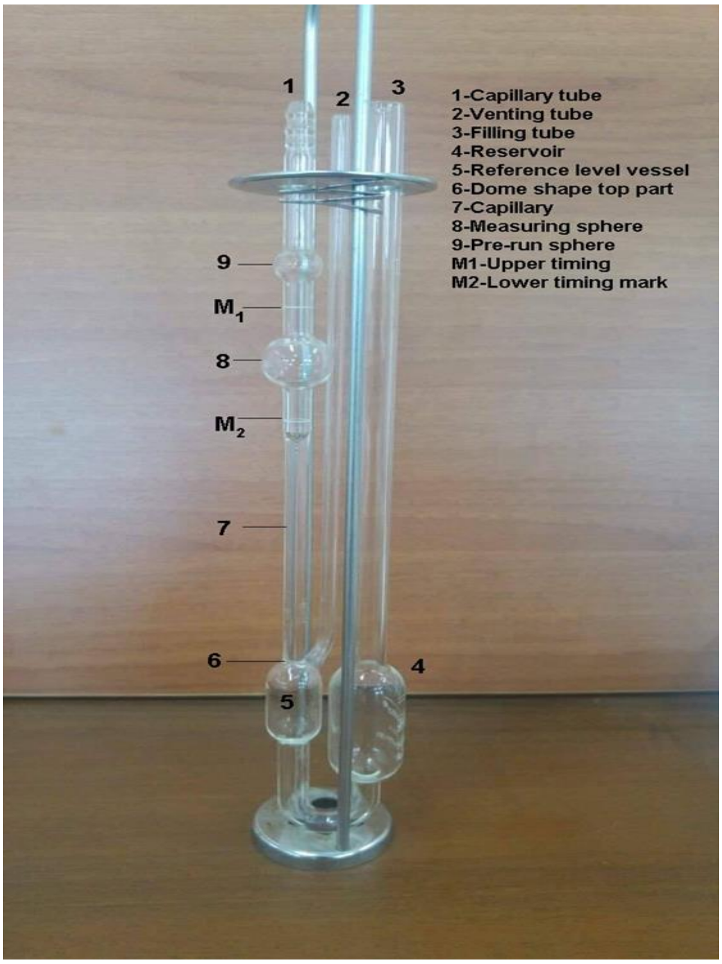

Figure 3.7: Ubbelohde type 525-10/I

Table 3.2: Correction of Kinetic Energy for a Range of Viscometers

Flow	**Capillary no**						
Time (s)	**0**	**0c**	**0a**	**I**	**Ic**	**Ia**	**1**
40	-[B]	-[B]	-[B]	1.03	0.45	0.15	-
50	-[B]	-[B]	-[B]	3.96	0.66	0.29	0.10
60	-[B]	-[B]	-[B]	2.75	0.46	0.20	0.07
70	-[B]	-[B]	-[B]	2.02	0.34	0.15	0.05
80	-[B]	-[B]	4.78[B]	1.55	0.26	0.11	0.04
90	-[B]	-[B]	3.78[B]	1.22	0.20	0.09	0.03
100	-[B]	7.07[B]	3.06[B]	0.99	0.17	0.07	0.02
110	-[B]	5.84[B]	2.53	0.82	0.14	0.06	0.02
120	-[B]	4.91[B]	2.13	0.69	0.12	0.05	0.02
130	-[B]	4.18[B]	1.81	0.59	0.10	0.04	0.01
140	-[B]	3.61[B]	1.56	0.51	0.08	0.04	0.01
150	-[B]	3.14[B]	1.36	0.44	0.07	0.03	0.01
160	-[B]	2.76	1.20	0.39	0.06	0.03	0.01
170	-[B]	2.45	1.06	0.34	0.06	0.02	0.01
180	-[B]	2.18	0.94	0.30	0.05	0.02	0.01
190	-[B]	1.96	0.85	0.28	0.05	0.02	0.01
200	10.33[B]	1.77	0.77	0.25	0.04	0.02	0.01
225	8.20	1.40	0.60	0.20	0.03	0.01	0.01
250	6.64	1.13	0.49	0.16	0.03	0.01	<0.01

Table 3.2: Continued

Flow	**Capillary no**						
Time (s)	**0**	**0c**	**0a**	**I**	**Ic**	**Ia**	**1**
350	3.39	0.58	0.25	0.08	0.01	0.01	
375	2.95	0.50	0.22	0.07	0.01	0.01	
400	2.59	0.44	0.19	0.06	0.01	<0.01	
425	2.30	0.66	0.29	0.09	0.01	<0.01	
450	2.05	0.58	0.25	0.08	0.01	<0.01	
475	1.84	0.50	0.22	0.07	0.01		
500	1.66	0.44	0.19	0.06	0.01		
550	1.37	0.23	0.1	0.03	0.01		
600	1.15	0.20	0.09	0.03	0.01		
650	0.98	0.17	0.07	0.03	<0.01		
800	0.65	0.11	0.05				
850	0.57	0.10	0.04				
900	0.51	0.09	0.04				
950	0.46	0.08	0.03				
1000	0.42	0.07	0.03				

[A] The correction seconds stated are related to the respective theoretical constant

[B] For precision measurement, these flow times should not be applied. Selection of a viscometer with a smaller capillary diameter is suggested

Table 3.3 shows the data given by the manufacturer. It is used to determine the viscosity constant K, (mm^2/s)/s.

Table 3.3: Ubbelohde Technical Data

Capillary No.	**Capillary Dia. I ± 0.01[mm]**	**Constant , K, (mm^2/s)/s**	**Measuring range [mm^2/s]**
0c	0.36	0.002856	0.6 ……… 3
I	0.58	0.009820	2 ………10
Ic	0.78	0.02944	6 ………30

The rectified flow time is multiplied by the constant K, for accurate measurement. This directly gives the kinematic viscosity [mm^2/s] as given in Equation 3.4;

$$v = K(t - y) \tag{3.4}$$

Where ν is the kinematic viscosity

K-the constant of calibration.

t-the measured time flow and

y-the correction on kinetic energy.

The kinetic energy correction y is provided by the producer of the viscometer and tabulated for each type of viscometer in term of flow time as shown in Table 3.2.

3.3.1 Procedure for measuring kinematic viscosity

The following are the instruments used in preparation and measuring of the kinematic viscosity.

Electromagnetic Heater and Stirrer

This is the devise used to heat up the water bath to 40 ^{O}C and maintain it at that temperature throughout the experiment. It is also called an induction heater and it heats the inductive metal through eddy currents. The apparatus is shown in Figure 3.8.

Figure 3.8: Electromagnetic Heater Heidolph MR Hei-Tec

Viscometer

For the measurement of the Kinematic Viscosity. As mentioned above, type 525-10/I, Figure 3.7, is used. Care must be taken when handling this instrument because it is fragile and expensive to replace.

Thermometer

This was used to regulate the temperature at an optimum 40^{O}C. The thermometer range is from 10 – 110^{O}C.

Viscometer stand

The viscometer stand is used to support the upright position of the viscometer and it is shown in Figure 3.9

Figure 3.9: Viscometer Stand

5000 ml Beaker

This is used as container for the water bath and the viscometer. It is not damaged by heat and is transparent enough for the contents to be seen.

Suction Syringe

This is used to pull the biodiesel through the venting tube on the viscometer. Figure 3.10 shows the suction syringe used in the experiment

Figure 3.10: Suction Syringe

Step 1 Clean the Viscometer

Cleanse the viscometer with the locally prepared detergent. The detergent should be 70% distilled water, 15% hydrogen peroxide, 15% muriatic acid%. Rinse well with pure acetone, a quick dryer, to round up the cleansing process. Rinse again with the sample to be tested.

Step 2 Prepare the Correct Amount of the Sample

Measure and charge the viscometer with the correct amount of biodiesel, usually 25ml. The biodiesel has to be between the two lines on the tube so that the amount of liquid charged will not obstruct the air tube during use.

Step 3 Insert the Viscometer into the Water Bath

Put the viscometer in a controlled water bath at $40^{O}C$. The capillary needs to be upright always. The sample must have a homogenous temperature with the bath, and this will take about 20 minutes.

Step 4 Suction of the Sample

Seal off venting tube and gently apply suction to the capillary tube with the suction syringe. Apply suction to the capillary tube to the point where the liquid fills the pre run bulb. Hold the liquid at this level by venting tube.

Step 5 Measure the Time Flow

Let go of the timing tube and leave the liquid to flow. Record the time, using seconds, it takes the fluid to flow from the first mark to the second bottom mark. Be consistent on how you measure. If you use the lower meniscus for the upper mark, be sure to use the same for the lower mark and throughout the whole experiment.

Step 6 Calculate the Kinematic Viscosity

Calculate the Kinematic viscosity of the sample using equation 3.4. Be sure to use the table 3.2 and 3.3 to get the kinetic energy correction factor and technical parameters and constant K of the time and viscometer respectively.

Step 7 Repeat the Process

Before moving on to the next sample, repeat the process three or 4 times and get the average kinematic viscosity. Make sure to keep checking the temperature so that it always stays at 40 ^{O}C.

Figure 3.11 shows the general set up of the experiment for kinematic viscosity.

Figure 3.11: Setup for Measuring Viscosity

3.4 Density

As explained in chapter 2, density is a key parameter which affects the spray quality. The density varies with temperature so the set temperature for this experiment was set at 15 ^{O}C. the following apparatus is used in measuring density;

2000 ml Beaker

This is the main container for the water bath in which the sample will be placed to attain an optimum temperature of 15 ^{O}C, as shown in Figure 3.3

Pycnometer

This is a device used to measure density, Figure 3.12. It is made of glass, with a tight glass cover which has a capillary in the centre of it, so that air bubbles and the excess liquid may flow out from the apparatus. This allows a liquid's density to be measured correctly by reference to an appropriate functional fluid, such as pure water.

Figure 3.12: 100ml Pycnometer

Electronic Balance Scale

This is a highly sensitive scale which measures mass of any substance within its range. The scale used in this experiment measures up to 250.000g. The scale has a spirit leveller to make sure the scale is well balanced when taking readings at any point of the procedure as shown in Figure 3.13.

Figure 3.13: Electronic Balance Scale

Thermometer

This is used to monitor the temperature of the water bath to keep it at 15 ^{O}C. The thermometer range was from 10-110 ^{O}C

3.4.1 Procedure for Measuring Density

Before measuring density, there are precautions to follow when using the pycnometer.

- Make sure not to trade neither the cover nor the bulb of the pycnometer with someone else since both the bulb and cover are labelled with the same number.
- Make sure the pycnometer is cleaned up and is dry before use.
- Use an appropriate apparatus such as a pipette or a funnel of the right size to fill the pycnometer to the middle of the neck and gently place the stopper
- Make sure that there are no air bubbles in the bulb or the capillary before u weigh.
- Wipe dry the pycnometer before putting it on the highly sensitive scale.
- Make sure the required temperature is maintained because the glass material used in manufacturing the pycnometer is sensitive to temperature and so is the biodiesel sample under study.
- Zero the electronic balance scale. Make sure the surface is clean and dry, with the spirit level indicating that it’s balanced. Set it on a surface which is stable and free from vibrations.

With the above precautions taken into the considerations, the following steps can be followed in measuring density.

Step 1

Wash the pycnometer with the locally prepared detergent. This detergent should 70% distilled pure water, 15% hydrogen peroxide, 15% muriatic acid%. Rinse with acetone for a quick dry to finish the washing process. Make sure the pycnometer gets dry.

Step 2

Measure the mass of the empty pycnometer and record the mass. Figure 3.14 shows the setup. Make sure that the surface of the weigh balance is dry and clean and that the pycnometer is dry both inside and outside.

Figure 3.14: Measuring Mass of Empty Pycnometer

Step 3

Fill the pycnometer with biodiesel as shown in Figure 3.15, carefully following the precautions. Any excess biodiesel or air bubbles will escape via the capillary opening on the stopper.

Figure 3.15: Pycnometer with Biodiesel

Wipe off any excess fluid on the pycnometer. Handle with clear as the biodiesel is a slippery fluid. Make use of a funnel of the correct size when filling the pycnometer. The stopper should also be clean and free from contamination as this will distort the mass to be recorded. The capillary opening on the stopper should not be blocked.

Step 4

Place the filled pycnometer into the water bath which is at the required 15 ^{O}C. Let the sample acclimatize to the required temperature for 20 mins. To achieve this temperature, you can use the electromagnetic heater to heat the water if it is too cold, Figure 3.16. When the water bath is above the required temperature, use a cooling bath to reduce the temperature. More about the cooling bath shall be discussed further in this chapter.

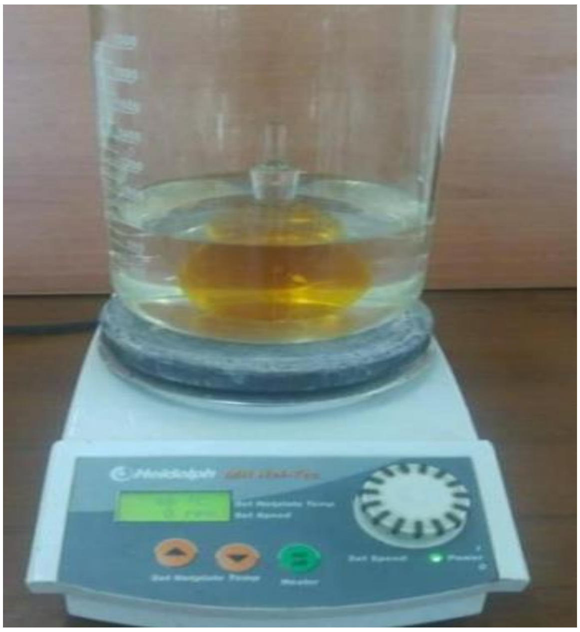

Figure 3.16: Set up for heating water bath to 15 ^{O}C

Step 5

Measure the mass of the filled pycnometer. Wipe it clean and dry after taking it from the water bath, Figure 3.17. Ensure the all surfaces are dry and the platform is level. Failure to achieve this will result in distorted recordings. Like mentioned before, the sample and the pycnometer are sensitive to temperature therefore the procedure has to be done with urgency. If there is any suspected loss of heat, repeat steps 4 and 5.

Figure 3.17: Measuring the mass of the sample

Step 6

Calculate the density following Equation 3.5;

$$\rho = \left(\frac{m_f - m_e}{V}\right) \times 1000 \tag{3.5}$$

Where ρ = density (g/ml)

m_f = Mass of Pycnometer filled with Biodiesel sample (g)

m_e = Mass of empty Pycnometer (g)

V = volume of sample (ml)

Multiplying by 1000 converts the units from g/ml to kg/m^3

3.5 Cooling Curve Analysis

This is used to analyse the behaviour of the fluid sample in respect to temperature drops. Solid and liquid fractions are determined and cold flow properties are determined from this experiment. The experiment can be divided into 3 main parts, which are;

1 The Data Collection Unit

This is the unit which has the instruments to collect information. In particular, temperature. This is used to analyse the fluid sample and come up with the required information. This unit consists of the Data Logger and a computer.

The data logger, Figure 3.18, used in this research is an Ordel Data Logger. It has 5 channels which are connected to thermocouples. Only four channels were used in this experiment to measure temperature.

Figure 3.18: Data Logger, ODEL UDL 100

A dedicated computer was used to capture the data from the data logger. Figure 3.19 shows the schematic setup of the system.

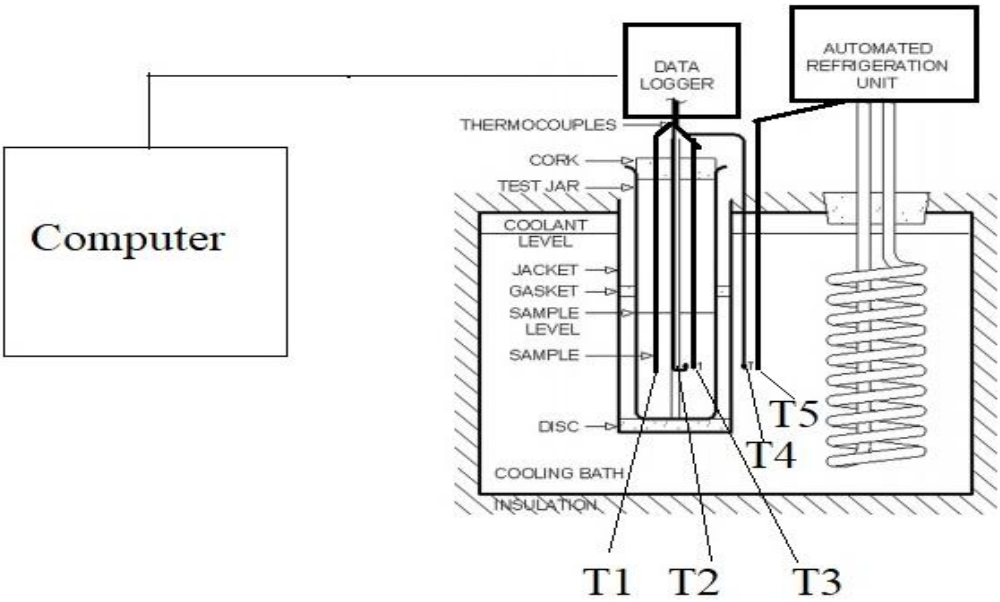

Figure 3.19: Schematic Setup

The computer is installed with the program software, Dali 08 Data Acquisition and Logging Interface, capable of reading signal from the data logger as shown in Figure 3.20.

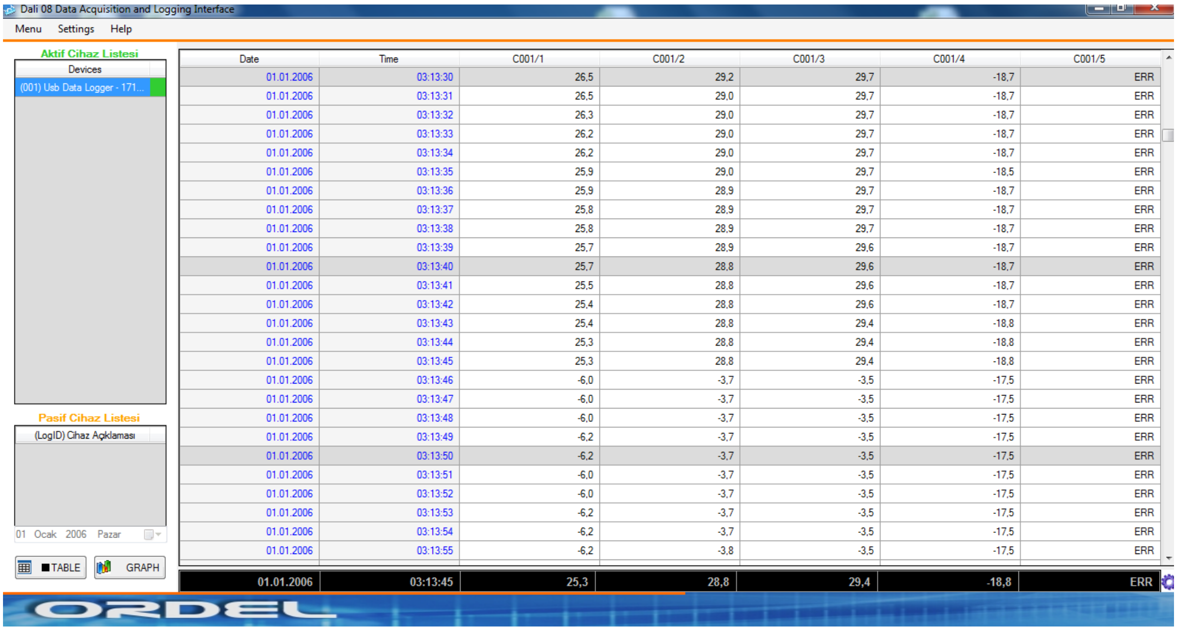

Date	Time	C001/1	C001/2	C001/3	C001/4	C001/5
01.01.2006	03:13:30	26,5	29,2	29,7	-18,7	ERR
01.01.2006	03:13:31	26,5	29,0	29,7	-18,7	ERR
01.01.2006	03:13:32	26,3	29,0	29,7	-18,7	ERR
01.01.2006	03:13:33	26,2	29,0	29,7	-18,7	ERR
01.01.2006	03:13:34	26,2	29,0	29,7	-18,7	ERR
01.01.2006	03:13:35	25,9	29,0	29,7	-18,5	ERR
01.01.2006	03:13:36	25,9	28,9	29,7	-18,7	ERR
01.01.2006	03:13:37	25,8	28,9	29,7	-18,7	ERR
01.01.2006	03:13:38	25,8	28,9	29,7	-18,7	ERR
01.01.2006	03:13:39	25,7	28,9	29,6	-18,7	ERR
01.01.2006	03:13:40	25,7	28,8	29,6	-18,7	ERR
01.01.2006	03:13:41	25,5	28,8	29,6	-18,7	ERR
01.01.2006	03:13:42	25,4	28,8	29,6	-18,7	ERR
01.01.2006	03:13:43	25,4	28,8	29,4	-18,8	ERR
01.01.2006	03:13:44	25,3	28,8	29,4	-18,8	ERR
01.01.2006	03:13:45	25,3	28,8	29,4	-18,8	ERR
01.01.2006	03:13:46	-6,0	-3,7	-3,5	-17,5	ERR
01.01.2006	03:13:47	-6,0	-3,7	-3,5	-17,5	ERR
01.01.2006	03:13:48	-6,0	-3,7	-3,5	-17,5	ERR
01.01.2006	03:13:49	-6,2	-3,7	-3,5	-17,5	ERR
01.01.2006	03:13:50	-6,2	-3,7	-3,5	-17,5	ERR
01.01.2006	03:13:51	-6,0	-3,7	-3,5	-17,5	ERR
01.01.2006	03:13:52	-6,0	-3,7	-3,5	-17,5	ERR
01.01.2006	03:13:53	-6,2	-3,7	-3,5	-17,5	ERR
01.01.2006	03:13:54	-6,2	-3,7	-3,5	-17,5	ERR
01.01.2006	03:13:55	-6,2	-3,8	-3,5	-17,5	ERR
01.01.2006	03:13:45	25,3	28,8	29,4	-18,8	ERR

Figure 3.20: Data Logger Interface

The system is highly interactive. The interface displays the readings of the thermocouples. It provides options of selecting the data to capture during the experiment. Options of saving are also available and it ca be set up to capture data every second, 30 seconds or hourly. During the run, it is best to capture the data every 30 seconds. Be sure to save the information every 10 minute intervals. This is done to ensure that data is stored for analysis in the event that a technical fault occurs. Monitor the thermocouples reading in the black panel readings, Figure 3.20. The bath reading should coincide with the digital thermostat.

However, this data is converted to a spreadsheet for analysis. Microsoft Excel was used to view the spreadsheet and perform extensive analysis of the data. Other software used include Matlab and Minitab. Figure 3.21 shows the screenshot of the data in Microsoft excel.

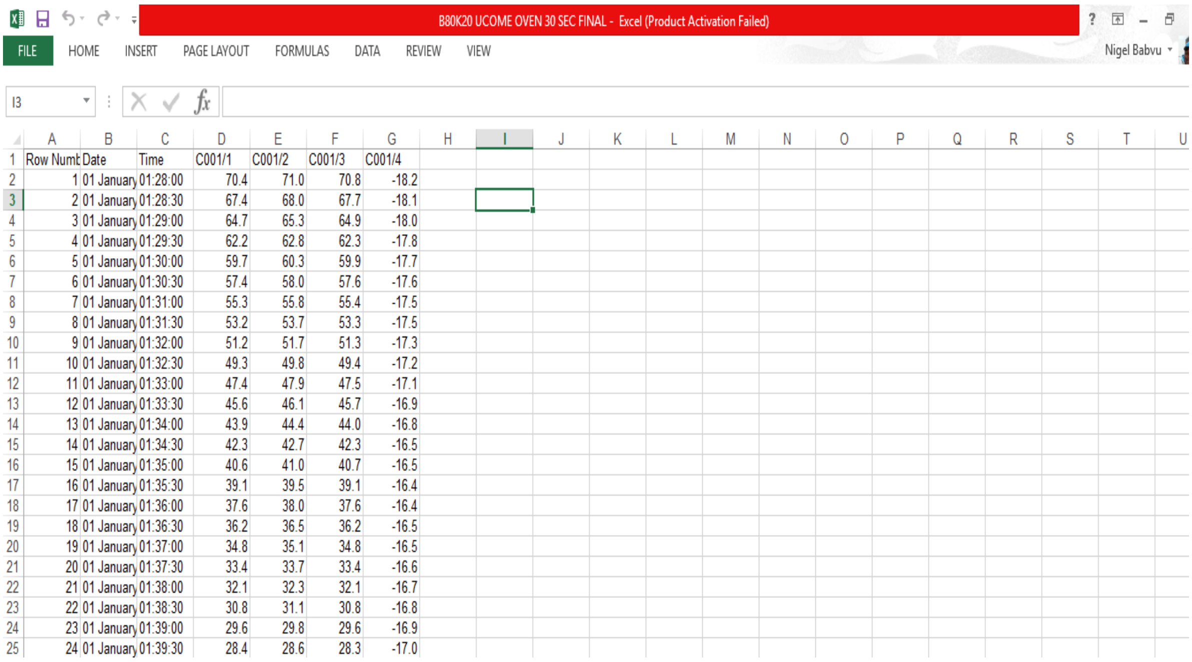

	A	B	C	D	E	F	G
1	Row Numb	Date	Time	C001/1	C001/2	C001/3	C001/4
2	1	01 January	01:28:00	70.4	71.0	70.8	-18.2
3	2	01 January	01:28:30	67.4	68.0	67.7	-18.1
4	3	01 January	01:29:00	64.7	65.3	64.9	-18.0
5	4	01 January	01:29:30	62.2	62.8	62.3	-17.8
6	5	01 January	01:30:00	59.7	60.3	59.9	-17.7
7	6	01 January	01:30:30	57.4	58.0	57.6	-17.6
8	7	01 January	01:31:00	55.3	55.8	55.4	-17.5
9	8	01 January	01:31:30	53.2	53.7	53.3	-17.5
10	9	01 January	01:32:00	51.2	51.7	51.3	-17.3
11	10	01 January	01:32:30	49.3	49.8	49.4	-17.2
12	11	01 January	01:33:00	47.4	47.9	47.5	-17.1
13	12	01 January	01:33:30	45.6	46.1	45.7	-16.9
14	13	01 January	01:34:00	43.9	44.4	44.0	-16.8
15	14	01 January	01:34:30	42.3	42.7	42.3	-16.5
16	15	01 January	01:35:00	40.6	41.0	40.7	-16.5
17	16	01 January	01:35:30	39.1	39.5	39.1	-16.4
18	17	01 January	01:36:00	37.6	38.0	37.6	-16.4
19	18	01 January	01:36:30	36.2	36.5	36.2	-16.5
20	19	01 January	01:37:00	34.8	35.1	34.8	-16.5
21	20	01 January	01:37:30	33.4	33.7	33.4	-16.6
22	21	01 January	01:38:00	32.1	32.3	32.1	-16.7
23	22	01 January	01:38:30	30.8	31.1	30.8	-16.8
24	23	01 January	01:39:00	29.6	29.8	29.6	-16.9
25	24	01 January	01:39:30	28.4	28.6	28.3	-17.0

Figure 3.21: Data Captured in Microsoft Excel

Once the data is converted to the spreadsheet, Figure 3.21, it is analysed using the tools provided for by the software. Using two software's enables comparison and verification. The

2 **The Cooling Bath System**

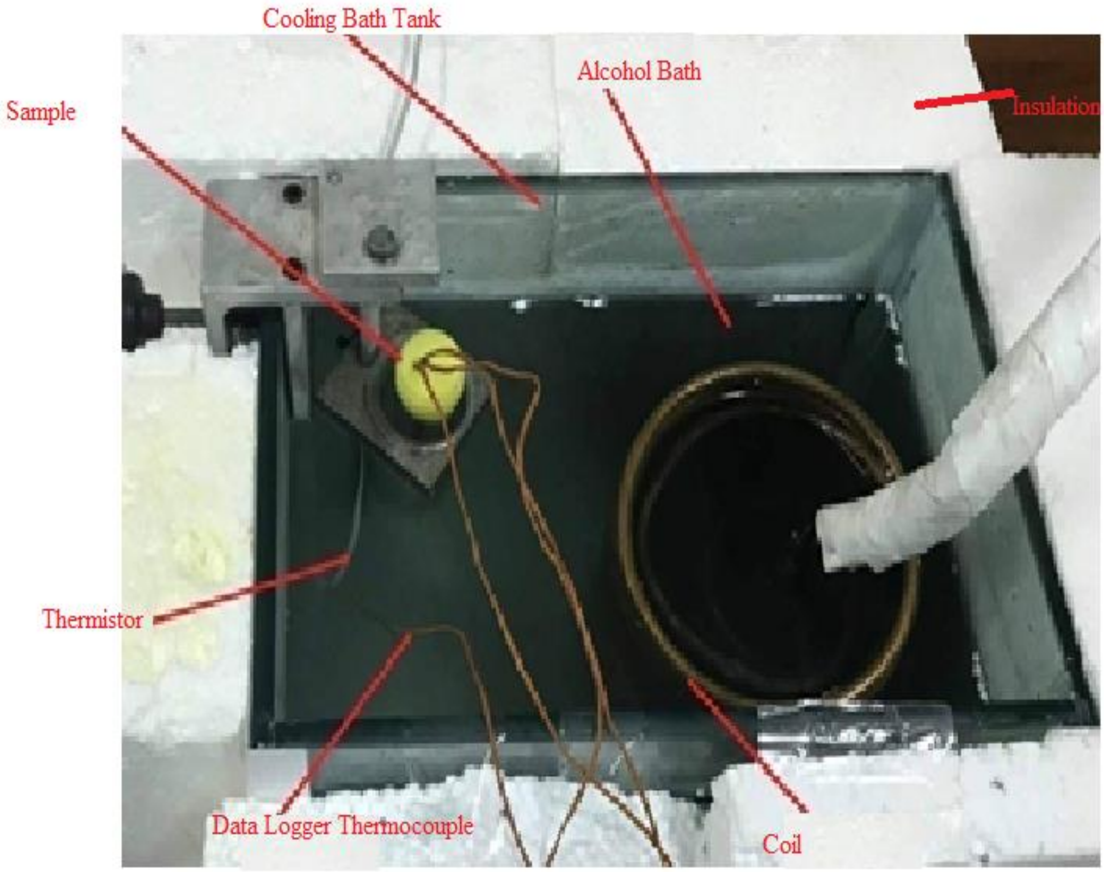

Figure 3.22: The Cooling Bath System

The above setup, Figure 3.22 is the general setup of the cooling bath that was used in the experiment.

The Cooling Bath Tank

It is made from thick glass which is a bad conductor of heat. Glass panels are joined together with silicone as a sealant to prevent loss off the alcohol bath.

Alcohol Bath

The alcohol used was ethyl alcohol or simply ethanol in its purest possible form. This was used because it freezes at a very low temperature, -114 ^{O}C.

Insulation

Styrofoam was used in this experiment. This is a very bad conductor of heat. I was used to cover the whole tank and the top part was the only detachable part. A small space was let clear to monitor the process inside.

Coil

This is the unit that carries the refrigerator gas to the compressor for heat exchange. It takes away the heat from the alcohol bath to the surroundings.

Data Logger Thermocouples

These are used to collect the temperature of the sample and the alcohol cooling bath. There are four in the setup, three are used to measure the temperature in the sample and the fourth one measures that of the cooling bath.

Thermistor

This is used to control the water bath temperature. It is connected to a temperature control unit in conjunction with the compressor.

Sample

Sample is mounted on a stand within the bath. It has thermocouples connected to it which gives readings of the sample.

3 The compression Unit

This comprises of a compressor and a digital temperature control unit as shown in Figure 3.23. The main purpose is to cool down the refrigerator gas which in turn, cools the alcohol bath. The temperature control unit is set up to a certain required temperature at it is let to run until it the bath gets to that temperature.

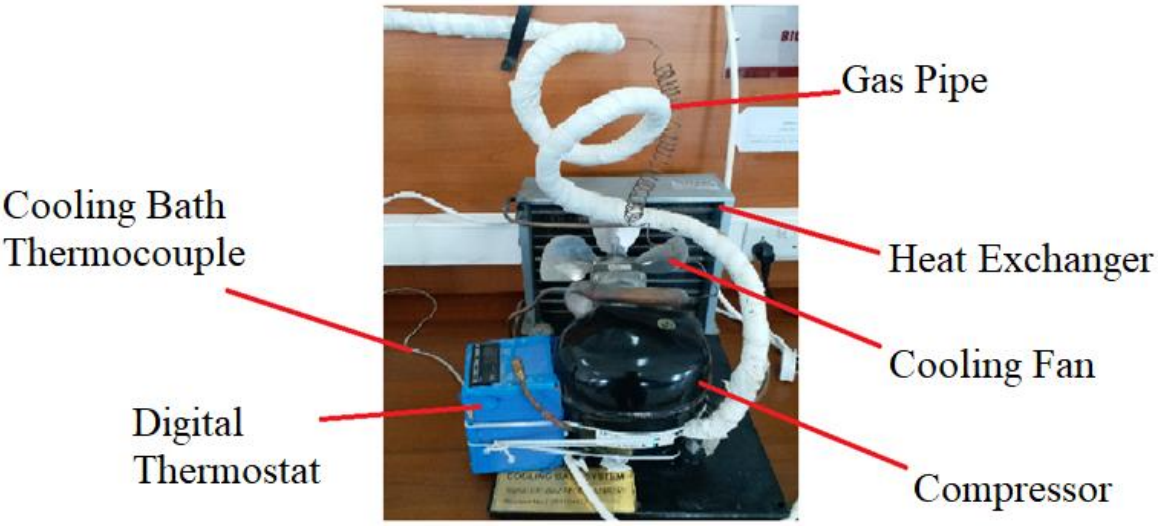

Figure 3.23: Compressor Unit

The compression unit in Figure 3.23 is switched on at least 2 hours before running the experiment. Depending on the ambient conditions, it takes almost 2 hours to get to the required -20 ^{O}C. However, it should not run for more than 10 hours in a day.

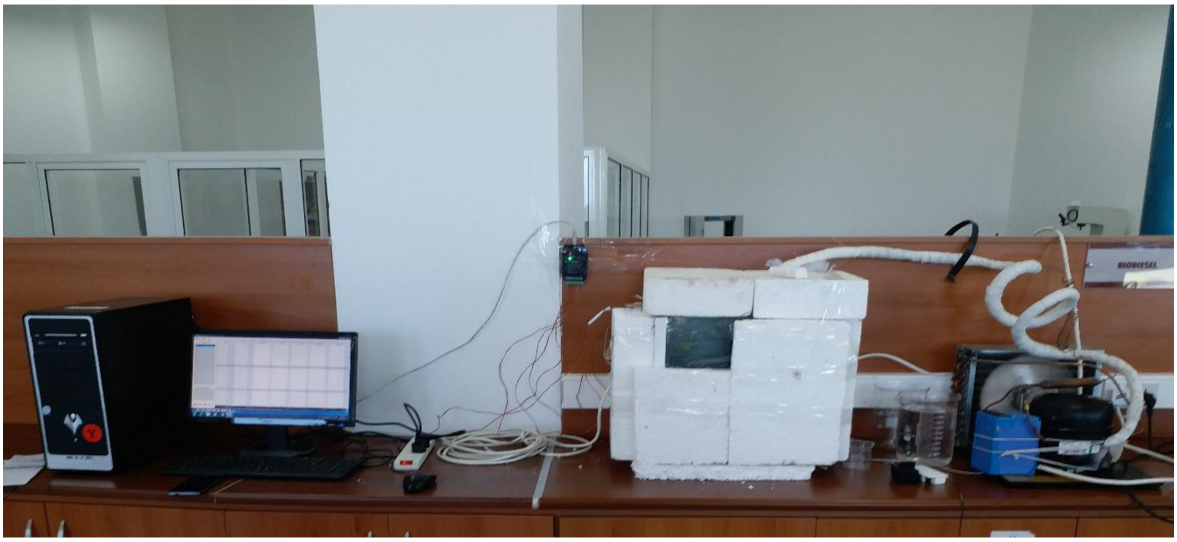

Figure 3.24: Complete Cooling Curve Analysis Setup

Figure 3.24 shows the complete set up of the cooling curve system.

3.5.1 Steps in Performing Cooling Curve

The following steps should be followed to perform a successful cooling curve analysis.

Step 1

Set the digital control unit to -20 ^{O}C and wait for the cooling bath to reach the required temperature.

Step 2

Measure 45ml of the sample into a measuring cylinder. This should be done while waiting the cooling bath is cooling off to the required temperature.

Step 3

Measure the Kinematic viscosity at 40 ^{O}C and Density at 15 ^{O}C of the sample following the steps outlined in the respective sections. This is done to study the effect of heating and cooling of the sample on kinematic viscosity and density. A smaller pycnometer of volume 25ml is used since the volume of the sample under study is not much.

Step 4

Pour the 45ml sample into a test jar. Place it into a water bath and heat the sample up to 70^{O}C. This is done to give room for transfer from the water bath into the cooling bath. The temperature of the sample will drop in the process.

Step 5

Set up the thermocouples as shown in Figure 3.25. This is done in accordance of with the standards for performing a Newtonian Thermal Analysis and a Fourier Thermal Analysis. Two thermocouples are needed for a NTA and three for FTA (FTA was not analysed in this work, however, the data was captured for future use). They are 10mm apart each other. Thermocouple 1 and 3 are 7.5mm from the wall with thermocouple 2 at the centre.

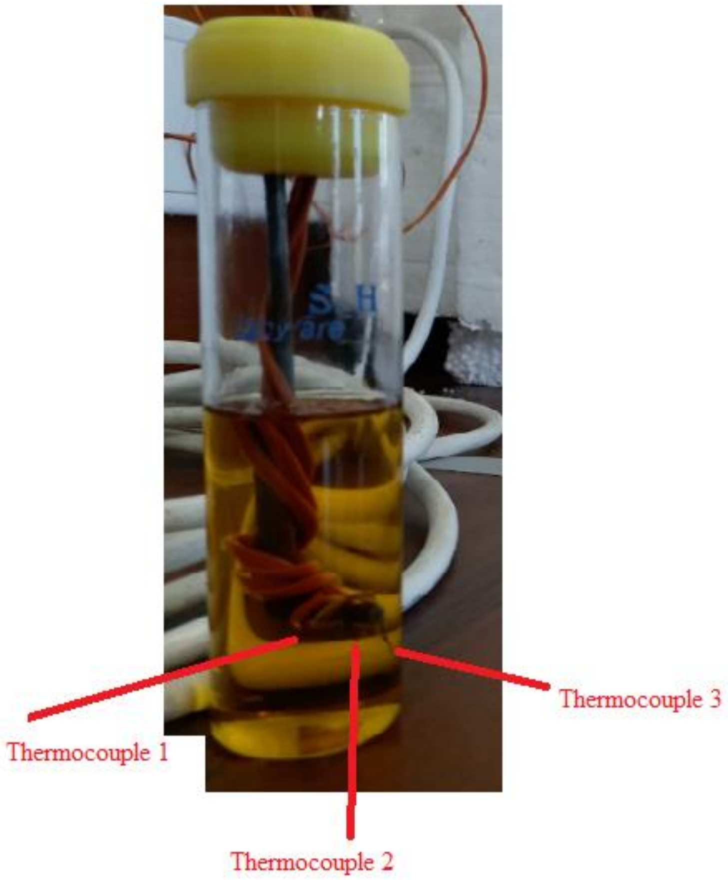

Figure 3.25: Thermocouple Setup for Thermal Analysis

Step 6

Place the glass test jar into a jacket cylinder and dip it not the cooling bath. Make sure the thermocouples are at the same level with that in the cooling bath.

Step 7

Monitor the cooling process. Save the data every 10 minutes from the moment the sample reading is 65 ^{O}C for four hours. Saving is done so as to have data stored just in case a fault occurs.

Step 8

Take out the frozen sample and reheat it. Measure the kinematic viscosity and density like before.

Step 9

Use Microsoft Excel or Matlab to analyse the data collected.

3.6 Cold Flow Properties

The cold flow properties measured here are Pour Point and Cloud Point. The Cold Filter Plugging Point is found in between these two points. The ASTM D 97-05 and ASTM 2500 were followed respectively. Both experiments can be done simultaneously.

3.6.1 Procedure

Step 1

Measure 45 ml of the sample and put in a glass test jar. The thermocouples should be set up as shown in figure 3.26. The lower thermocouple measures the Cloud point and the upper thermocouple the Pour point. Be sure to label the thermocouples.

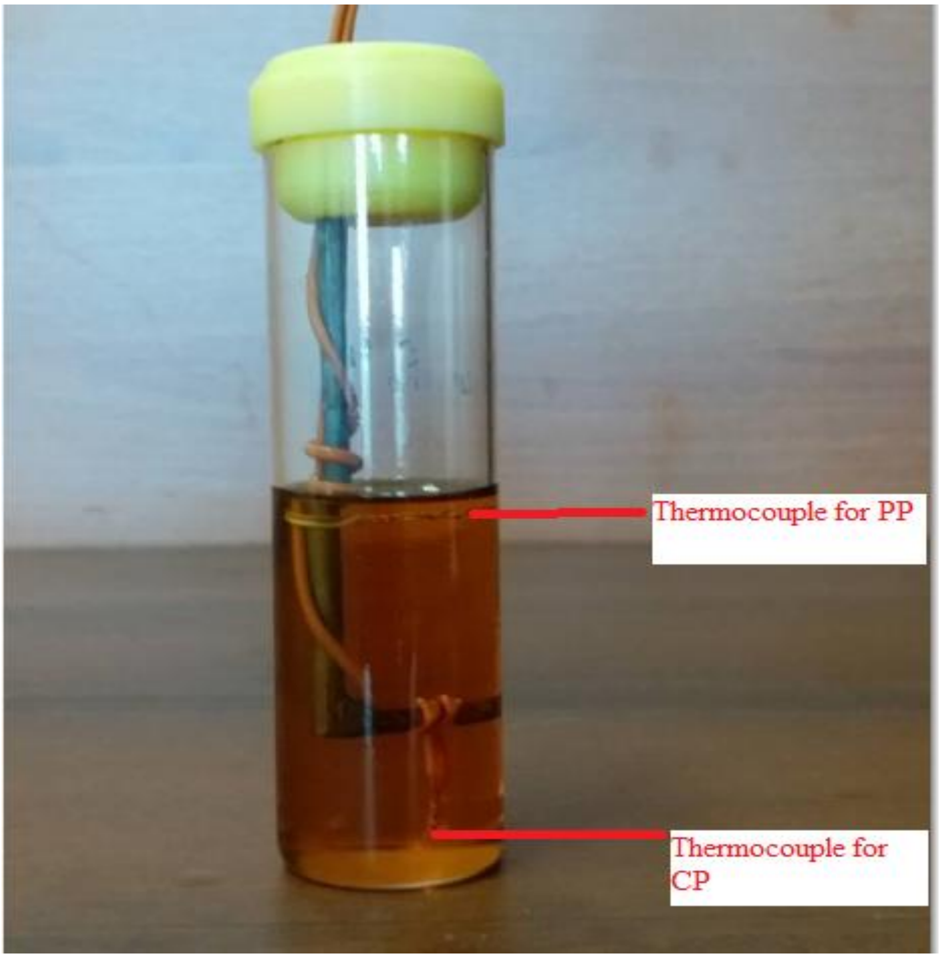

Figure 3.26: Setup for Cold Flow Properties

Step 2

Place the test jar in jacket cylinder and make sure the temperature of the cooling bath is at negative 20 ^{O}C.

Step 3

Continuously check for on the sample visually with every $1^{O}C$ temperature drop.

Step 4

Once Crystal like particles begin to form up at the bottom, the cloud point has been reached. Record the temperature reading on the thermocouple assigned to the reading of the cloud point.

Step 5

Continue the process from step 3.

Step 6

Once the sample is no longer flowing, even at a tilt, it has reached the pour point. Record this temperature using the thermocouple assigned for pour point.

Step 7

Compare and contrast the results obtained visually with that of the cooling curve.

3.7 Acid Number and Oxidation Stability

These tests were done at Tubitak Marmara Research Centre in Gebze, Kocaeli Province, Turkey. They followed the EN 14104 standard for Acid Number and EN 14112 for Oxidation Stability.

CHAPTER 4

RESULTS AND DISCUSSIONS

The analytical results of the experimental work is explained in this chapter. All the data used during the analysis was obtained from the experimental work. The constants used in the calculations were from the referenced sources and manufacturers data sheets as described in previous chapters. The information will be presented in the form of graphs and tables and a brief discussion precedes.

4.1 Calibration and Reliability

The equipment used in this work were tested against known standard values of pure water in kinematic viscosity at 40 ^{O}C and density at 15 ^{O}C. the percentage error in the viscometer was less than 1% and that of the pycnometer was 0.11%. The thermocouples and thermometers were used to measure a known temperature of water and all produced the accurate value within a 0.5% margin of error. The experiments conducted in this research have been repeated at least three times so as to get accurate results. In the case of cooling curve, analysis, the experiment ran for four hours so as to attain more data and accurate results. Kinematic Viscosity was measured at 40 ^{O}C and Density at 15 ^{O}C throughout.

4.2 Effects Storage Period and Methods on Kinematic Viscosity

This section is focused on establishing the effect of storage time on kinematic viscosity of the different blends of biodiesel samples used.

Table 4.1: Kinematic Viscosity Values of Samples in Ambient Conditions

	UCOME STORED IN AMBIENT CONDITIONS				
	Viscosity in mm^2/s				
Time (Days)	**B100**	**B95**	**B90**	**B85**	**B80**
10	4.4734	4.178	3.9495	3.5904	3.3499
20	4.5165	4.1861	3.8921	3.6484	3.4197
30	4.5222	4.2252	3.9114	3.6589	3.3765
40	4.5391	4.2418	3.9806	3.6993	3.4355
50	4.5515	4.2819	3.9891	3.7001	3.4368
60	4.5992	4.2851	3.9953	3.7147	3.4638
80	4.6031	4.3058	3.9797	3.7158	3.4820
100	4.7130	4.3256	3.9854	3.7431	3.5264
MEAN	4.5647	4.2536	3.9603	3.6838	3.4363
SD	0.0736	0.0546	0.0389	0.0486	0.0564

The first measurement of the samples was recorded as day 10. The corresponding graph of Table 4.1 is shown in Figure 4.1. From the graph, it is evident that the kinematic viscosity of the samples generally increases with time. Even though some of the samples show a decrease at first, they continue to exhibit signs of an increasing viscosity as the number of day's progresses. This is due to the formation of insoluble waxes that form during oxidation.

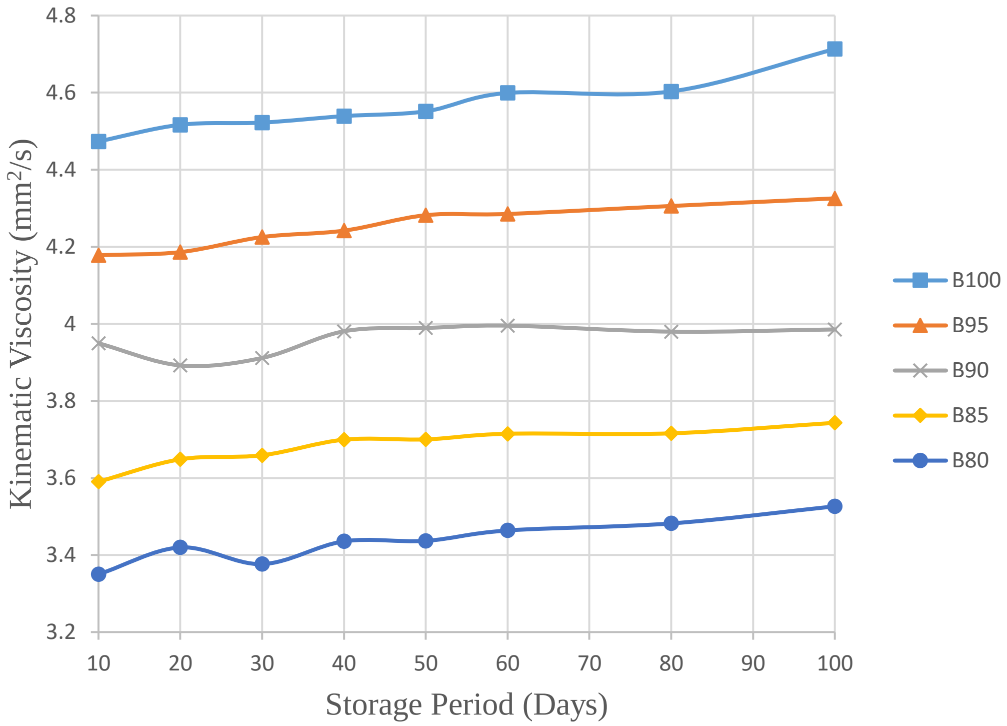

Figure 4.1: Kinematic Viscosity against Time

The graph above shows the trends of the samples. As discussed above, there is a general increase in viscosity. Samples B95 and B85 show a steady increase in viscosity without the values dipping lower. The general conclusion that can be drawn from this graph is that the storage period affects the kinematic viscosity of UCOME biodiesel. The sample needs to be constantly checked to see if it lies within the standards of the region.

Table 4.2 shows the values of the kinematic viscosity of the samples of blended biodiesel stored at 40 ^{O}C in an oven. This was done to study the effect of temperature storage on kinematic viscosity.

Table 4.2: Kinematic Viscosity Values for Samples Stored in the Oven

UCOME STORED AT 40 ^{O}C					
	Viscosity in mm^2/s				
Time (Days)	**B100**	**B95**	**B90**	**B85**	**B80**
10	4.45	4.1542	3.8974	3.5804	3.3332
20	4.5681	4.2087	3.9283	3.7053	3.3983
30	4.506	4.2165	3.9565	3.6698	3.4153
40	4.5687	4.2265	3.9607	3.7221	3.456
50	4.5765	4.2615	3.9882	3.7459	3.4756
60	4.6095	4.2716	4.0274	3.7607	3.4801
80	4.6515	4.2939	4.0897	3.7636	3.4948
100	4.7031	4.3523	4.1372	3.8010	3.5136
MEAN	4.5791	4.2481	3.9981	3.7186	3.4458
SD	0.0790	0.0603	0.0817	0.0686	0.0597

The corresponding graph is shown in Figure 4.2. Take note of the amount of kerosene.

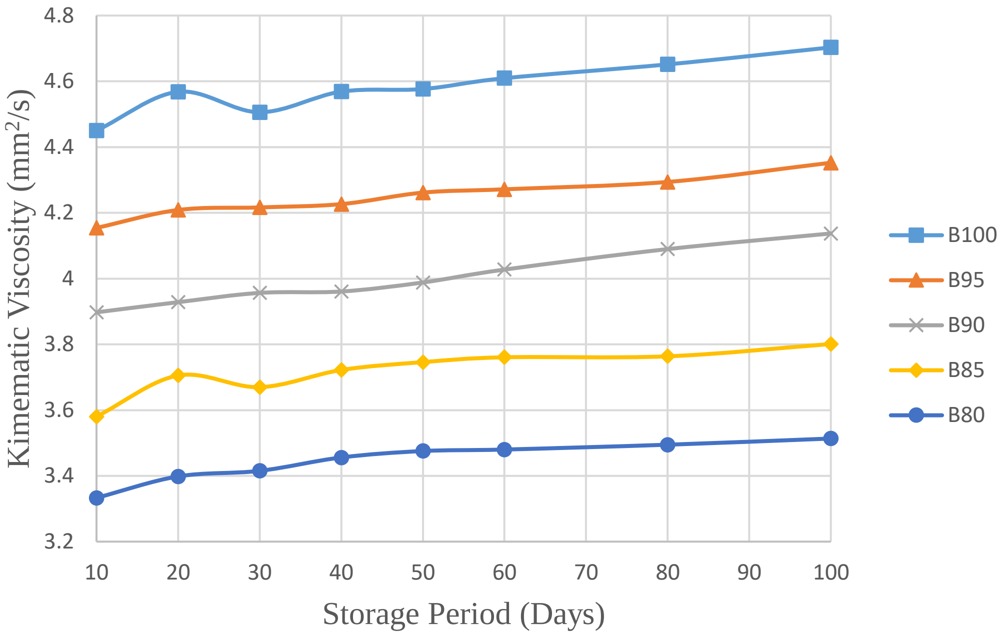

Figure 4.2: Kinematic Viscosity of Samples kept at 40 ^{O}C against Time

Figure 4.2 shows the behaviour of the kinematic viscosity of the samples against time in days. There is a general increase in kinematic viscosity across all samples. B100 and B85 only show a small deviation after 30 days, however, they continue to follow a common trend.

The graphs as well show that the kinematic viscosity decreases with an increase in kerosene volume in each blend sample. The Following graphs show the samples of the blend compared with the identical ratio but stored in separate conditions.

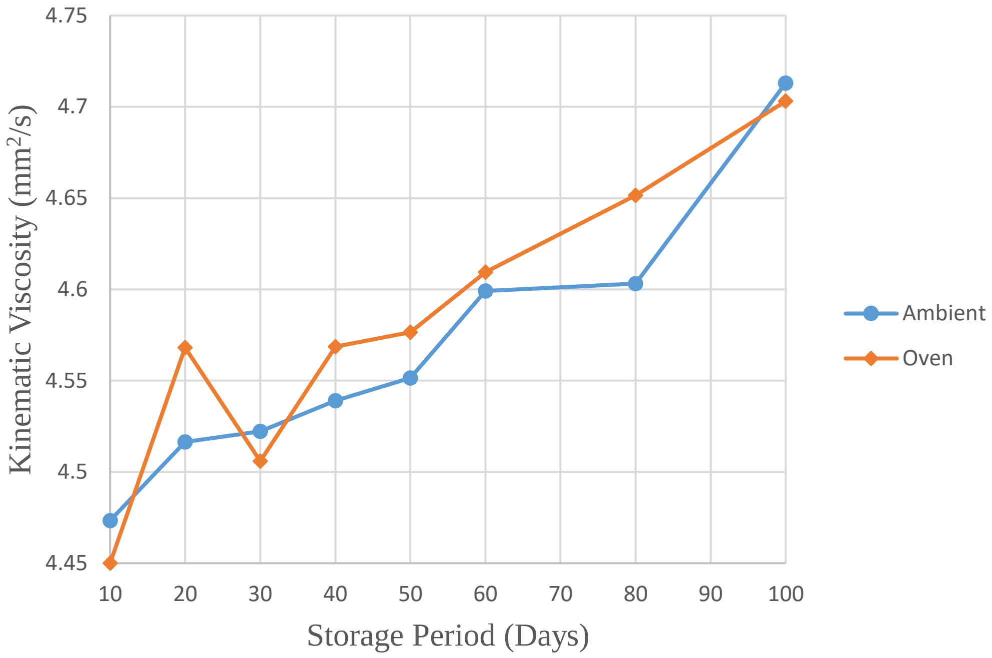

Figure 4.3: B100 Stored at 40 ^{O}C and Ambient Condition Samples: KV

The graph in Figure 4.3 shows that the ambient samples has a lower viscosity than that of the oven sample.

Further comparisons of the samples are shown in the following graphs.

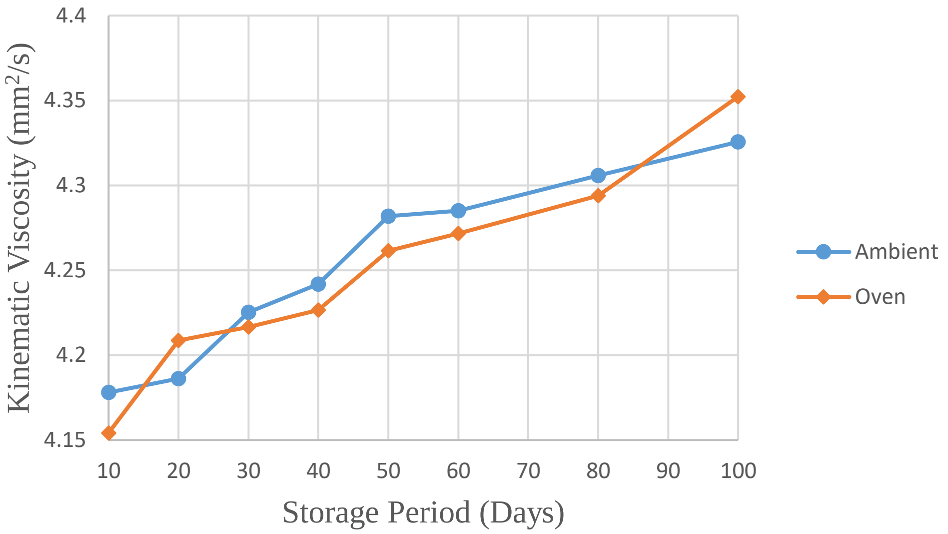

Figure 4.4: B95K5 Sored at 40 ^{O}C and Ambient Sample Comparison: KV

In Figure 4.4, the ambient sample has a higher viscosity generally. It does not follow expectations. Figure 4.5 shows that the ambient sample oscillates and it is clearly having a lower kinematic viscosity over a period of hundred days. This is in line with the expectations.

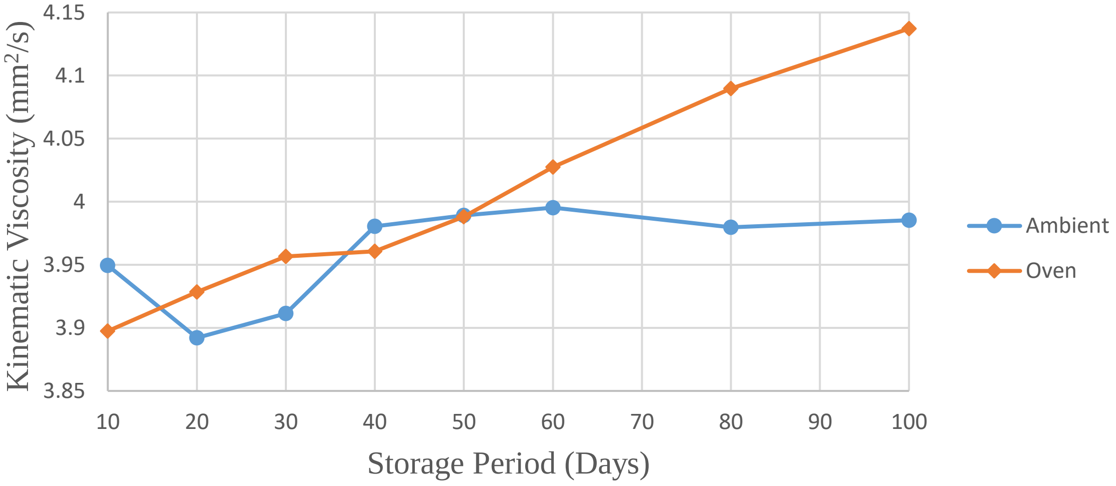

Figure 4.5: B95 Stored at 40 ^{O}C and Ambient Conditions Samples: KV

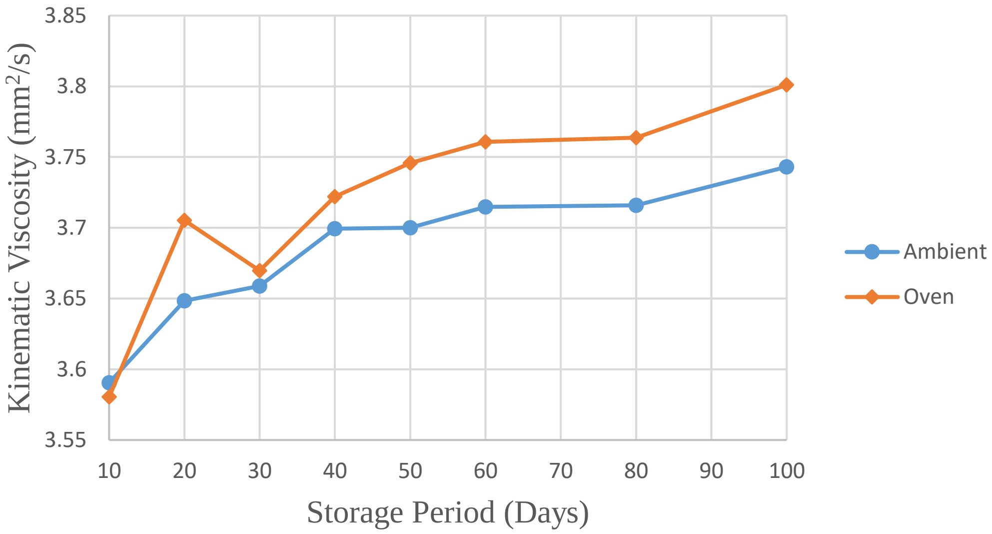

Figure 4.6: B85 Stored at 40 ^{O}C and Ambient Conditions Samples: KV

In this sample, Figure 4.6, we see that the oven sample has a higher viscosity in general. However, it starts lower and takes a dip on day 30. Figure 4.7 shows that the ambient sample has generally higher viscosity as expected.

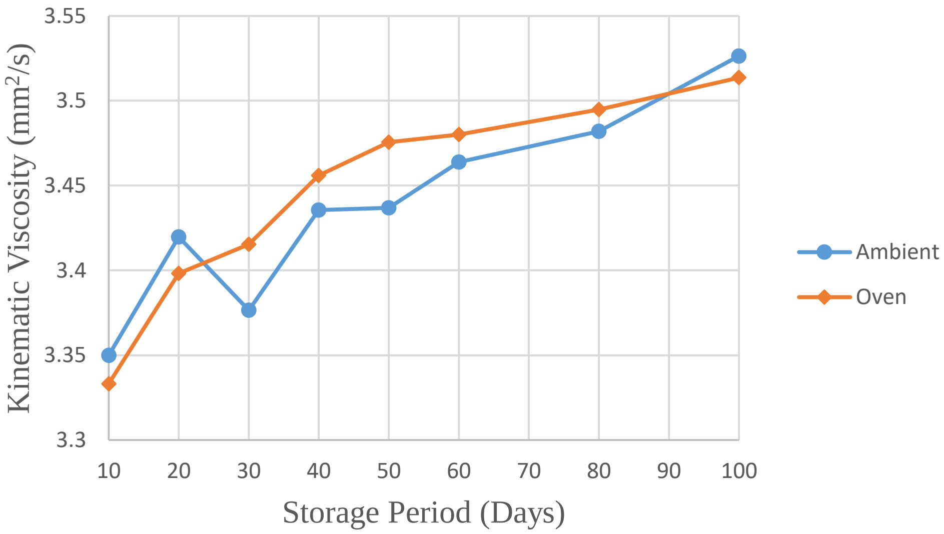

Figure 4.7: B80K20 Stored at 40 ^{O}C and Ambient Conditions Sample: KV

4.2 Effect of Storage Period and Method on Density

This section is focused on establishing the effect of storage time on density of the different blends of biodiesel samples used.

Table 4.3: Values for Density of Samples in Ambient Conditions

	UCOME STORED IN AMBIENT CONDITIONS				
		Density kg/m^3			
Time (Days)	**B100**	**B95**	**B90**	**B85**	**B80**
20	871.987	868.025	863.15	859.208	855.115
30	873.532	868.567	865.868	861.003	858.636
40	873.313	870.733	866.089	863.12	858.894
50	874.134	872.529	866.269	863.631	859.097
60	877.153	873.506	867.533	864.213	859.398
80	877.468	873.83	867.915	864.862	859.76
100	878.437	875.1128	869.2684	866.4500	860.2391
MEAN	875.145	871.7573	866.5842	863.2123	858.7341
SD	2.48905	2.7192	1.93695	2.425768	1.684304

The first measurement of the samples in Table 4.3 were recorded as day 20. The corresponding graph of the table above is shown in Figure 4.8.

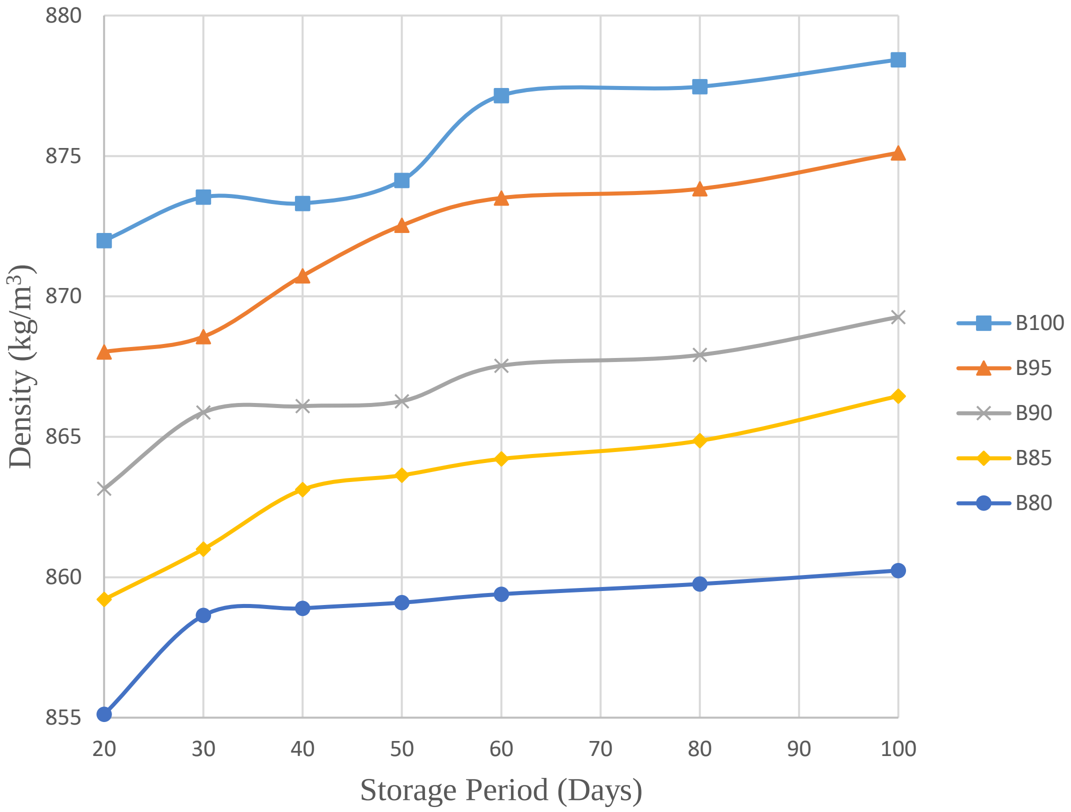

Figure 4.8: Ambient Samples Density Curves

From the graph, Figure 4.8, it is evident that the density of the samples generally increases with time.

The Table 4.4 shows the values of density of samples stored at 40 ^{O}C.

Table 4.4: Density Values for Samples Stored at 40 ^{O}C

	UCOME STORED AT 40^{O}C				
		Density kg/m^3			
Time (Days)	**B100**	**B95**	**B90**	**B85**	**B80**
20	873.522	868.637	865.276	861.956	857.583
30	873.582	869.76	866.029	861.455	857.693
40	873.973	869.82	866.079	862.518	858.345
50	874.886	871.195	866.52	863.16	859.188
60	876.09	870.844	867.654	863.651	859.79
80	877.514	873.201	868.446	864.524	861.194
100	878.0263	874.3222	868.2712	865.7374	861.6260
MEAN	875.370	871.111	866.896	863.2859	859.345
SD	1.8694	2.01537	1.22829	1.494639	1.61646

The density is expected to increase more steadily as these samples were subjected to stable temperatures. The increment of density may also be attributed to the formation of insoluble waxes that are produced during oxidation.

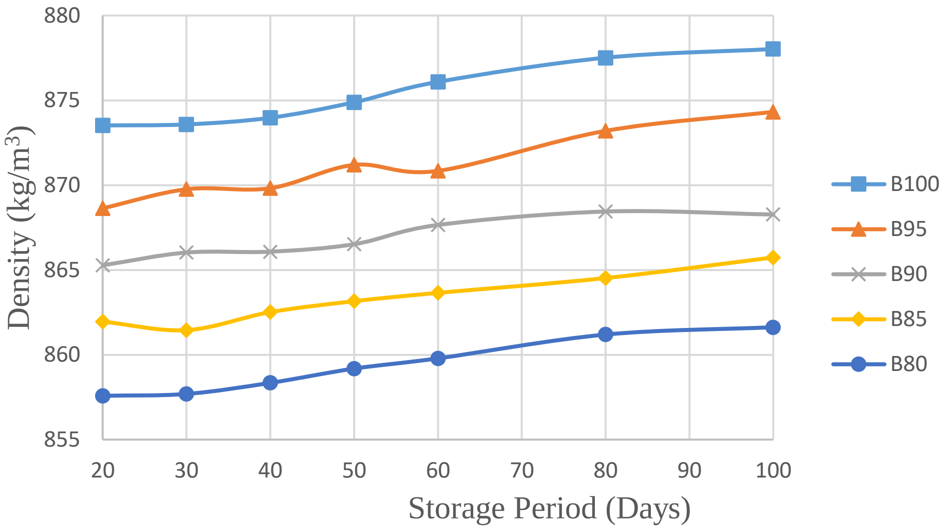

Figure 4.9: Density Values of Oven Samples

Figure 4.9 shows the behaviour of the density of the samples against time passed, in days. There is a general increase in density across all samples. B90 and B85 only show a small deviation, however, they continue to follow a common trend.

The graphs as well show that the density decreases with an increase in kerosene volume in each blend sample. The Following graphs show the samples of the blend compared with the identical ratio but stored in separate conditions.

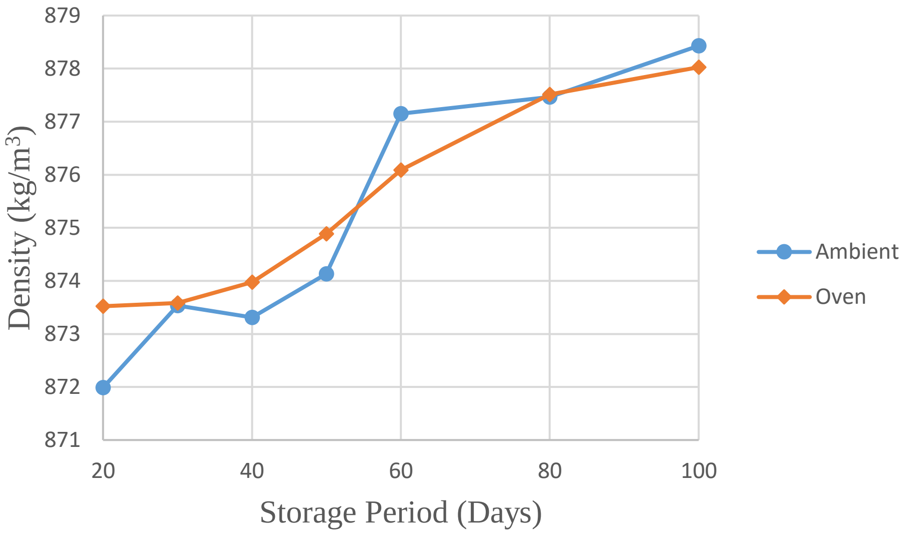

Figure 4.10: B100 Stored at 40^{O}C and Ambient Condition Sample: Density

The Figure 4.10 Shows samples of B100 stored in ambient and oven conditions. It is evident that the oven sample stored at 40 ^{O}C that the increase in density is uniform and almost linear. The ambient sample is subjected to different temperatures hence the haphazard growth. The same can be said about the sample in Figure 4.11.

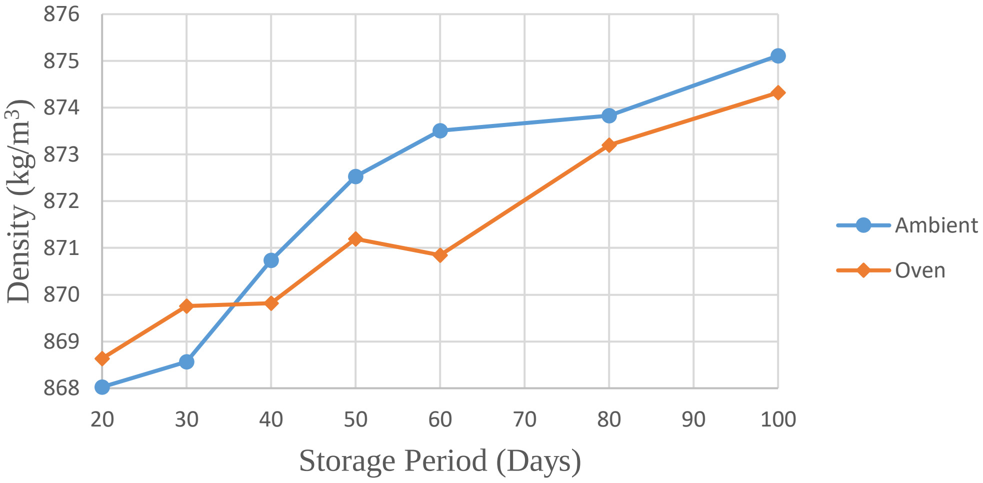

Figure 4.11: B95 Stored at 40 ^{O}C and Ambient Condition Sample: Density

The oven sample follows a pattern which can easily defined by the equation of a line. In this sample, the ambient sample is generally having a higher density value. The fluctuating temperatures have an effect on this particular property.

As expected, the sample shown in Figure 4.12, the oven sample has a higher viscosity over the period of time measured. However, it falls on day 100.

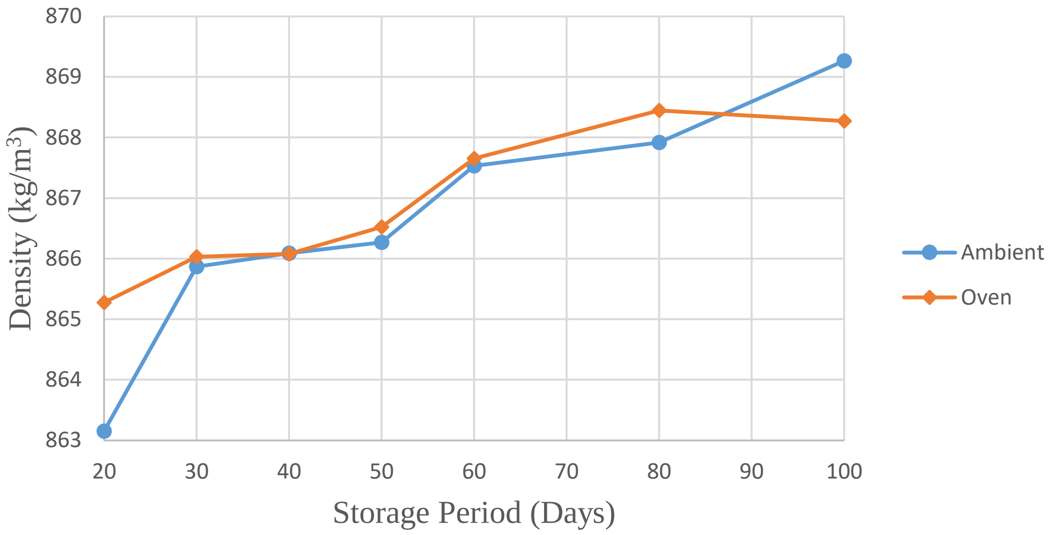

Figure 4.12: B90 K10 Oven and Ambient Sample Comparison for Density

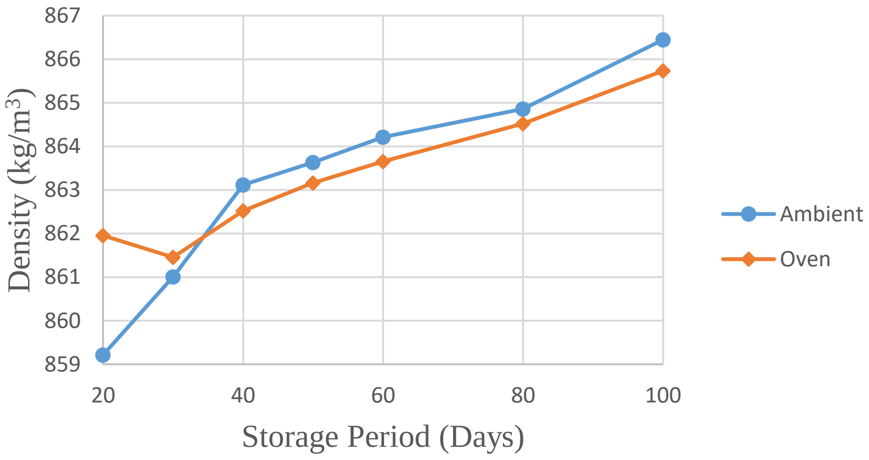

Figure 4.13: B90 Stored at 40 ^{O}C and Ambient Condition Sample: Density

In this particular sample, Figure 4.13, both samples grow steadily but, the start differs a bit. The oven sample starts of higher then falls below the sample in ambient conditions.

Figure 4.14 shows the B80K20 sample. The oven sample generally has an expectedly higher density value.

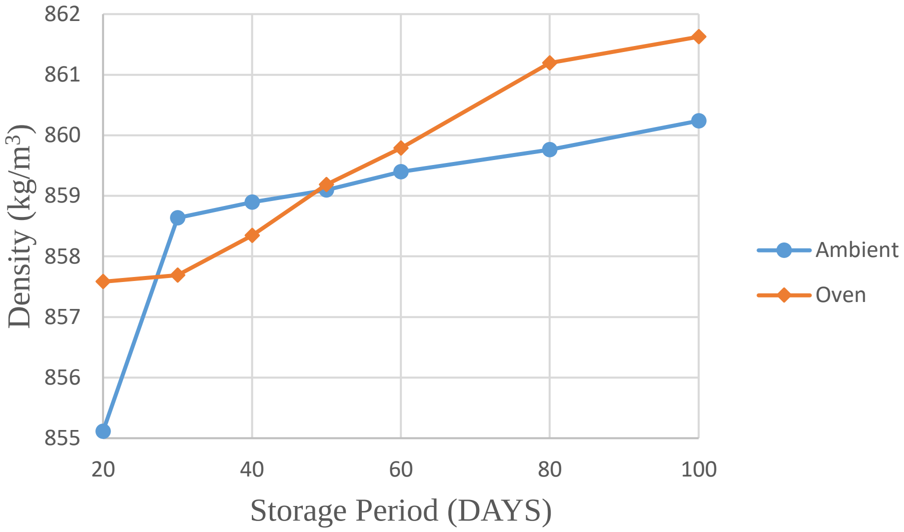

Figure 4.14: B80 Stored at 40 ^{O}C and Ambient Condition Sample: Density

4.3 Acid value and Oxidation Stability

These tests were done at Tubitak Marmara Research Centre in Gebze, Kocaeli Province, Turkey. They followed the EN 14104 standard for Acid Number and EN 14112 for Oxidation Stability. The following tables show the results of the tests.

The oxidation stability, Table 4.5 increased with an increase in kerosene percentage. However, the difference of the acid value seems to have reduced with the increase in kerosene amount, though the difference is small. With time progression, we see that the acid number increases due formation of more fatty acids. As expected from literature, the oxidation stability reduced considerably.

Table 4.5: Acid Number and Oxidation Stability Values for B90 K10

	B90K10 Sample			
Analysis Test Units	**Standard**	**Specific Limits**	**Results (Day 30)**	**Results (Day 90)**
Total Acid Number (mgKOH/g)	EN14104	0.5	0.43	1.04*
Oxidation Stability (110 ^{O}C)(Hours)	EN14112	3	2.23	1.83

* ASTM D 664 was used.

The oxidation stability is measured in hours. The sample with the data in Table 4.5 does not meet the regular standards. It is below with a small margin at day 30, and at day 90, it has gone below 2 hours. The acid number more than doubles over a period of 60 days.

The oxidation stability, Table 4.6, increased with an increase in kerosene percentage. However, the difference of the acid value seems to have reduced with the increase in kerosene amount, though the difference is small. With time progression, we see that the acid number increases due formation of more fatty acids. As expected from literature, the oxidation stability reduced considerably.

Table 4.6: Acid Number and Oxidation Stability for B80K20

	B80 K20 Sample			
Analysis Test Units	**Standard**	**Specific Limits**	**Results (Day 30)**	**Results (Day 90)**
Total Acid Number (mgKOH/g)	EN14104	-	0.41	0.94*
Oxidation Stability (110 ^{O}C)(Hours)	EN14112	-	3.38	2.20

* ASTM D 664 was used.

The oxidation stability is measured in hours. The sample with the data in Table 4.6 does meet the regular standards at day 30, but at day 90, it has gone below 3 hours. The acid number more than doubles over a period of 60 days.

In comparison, the B80K20 exhibited better quality as compared to the B90K10.

4.4 Cold Flow Properties of UCOME

B90 and B80 were used for this experiment. The cold flow properties, CP and PP, were determined visually following the respective standards. The visually obtained values were compared to the values derived from the cooling curve analysis.

Table 4.7 shows the values of the experimentally obtained CP and PP.

Table 4.7: B90 K10 Experimental Cold Flow Property Values

Sample	Property	Standard	Value (^{O}C) (Day 30)	Value (^{O}C) (Day 90)
Ambient	CP	ASTM D2500	8.4	8.0
	PP	ASTM D97-05	5.4	5.8
Oven	CP	ASTM D2500	7.1	8.5
	PP	ASTM D97-05	4.3	5.9

The accuracy of the experiment is +/- 1.5 ^{O}C. The value of the CP of the ambient sample differs from that of the oven sample. It dropped to 7.1 ^{O}C from 8.4 ^{O}C. The PP also followed suit and dropped to 4.3 ^{O}C from 5.4 ^{O}C. The storage conditions had an effect on the oven samples. Table 4.8 shows the experimental cold flow properties of the B80K20 sample.

Table 4.8: B80K20 Experimental Cold Flow Property Values

Sample	Property	Standard	Value (^{O}C) (Day 30)	Value (^{O}C) (Day 90)
Ambient	CP	ASTM D2500	6.9	-
	PP	ASTM D97-05	2.4	-
Oven	CP	ASTM D2500	6.5	4.1
	PP	ASTM D97-05	2.3	2.2

There is a difference of 0.4 ^{O}C in the in CP of the ambient and oven samples. This is within the range of +/- 1.5 ^{O}C margin of error, hence can be said to have the same value. The ambient having the higher value of 6.9 ^{O}C. The PP of the oven is higher at 2.5 ^{O}C as compared to 2.4 ^{O}C of the ambient sample.

The kinematic viscosity and density of the samples were measured before and after the process of cooling from 65 ^{O}C. This was done to establish the immediate effect of heating and cooling of the fuel samples. Table 4.9 below shows the recorded values.

Table 4.9: Kinematic Viscosity and Density Before and After Cooling Curve Analysis

Sample	**Kinematic Viscosity Before (mm^2/s)**	**Kinematic Viscosity After (mm^2/s)**	**Density Before (kg/m^3)**	**Density After (kg/m^3)**
B90 K10 Ambient	3.9471	3.9706	862.0717	866.8813
B90 K10 Oven	3.9410	4.0225	865.1324	874.7913
B80 K20 Ambient	3.4200	3.4574	857.1031	860.0048
B80 K20 Oven	3.4756	3.4972	863.3437	870.6972

From Table 4.9, it is clear that there is a general increment of density and kinematic viscosity of the samples after the cooling curve analysis. This will affect the fuel quality especially ignition point. The physical properties are affected and the long chain hydrocarbons end up densely packed close to each other hence the increase in density.

4.5 Thermal Analysis

From the cooling curve, the first derivative of the curve is derived. This is the cooling rate, which is used in conjunction with the cooling curve to graphically determine the CP and PP of the samples. The first derivative is also used in calculating the solid fraction of the sample during the freezing of the biodiesel samples. Figure 4.5 shows the graph of rate vs the difference of the of the sample and bath temperature.

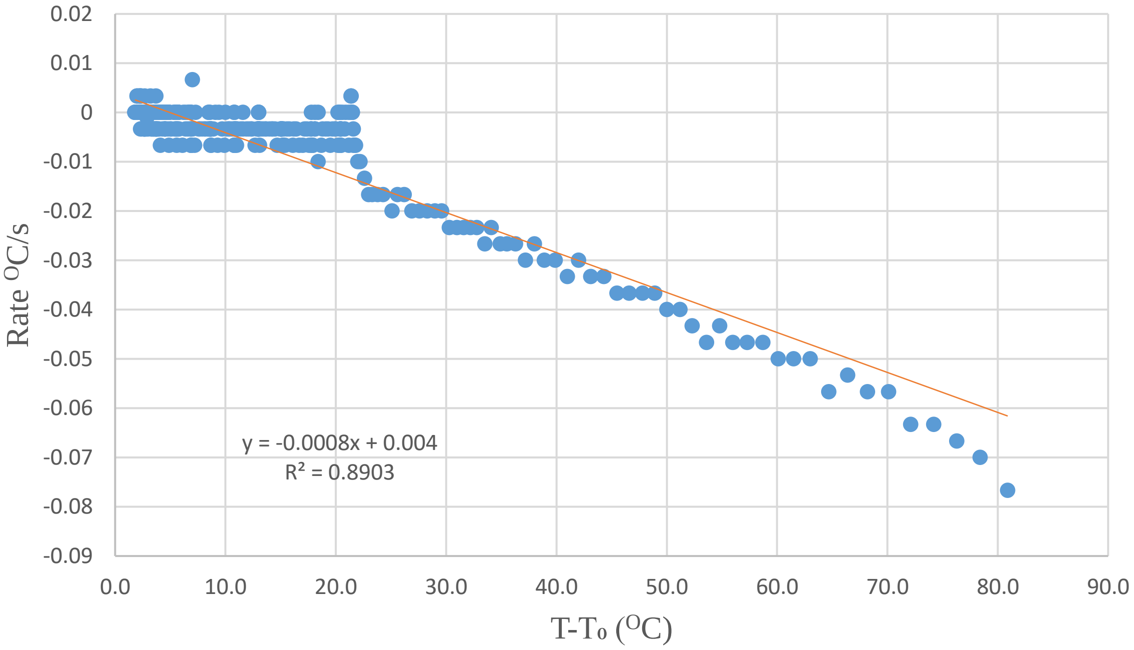

Figure 4.15: Rate vs Sample-Bath Temperature Difference for B90 K10 Ambient

Using the equation of y shown in Figure 4.15, we derive the Newtonian Zero Line, Z_n.

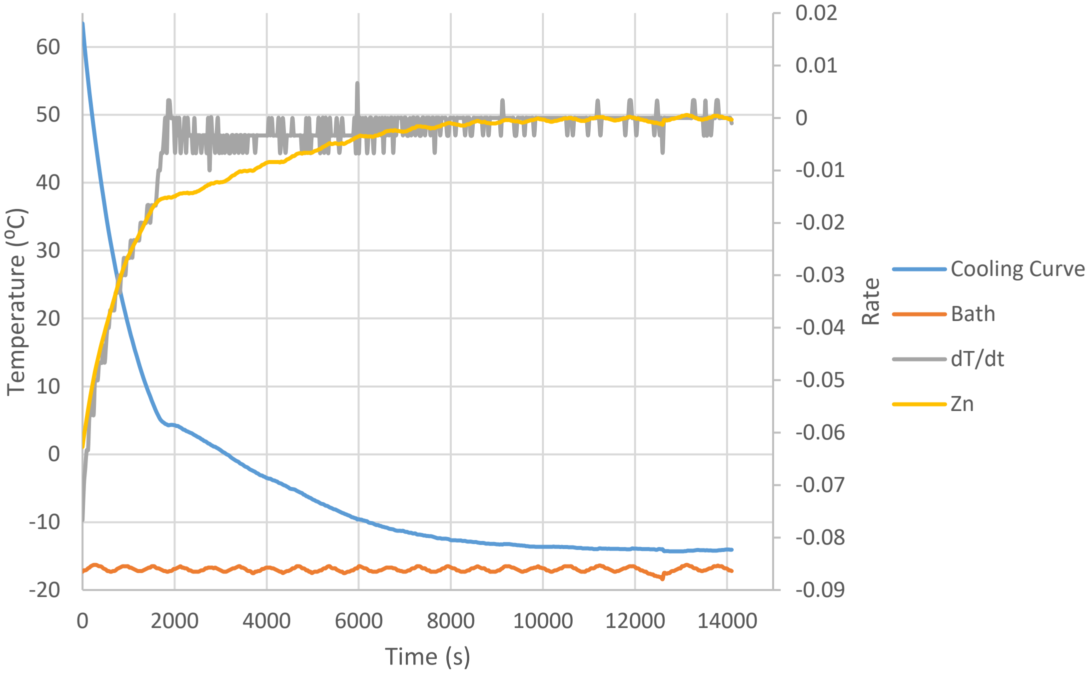

Figure 4.16: CCA for B90 K10 Ambient.

The graph in Figure 4.15 shows the equation of the line used to produce the Newtonian Zero curve. This curve is used in conjunction with that of the rate against time to calculate the solid fraction in the two phase liquid state, that is, the solid-liquid phase. Figure 4.16 shows a compound graph which has, the Cooling Curve, Bath curve, Rate and the Newtonian Zero curve respectively. From this data, the solid fraction during freezing can be determined.

Equation 4.1 shows how to calculate the solid fraction using the graph in figure 4.16.

$$(Fs)n = \frac{A_n}{A_{Total}} \tag{4.1}$$

Where A_n is the area between the Rate graph and the zero line, Zn. This is expressed by the trapezoidal rule in Equation 4.2

$$An = \sum_{i=1}^{n} [\frac{1}{2}(T'_i + T'_{i+1}) - \frac{1}{2}(Z_i + Z_{i+1})] \times (t_{i+1} - t_i) \tag{4.2}$$

Where T'_i is the point i on the rate graph, Z_i is the point i on the Zn graph and t_i is the corresponding temperature of both points.

Equation 4.3 shows the calculation of the total area, which is basically a cumulative sum of all cumulating A_n points.

$$A_{Total} = \sum_{i=1}^{n} A_n \tag{4.3}$$

Figure 4.17 shows the corresponding solid fraction graph.

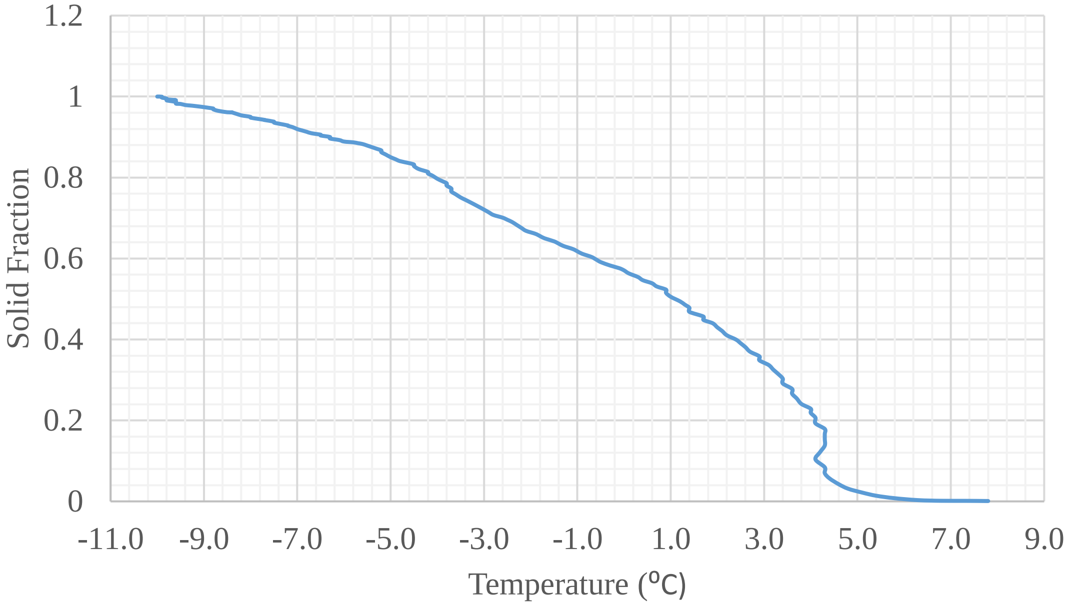

Figure 4.17: Solid Fraction for B90K10 Sample in Ambient Conditions

Figure 4.18 shows the graph used to generate the Zn equation for the B90 oven sample.

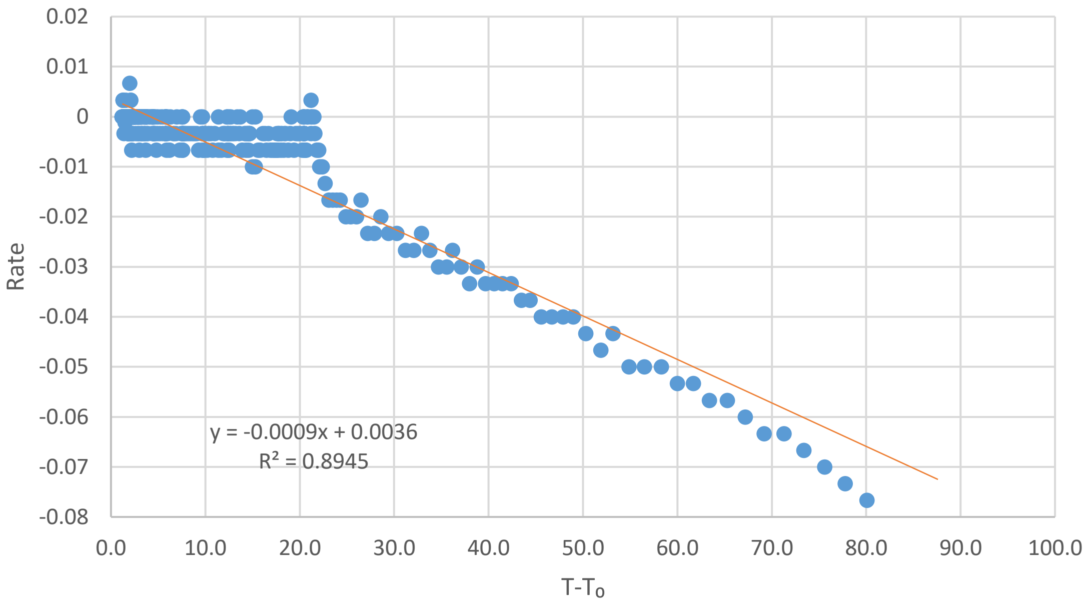

Figure 4.18: Rate vs Sample-Bath Temperature for B90 Oven

The points in the two phase region, the space at which the majority of the points deviates from the trend line, are not used in the equation generation. This is because the theory assumes that there is no latent heat that is lost during solidification.

The corresponding compound graph is in Figure 4.19

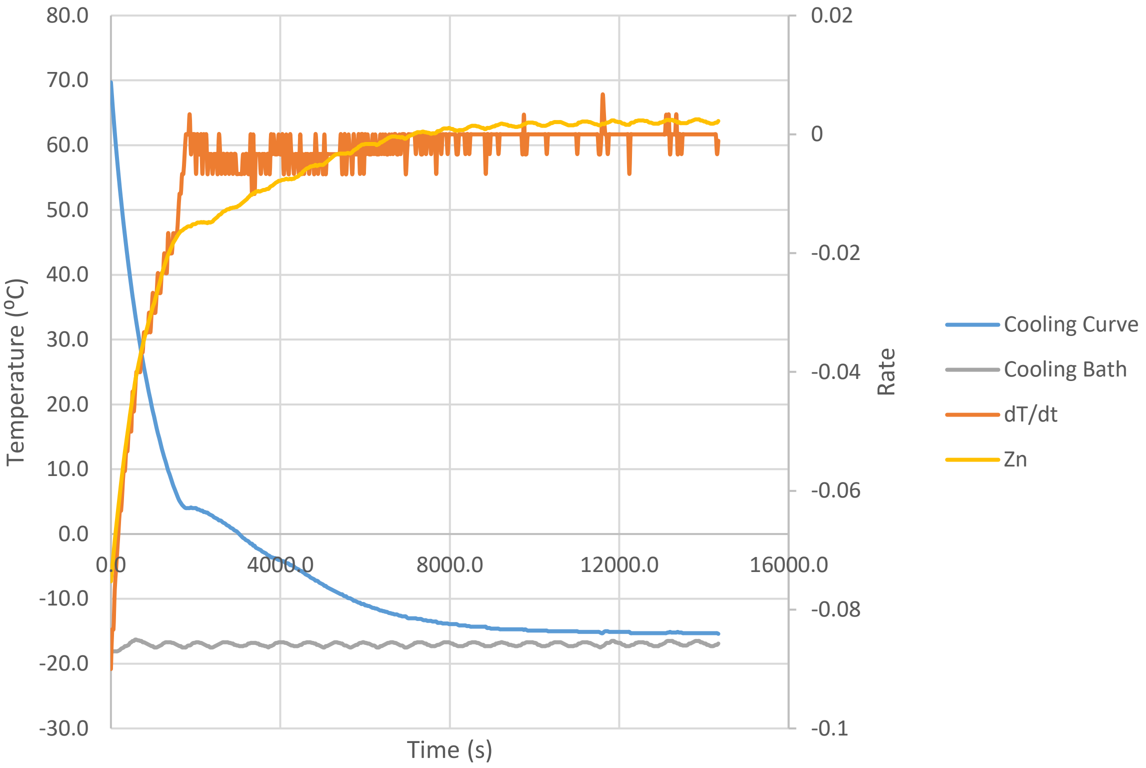

Figure 4.19: CCA for B90 K10 Oven Sample

From Figure 4.16 and 4.19, we see that the Newtonian Zero curve and the Rate are moving combined together up to the point where solidification starts. This is the two phase, solid-liquid phase. The area in between the two curves has a direct relation to the value of the latent heat of solidification. The graphs almost join after the solidification and continue in the solid phase.

Figure 4.20 shows the graph of the corresponding solid fraction.

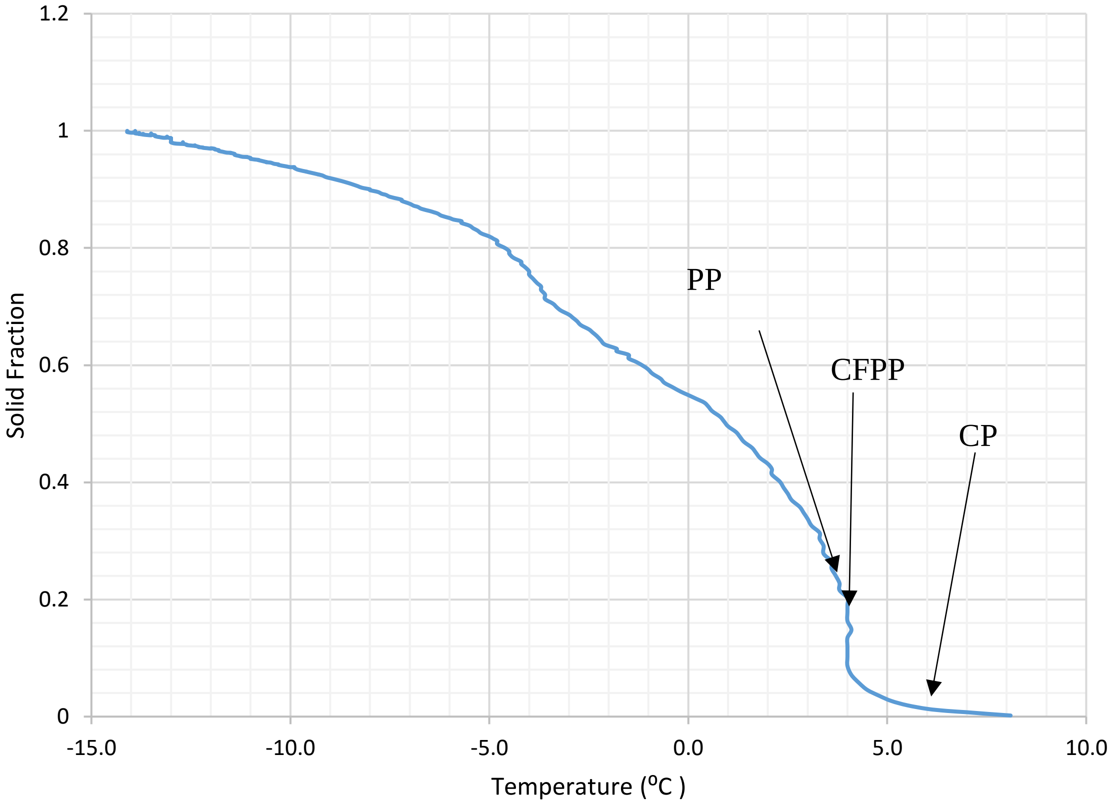

Figure 4.20: Solid Fraction for B90K10 sample stored at 40 ^{O}C

From the graph, Figure 4.20, it is clear that the solid matter will be enough to plug a fuel filter before 30% of the sample has solidified. The cold flow property temperature values are indicated. This shows how temperature sensitive the sample is. It seizes to flow properly with almost 30% of the sample being solid.

The same approach for B80 K20 sample was done. The samples were all left to cool or a period of 4 hours and produced almost similar graphs. The values differ and this was contributed by the amount of kerosene in the samples mainly and, to a certain extent, the method of storage.

Figure 4.21 shows the graph used to generate the Zn equation for the B80 ambient sample.

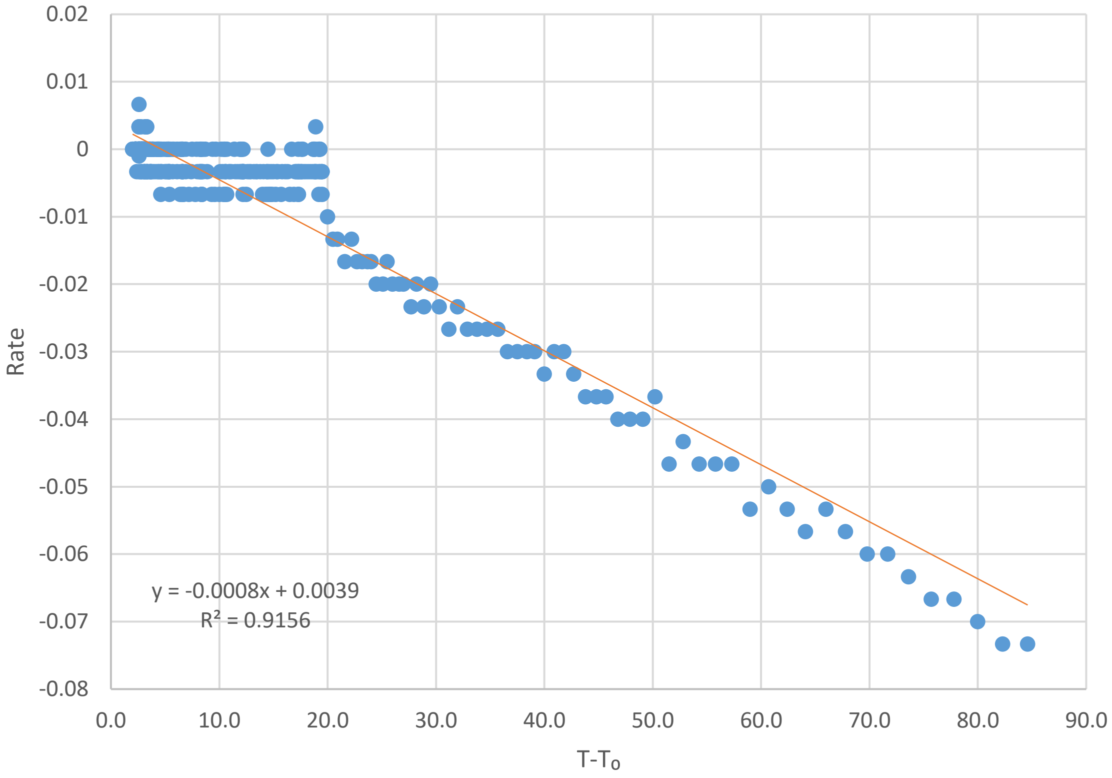

Figure 4.21: Rate vs Sample-Bath Temperature Difference for B80 K20 Ambient

The points in the two phase region, the space at which the majority of the points deviates from the trend line, are not used in the equation generation. This is because the theory assumes that there is no latent heat that is lost during solidification.

The corresponding compound graph is in Figure 4.22.

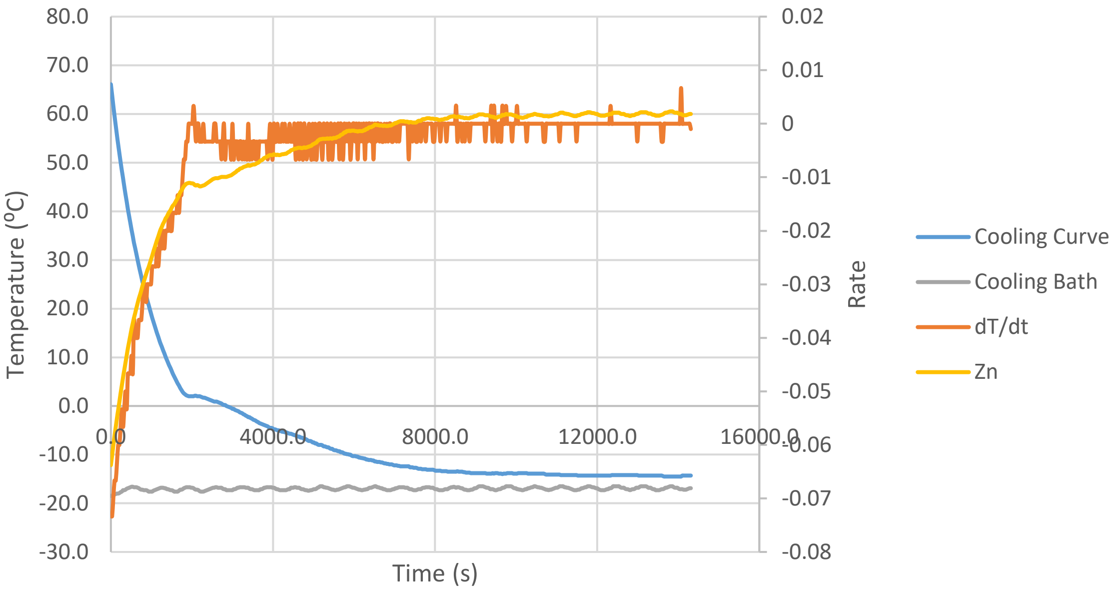

Figure 4.22: CCA for B80 K20 Ambient.

From Figure 4.22, the Newtonian Zero curve and the Rate are moving combined together up to the point where solidification starts. This is the two phase, solid-liquid phase. The area in between the two curves has a direct relation to the value of the latent heat of solidification.

Figure 2.23 shows the corresponding solid fraction graph of the B80K20 sample stored at ambient conditions.

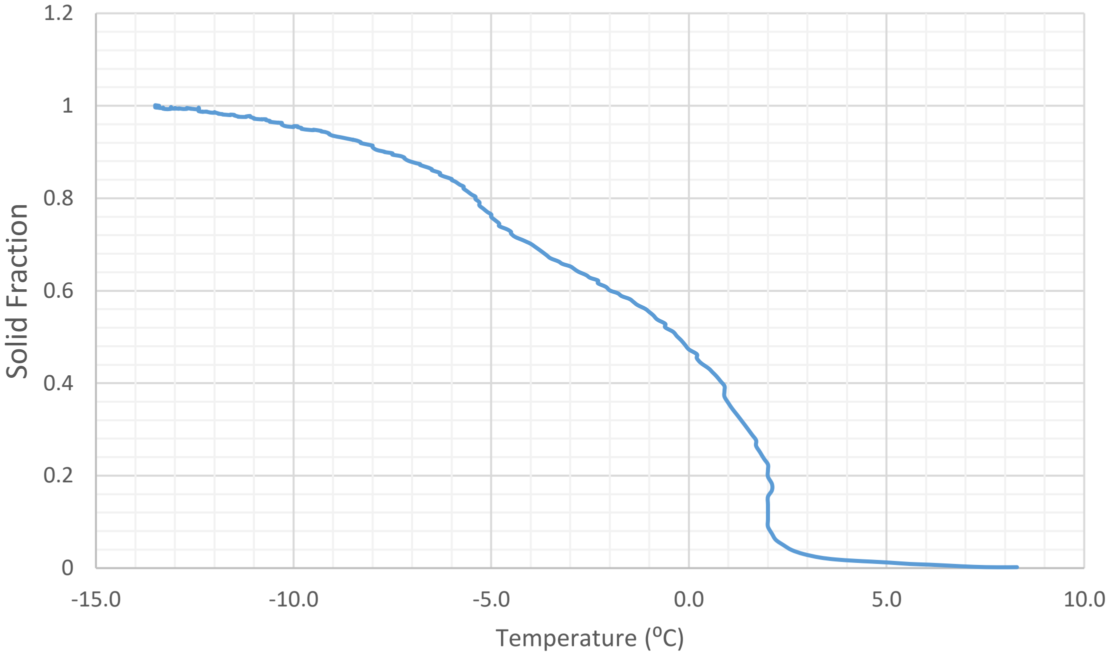

Figure 4.23: Solid Fraction for B80K20 Ambient

From Figure 4.23, it is clear that the sample reaches the pour point before it reaches 30% solidification. This is more evidence of it being cold flow intolerant. However, it has better properties in terms of temperature as compared to the B90K10 sample.

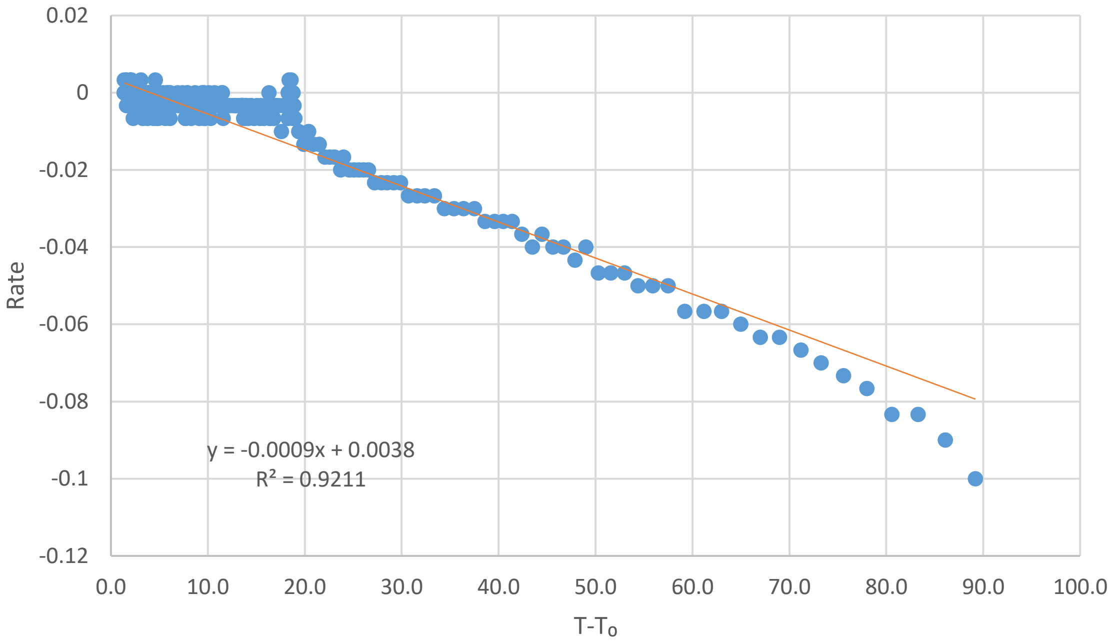

Figure 4.24: Rate vs Sample-Bath Temperature for B80 K20 Oven

The points in the two phase region, Figure 4.24, the space at which the majority of the points deviates from the trend line, are not used in the equation generation. This is because the theory assumes that there is no latent heat that is lost during solidification.

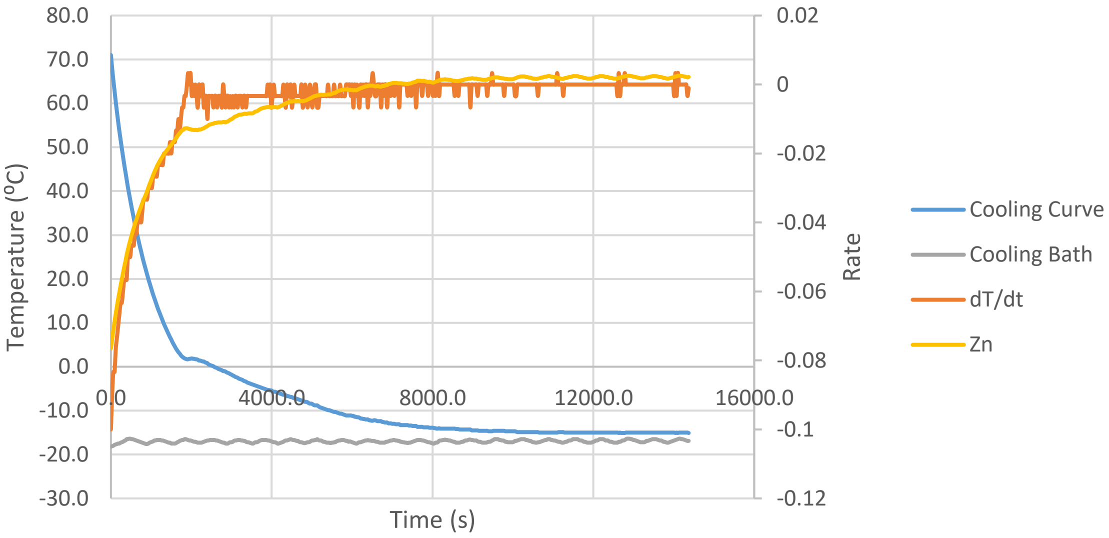

Figure 4.25: CCA for B80K20 Oven Sample.

From Figure 4.25, the Newtonian Zero curve and the Rate are moving combined together up to the point where solidification starts. This is the two phase, solid-liquid phase. The area in between the two curves has a direct relation to the value of the latent heat of solidification. Figure 4.26 shows the solid fraction graph for the oven sample.

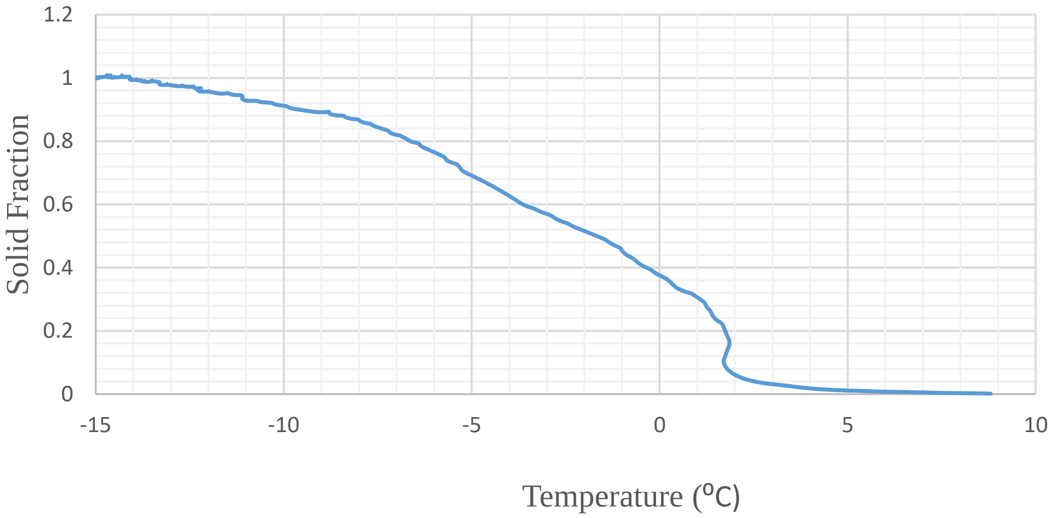

Figure 4.26: Solid Fraction for B80K20 Oven Sample

Table 4.10 shows a comparison of the graph values as compared to the experimental values.

Table 4.10: Comparison of Cold Flow Properties with Different Methods

Sample	**ASTMD 2500 CP (^OC)**	**ASTMD 97-05 PP (^OC)**	**CCA CP (^OC)**	**CCA PP (^OC)**	**Fs CP (^OC)**	**Fs PP (^OC)**	**Fs CFPP (^OC)**
B90 K10 Ambient	8.4	5.4	6.4	4.0	5.8	4.1	4.3
B90 K10 Oven	7.1	4.3	6.0	3.8	7.5	3.8	4.0
B80 K20 Ambient	6.9	2.4	5.1	1.7	6.1	1.9	2.0
B80 K20 Oven	6.5	2.3	4.1	1.4	7.0	1.6	1.9

From Table 4.10 above, we see that the values from the graph are lower in every property. However, the difference can be attributed to poor eyesight or error in judgement. There is a 2 degree difference in the ambient sample of B90 on the CP, with a 1.4 degree difference on the PP. The value of the properties decrease with an increase kerosene percentage. The storage method has an effect to the cold flow properties. The values of the CP and PP of the oven samples are lower than that their identical ambient doubles. The solid fraction (Fs) values also offer better insights to the properties. The temperature values for cold filter plugging point are also found on the graph. Table 4.11 shows the sample solid fractions at the corresponding cold flow properties.

Table 4.11: Solid Fraction at Cold Flow Properties

Sample	Fs at CP	Fs at CFPP	Fs at PP
B90K10 Ambient	0.008	0.057-0.179	0.193
B90K10 Oven	0.005	0.071-0.203	0.216
B80K20 Ambient	0.007	0.090-0.224	0.237
B80K20 Oven	0.005	0.061-0.155	0.169

The solid fraction of the B80K20 sample shows a more consistent trend. The oven sample has lower amount of solid fraction throughout the properties. However, for the B90 sample, the fraction at the cloud point of the oven sample is lower than that of the ambient sample. For pour point and the CFPP, the oven sample is higher.

CHAPTER 5

CONCLUSIONS AND RECOMMENDATIONS

From the work completed in this research, a concise conclusion was drawn. Recommendations provided were based upon the success of the experiments conducted by the researcher. The samples were studied in the Mechanical Engineering Department Laboratory of Near East University. A strict adherence to the ASTM and EN standards was done. For CP and PP, ASTM D2500 and ASTM D 97-05 were followed.

5.1 Conclusions

The researcher concluded that:

- The kinematic viscosity and density of the all UCOME samples increase with the storage period increment.
- The kinematic viscosity and density of the oven samples have a steady increment as compared to the samples stored in ambient conditions. This is because of the temperature flatulence in the ambient conditions.
- An increase in kerosene percentage has an effect on both the kinematic viscosity and density. The values reduced with the increment of the amount of kerosene.
- The thermal analysis was useful in determining the fraction of solid in the two phase stage during the solidification of the samples. It also provides information on cold flow properties and their corresponding solid fractions.
- Thermal analysis is accurate and simple in determining the cold flow properties. The experimental method is more difficult.
- Rapid heating and cooling of the sample has an immediate effect on the samples. This is evidenced by the change in the viscosity and density before and after the cooling curve analysis.

- The storage method has an effect on the cold flow properties and affects also the differences obtained.
- Kerosene is a very good additive to biodiesel. This is because it affects the high performance and efficiency of the fuel to a very less extent. It also improves its cold flow properties
- UCOME is highly sensitive to temperature and cannot withstand cold temperatures under 7 ^{O}C. This is evidenced by the high cold flow properties. The solid fraction graphs show us that at 30% solid fraction, the sample would have reached its pour point.

5.2 Recommendations

The success of the work has led to more questions than not. The researcher deemed it necessary to recommend the following

- To store the same samples in a constant temperature of 10 ^{O}C to study how it will perform in regions with similar conditions.
- To study further mixtures of the blend, up to B50 K50 at the same conditions. This is because of the successful use of kerosene as a blending additive.
- To study a three way blend of UCOME, Euro-Diesel and Kerosene in the same conditions so as to establish the effect on the cold flow properties.
- To study the effect of storage materials, such as HDPE and metal containers, in the same conditions so as to establish the effect on the chemical and physical properties.
- To study the Fourier Thermal Analysis for the same samples.

REFERENCES

Argawal, AK.,. (2007). Biofuels (alcohols and biodiesel) applications as fuels in internal combustion engines. *Progr Energy Combust Sci*, 233–271.

Aydin, H., Bayindir, H., & Ilkilic, C. (2010). Emissions From an Engine Fueled With Biodiesel Kerosene Blends. *Energy Sources*, 130-137.

Barlow, J., & Stefanescu, D. (1997). Computer-aided cooling curve analysis revisited. *AFS Trans*, 349–354.

Canon, M. R., & Fenske, M. R. (1938). Viscosity measurement. *Industrial and Engineering chemistry. Analytical Edition. ANCHA*, *10*, 297-298.

Chu, J., Xu, X., & Zhang, Y. (2013). Production and properties of biodiesel produced from Amygdalus pedunculata Pall. *Bioresource Technology 134*, 374–376.

Corach, J., Colman, M., Sorichettic, P.A., & Romano, S.D. (2017). Kinematic viscosity of soybean biodiesel and diesel fossil fuel blends: Estimation from permittivity and temperature. *Fuel Volume 207*, 488-492.

Demirbas, A. (2005). Biodiesel production from vegetable oils via catalytic and non-catalytic supercritical methanol transesterification methods. *Progr Energy Combust Sci*, 466-487.

Demirbas, A. (2008). Relationships derived from physical properties of vegetable oil and biodiesel fuels . *Fuel 87*, 1743–1748.

Emadi, D., & Whiting, L. (2002). Determination of Solidification Characteristics of Al-Si Alloys by Thermal Analysis. *AFS Transactions, Vol. 110*, 285-296.

Evcil, A., Al-Shanableh, F., & Savas, M. A. (2018). Variation of solid fraction with cold flow properties of biodiesel produced from waste frying oil. *Fuel*, 522-527.

Ferrari, R., Oliveira, V., & Scabio, A. (2005). Oxidative stability of biodiesel from soybean oil fatty acid ethyl esters. *Sci. Agric. 62*, 291–295.

Fras, E., Kapturkiewicz, W., Burbielko, A., & Lopez, H. (1993). A new concept in thermal analysis of castings. *AFS Trans vol. 101*, 505–511.

Fox, R. W., McDonald, A. T., Pritchard, P. J. (2012). *Fluid Mechanics*. Asia: Wiley and Sons

Gabroski, M.S & McCormick, RL. (1998). Combustion of fat and vegetable oil derived fuels in diesel engines. *Progr Energy Combust Sci*, 125–64.

Giakoumis, E.G. (2013). A statistical investigation of biodiesel physical and chemical properties, and their correlation with the degree of unsaturation. *Renewable Energy*, 858-878.

Giakoumis, E. G., & Sarakatsanis, C. K. (2018). Estimation of biodiesel cetane number, density, kinematic viscosity and heating values from its fatty acid weight composition. *Fuel 222 (2018) Science direct.*, 574–585.

Giakoumis, E., Rakopoulos, C., Dimaratos, A., & Rakopoulos, D. (2012). Exhaust emissions of diesel engines operating under transient conditions with biodiesel fuel blends. *Progr Energy Combust Sci*, 691-715.

Hasan, A., Mashkour, M. A., & Mohammed, A. A. (2016). Experimental study of kerosene additive to waste oil biodiesel for using as alternative diesel fuel. *International Journal of Engineering Research and Modern Education (IJERME)*, 246-250.

Hoekman, S., Broch, A., Robbins, C., Ceniceros, E., & M. Natarajan. (2012). Review of biodiesel composition, properties and specifications. *Renew. Sust. Energ. Rev. 16*, 143–169.

Kierkus, W., & J. H. Sokolowski. (1999). Recent Advances in CCA: A New Method of Determining 'Baseline' Equation. *AFS Transactions v66*, 161-167.

Knothe, G. (2006). Analyzing biodiesel: standards and other methods. *American Oil Chemists' Society (AOCS)*, 823–833.

Krisnangkura, K., Yimsuwan, T., & Pairintra, R. (2006). An empirical approach in predicting biodiesel viscosity at various temperatures. *Fuel, Volume 85,*, 107-113.

Kumar, D., Singh, B., Banerjee, A., & Chatterjee, S. (2018). Cement wastes as transesterification catalysts for the production of biodiesel from Karanja oil. *Journal of Cleaner Production*, 26-34.

Loong, T. C., & Idris, A. (2017). One step transesterification of biodiesel production using simultaneous cooling and microwave heating. *Journal of Cleaner Production*, 57-62.

McCormick, R. L., Graboski, M. S., Alleman, T. L., Herring, A. M., & Tyson, K. S. (2001). Impact of Biodiesel Source Material and Chemical Structure on Emissions of Criteria Pollutants from a Heavy-Duty Engine. *Environmental Science and Technology*, 1742-1747.

Meiraa, M., Quintellaa, C. M., Tanajuraa, A. d., Silvaa, H. R., Fernando, J. D., Netoc, P. R., . . . Nascimento, L. L. (2011). Determination of the oxidation stability of biodiesel and oils by spectrofluorimetry and multivariate calibration . *Talanta 85*, 430-434.

National Biodiesel Board. (2014). *Biodiesel Cold Flow Basics 2014; Information for Petroleum Distributors, Blenders, and End-Users on Issues Affecting Biodiesel in the Winter Months.* National Biodiesel Board.

National Biodiesel Board. (2018, March 31). *Biodiesel Americas Advanced Biofuels*. Retrieved from http://www.biodiesel.org

Olah, G., Goeppert, A., & Prakash, G. (2006). *Beyond Oil and Gas: The Methanol Economy.* John Wiley & Sons.

Oxford. (2018, April 4). *Oxford living Dictionaries*. Retrieved from https://en.oxforddictionaries.com/definition/non-renewable

Paulik, F., Paulik, J., & Erdey, L. (1966). Derivatography A complex method in thermal analysis. *Talanta 13,* 1405-1430.

Pratas, M. J., Freitas, S., Oliveira, M. B., Monteiro, S. C., Lima, A. S., & Coutinho, J. (2010). Densities and Viscosities of fatty acid methyl and ethyl esters. . *Journal of Chemical and Engineering Data, 55(4),*, 83–90.

Saint clair systems norcross. (2018, April 11). *Temperature and Viscosity Control.* Retrieved from Temperature and Viscosity Control.: https://blog.viscosity.com/blog/6-different-types-of-viscometers-how-they-work

Sidjabat, O. (2013). The characteristics of a mixture of kerosene and biodiesel as a substituted diesel fuel. *Scientific Contributions Oils and Gas Vol 36 No.1,* 37-44.

Soares, S., Lima, M. J., & Rocha, F. R. (2017). A spot test for iodine value determination in biodiesel based on digital images exploiting a smartphone. *Microchemical Journal 133*, 195–199.

The Physics hyper textbook. (2018, April 10). Retrieved from *The Physics hyper textbook:* https://physics.info/viscosity/

Thomas, A. (2002). Fats and Fatty Oils. *Ullmann's Encyclopedia of Industrial Chemistry*.

Xiea, W.-Q., Gonga, Y.-X., & Yuc, K.-X. (2017). A rapid method for the quantitative analysis of total acid number in biodiesel based on headspace GC technique. *Fuel 210*, 236–240.

APPENDICES

APPENDIX 1

ASTM D 2500 Test Method for Cloud Point of Petroleums

Designation: D 2500 – 09

An American National Standard
British Standard 4458

Designation: 219/82

Standard Test Method for Cloud Point of Petroleum Products[1]

This standard is issued under the fixed designation D 2500; the number immediately following the designation indicates the year of original adoption or, in the case of revision, the year of last revision. A number in parentheses indicates the year of last reapproval. A superscript epsilon (ε) indicates an editorial change since the last revision or reapproval.

This standard has been approved for use by agencies of the Department of Defense.

1. Scope*

1.1 This test method covers only petroleum products and biodiesel fuels that are transparent in layers 40 mm in thickness, and with a cloud point below 49°C.

NOTE 1—The interlaboratory program consisted of petroleum products of Test Method D 1500 color of 3.5 and lower. The precisions stated in this test method may not apply to samples with ASTM color higher than 3.5.

1.2 The values stated in SI units are to be regarded as standard. No other units of measurement are included in this standard.

1.3 *This standard does not purport to address all of the safety concerns, if any, associated with its use. It is the responsibility of the user of this standard to establish appropriate safety and health practices and determine the applicability of regulatory limitations prior to use.* For specific hazard statements, see Section 7.

2. Referenced Documents

2.1 *ASTM Standards:*[2]

D 1500 Test Method for ASTM Color of Petroleum Products (ASTM Color Scale)

E 1 Specification for ASTM Liquid-in-Glass Thermometers

2.2 *Energy Institute Standard:*[3]

Specifications for IP Standard Thermometers

3. Terminology

3.1 *Definitions of Terms Specific to This Standard:*

3.1.1 *biodiesel*, *n*—a fuel comprised of mono-alkyl esters of long chain fatty acids derived from vegetable oils or animal fats, designated B100.

3.1.1.1 *Discussion*—Biodiesel is typically produced by a reaction of vegetable oil or animal fat with an alcohol such as methanol or ethanol in the presence of a catalyst to yield mono-esters and glycerin. The fuel typically may contain up to 14 different types of fatty acids that are chemically transformed into fatty acid methyl esters (FAME).

3.1.2 *biodiesel blend*, *n*—a blend of biodiesel fuel with petroleum-based diesel fuel designated BXX, where XX is the volume % of biodiesel.

3.1.3 *cloud point*, *n—in petroleum products and biodiesel fuels,* the temperature of a liquid specimen when the smallest observable cluster of hydrocarbon crystals first occurs upon cooling under prescribed conditions.

3.1.3.1 *Discussion*—To many observers, the cluster of wax crystals looks like a patch of whitish or milky cloud, hence the name of the test method. The cloud appears when the temperature of the specimen is low enough to cause wax crystals to form. For many specimens, the crystals first form at the lower circumferential wall of the test jar where the temperature is lowest. The size and position of the cloud or cluster at the cloud point varies depending on the nature of the specimen. Some samples will form large, easily observable, clusters, while others are barely perceptible.

3.1.3.2 *Discussion*—Upon cooling to temperatures lower than the cloud point, clusters of crystals will grow in multiple directions; for example, around the lower circumference of the test jar, towards the center of the jar, or vertically upwards. The crystals can develop into a ring of cloud along the bottom circumference, followed by extensive crystallization across the bottom of the test jar as temperature decreases. Nevertheless, the cloud point is defined as the temperature at which the crystals first appear, not when an entire ring or full layer of wax has been formed at the bottom of the test jar.

3.1.3.3 *Discussion*—In general, it is easier to detect the cloud point of samples with large clusters that form quickly, such as paraffinic samples. The contrast between the opacity of the cluster and the liquid is also sharper. In addition, small brightly-reflective spots can sometimes be observed inside the cluster when the specimen is well illuminated. For other more difficult samples, such as naphthenic, hydrocracked, and those samples whose cold flow behavior have been chemically

---

[1] This test method is under the jurisdiction of ASTM Committee D02 on Petroleum Products and Lubricants and is the direct responsibility of Subcommittee D02.07 on Flow Properties.

Current edition approved April 15, 2009. Published April 2009. Originally approved in 1966. Last previous edition approved in 2005 as D 2500–05.

[2] For referenced ASTM standards, visit the ASTM website, www.astm.org, or contact ASTM Customer Service at service@astm.org. For *Annual Book of ASTM Standards* volume information, refer to the standard's Document Summary page on the ASTM website.

[3] Available from Energy Institute, 61 New Cavendish St., London, WIG 7AR, U.K., http://www.energyinst.org.uk.

***A Summary of Changes section appears at the end of this standard.**

altered, the appearance of the first cloud can be less distinct. The rate of crystal growth is slow, the opacity contrast is weak, and the boundary of the cluster is more diffuse. As the temperature of these specimens decrease below the cloud point, the diffuse cluster will increase in size and can form a general haze throughout. A slight haze throughout the entire sample, which slowly becomes more apparent as the temperature of the specimen decreases, can also be caused by traces of water in the specimen instead of crystal formation (see Note 3). With these difficult samples, drying the sample prior to testing can eliminate this type of interference.

3.1.3.4 *Discussion*—The purpose of the cloud point method is to detect the presence of the wax crystals in the specimen; however trace amounts of water and inorganic compounds may also be present. The intent of the cloud point method is to capture the temperature at which the liquids in the specimen begin to change from a single liquid phase to a two-phase system containing solid and liquid. It is not the intent of this test method to monitor the phase transition of the trace components, such as water.

4. Summary of Test Method

4.1 The specimen is cooled at a specified rate and examined periodically. The temperature at which a cloud is first observed at the bottom of the test jar is recorded as the cloud point.

5. Significance and Use

5.1 For petroleum products and biodiesel fuels, cloud point of a petroleum product is an index of the lowest temperature of their utility for certain applications.

6. Apparatus (see Fig. 1)

6.1 *Test Jar*, clear, cylindrical glass, flat bottom, 33.2 to 34.8-mm outside diameter and 115 and 125-mm height. The inside diameter of the jar may range from 30 to 32.4 mm within the constraint that the wall thickness be no greater than 1.6 mm. The jar should be marked with a line to indicate sample height 54 ± 3 mm above the inside bottom.

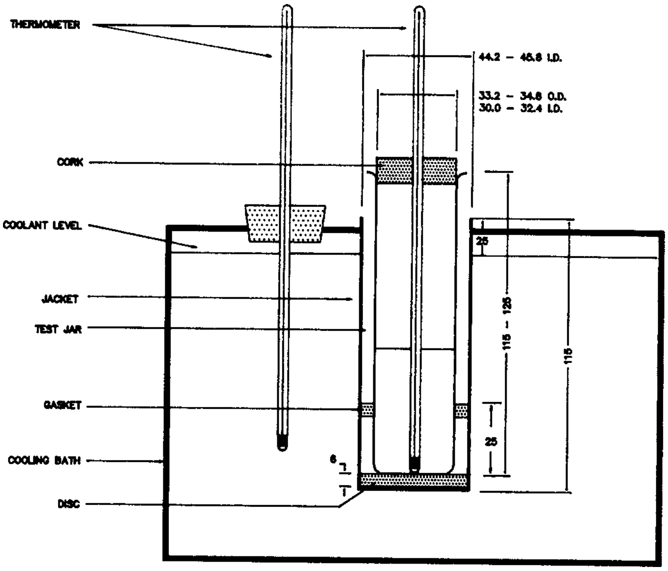

NOTE—All dimensions are in milllimetres.

FIG. 1 Apparatus for Cloud Point Test

6.2 *Thermometers*, having ranges shown below and conforming to the requirements as prescribed in Specification E 1 or Specifications for IP Standard Thermometers.

Thermometer	Temperature Range	Thermometer Number ASTM	 IP
High cloud and pour	−38 to +50°C	5C	1C
Low cloud and pour	−80 to +20°C	6C	2C

6.3 *Cork*, to fit the test jar, bored centrally for the test thermometer.

6.4 *Jacket*, metal or glass, watertight, cylindrical, flat bottom, about 115 mm in depth, with an inside diameter of 44.2 to 45.8 mm. It shall be supported free of excessive vibration and firmly in a vertical position in the cooling bath of 6.7 so that not more than 25 mm projects out of the cooling medium.

6.5 *Disk*, cork or felt, 6-mm thick to fit loosely inside the jacket.

6.6 *Gasket*, ring form, about 5 mm in thickness, to fit snugly around the outside of the test jar and loosely inside the jacket. The gasket may be made of rubber, leather, or other material that is elastic enough to cling to the test jar and hard enough to hold its shape. Its purpose is to prevent the test jar from touching the jacket.

6.7 *Bath or Baths*, maintained at prescribed temperatures with a firm support to hold the jacket vertical. The required bath temperatures may be maintained by refrigeration if available, otherwise by suitable cooling mixtures. Cooling mixtures commonly used for bath temperatures shown are in Table 1.

7. Reagents and Materials

7.1 *Acetone*—Technical grade acetone is suitable for the cooling bath, provided it does not leave a residue on drying. (**Warning**—Extremely flammable.)

7.2 *Carbon Dioxide (Solid) or Dry Ice*—A commercial grade of dry ice is suitable for use in the cooling bath.

7.3 *Petroleum Naphtha*—A commercial or technical grade of petroleum naphtha is suitable for the cooling bath. (**Warning**—Combustible. Vapor harmful.)

7.4 *Sodium Chloride Crystals*—Commercial or technical grade sodium chloride is suitable.

7.5 *Sodium Sulfate*—A reagent grade of anhydrous sodium sulfate should be used when required (see Note 3).

TABLE 1 Cooling Mixtures and Bath Temperatures

	Bath Temperature
Ice and water	0 ± 1.5°C
Crushed ice and sodium chloride crystals, or acetone or petroleum naptha (see 7) with solid carbon dioxide added to give the desired temperature	−18 ± 1.5°C
Acetone or petroleum naptha (see 7) with solid carbon dioxide added to give the desired temperature	−33 ± 1.5°C
Acetone or petroleum naptha (see 7) with solid carbon dioxide added to give the desired temperature	−51 ± 1.5°C
Acetone or petroleum naptha (see 7) with solid carbon dioxide added to give the desired temperature	−69 ± 1. 5°C

8. Procedure

8.1 Bring the sample to be tested to a temperature at least 14°C above the expected cloud point. Remove any moisture present by a method such as filtration through dry lintless filter paper until the oil is perfectly clear, but make such filtration at a temperature of at least 14°C above the approximate cloud point.

8.2 Pour the sample into the test jar to the level mark.

8.3 Close the test jar tightly by the cork carrying the test thermometer. Use the high cloud and pour thermometer if the expected cloud point is above −36°C and the low cloud and pour thermometer if the expected cloud point is below −36°C. Adjust the position of the cork and the thermometer so that the cork fits tightly, the thermometer and the jar are coaxial, and the thermometer bulb is resting on the bottom of the jar.

NOTE 2—Liquid column separation of thermometers occasionally occurs and may escape detection. Thermometers should be checked periodically and used only if their ice points are 0 ± 1°C, when the thermometer is immersed to the immersion line in an ice bath, and when the emergent column temperature does not differ significantly from 21°C. Alternatively, immerse the thermometer to a reading and correct for the resultant cooler stem temperature.

8.4 See that the disk, gasket, and the inside of the jacket are clean and dry. Place the disk in the bottom of the jacket. The disk and jacket shall have been placed in the cooling medium a minimum of 10 min before the test jar is inserted. The use of a jacket cover while the empty jacket is cooling is permitted. Place the gasket around the test jar, 25 mm from the bottom. Insert the test jar in the jacket. Never place a jar directly into the cooling medium.

NOTE 3—Failure to keep the disk, gasket, and the inside of the jacket clean and dry may lead to frost formation, which may cause erroneous results.

8.5 Maintain the temperature of the cooling bath at 0 ± 1.5°C.

8.6 At each test thermometer reading that is a multiple of 1°C, remove the test jar from the jacket quickly but without disturbing the specimen, inspect for cloud, and replace in the jacket. This complete operation shall require not more than 3 s. If the oil does not show a cloud when it has been cooled to 9°C, transfer the test jar to a jacket in a second bath maintained at a temperature of −18 ± 1.5°C (see Table 2). Do not transfer the jacket. If the specimen does not show a cloud when it has been cooled to −6°C, transfer the test jar to a jacket in a third bath maintained at a temperature of −33± 1.5°C. For the determination of very low cloud points, additional baths are required, each bath to be maintained in accordance with Table 2. In each case, transfer the jar to the next bath, if the specimen does not exhibit cloud point and the temperature of the specimen reaches the lowest specimen temperature in the range identified for the current bath in use, based on the ranges stated in Table 2.

TABLE 2 Bath and Sample Temperature Ranges

Bath	Bath Temperature Setting, °C	Sample Temperature Range, °C
1	0 ± 1.5	Start to 9
2	−18 ± 1.5	9 to −6
3	−33 ± 1.5	−6 to −24
4	−51 ± 1.5	−24 to −42
5	−69 ± 1.5	−42 to −60

8.7 Report the cloud point, to the nearest 1°C, at which any cloud is observed at the bottom of the test jar, which is confirmed by continued cooling.

NOTE 4—A wax cloud or haze is always noted first at the bottom of the test jar where the temperature is lowest. A slight haze throughout the entire sample, which slowly becomes more apparent as the temperature is lowered, is usually due to traces of water in the oil. Generally this water haze will not interfere with the determination of the wax cloud point. In most cases of interference, filtration through dry lintless filter papers, such as described in 8.1, is sufficient. In the case of diesel fuels, however, if the haze is very dense, a fresh portion of the sample should be dried by shaking 100 mL with 5 g of anhydrous sodium sulfate for at least 5 min and then filtering through dry lintless filter paper. Given sufficient contact time, this procedure will remove or sufficiently reduce the water haze so that the wax cloud can be readily discerned. Drying and filtering should be done always at a temperature at least 14°C above the approximate cloud point but otherwise not in excess of 49°C.

9. Report

9.1 Report the temperature recorded in 8.7 as the cloud point, Test Method D 2500.

10. Precision and Bias

10.1 The precision of this test method as determined by statistical examination of interlaboratory results is as follows:

10.1.1 *Repeatability*—The difference between two test results, obtained by the same operator with the same apparatus under constant operating conditions on identical test material, would in the long run, in the normal and correct operation of this test method, exceed 2°C only in 1 case in 20.

10.1.2 *Reproducibility*—The difference between two single and independent results obtained by different operators working in different laboratories on identical test material, would in the long run, in the normal and correct operation of this test method, exceed 4°C only in 1 case in 20.

10.1.3 The precision statements were derived from a 1990 interlaboratory cooperative test program.[4] Participants analyzed 13 sample sets comprised of various distillate fuels and lubricating oils with temperature range from -1 to -37°C. Eight laboratories participated with the manual D 2500/IP219 test method. Information on the type of samples and their average cloud points are in the research report.

10.2 *Bias*—The procedure in this test method has no bias, because the value of cloud point can be defined only in terms of a test method.

10.3 *Precision for Biodiesel Products*[5]—The precision of this test method as determined by statistical examination of interlaboratory results is as follows:

10.3.1 *Repeatability for Blends of Biodiesel in Diesel*—The difference between successive test results obtained by the same operator, using the same apparatus, under constant operating

---

[4] Supporting data have been filed at ASTM International Headquarters and may be obtained by requesting Research Report RR: D02–1444.

[5] Supporting data (the results of the 2001 interlaboratory cooperative test program) have been filed at ASTM International Headquarters and may be obtained by requesting Research Report RR: D02–1524.

conditions, on identical test material would, in the long run, in the normal and correct operation of this test method, exceed 2°C only in 1 case in 20.

10.3.2 *Reproducibility for Blends of Biodiesel in Diesel*—The difference between two single and independent test results obtained by different operators, working in different laboratories, on identical test material would, in the long run, in the normal and correct operation of this test method, exceed 3°C only in 1 case in 20.

NOTE 5—The precision for blends of biodiesel in diesel samples comprised cloud points from about −2 to +10°C.

10.3.3 The precision statements were derived from a 2001 interlaboratory cooperative test program.[5] Participants analyzed eleven sample sets comprised of different blends of two petroleum distillate fuels, diesel and kerosene, with various biodiesel fuels with temperature range from +10 to −45°C. Ten laboratories participated with the manual D 2500/IP219 test method. Information on the type of samples and their average cloud points are in the research report.

NOTE 6—One of the outcomes of the interlaboratory study was the selection of the sample types, since the ones used in the study contributed to a difficulty in determining the precision statement. Kerosene is a sufficiently different fuel type from biodiesel to cause some slight separation of phases upon cooling when in B20 blends. Also, the particular kerosene sample used was atypical, which complicated the study further. Therefore, data from the blends of kerosene in biodiesel were not used in the precision statement. In addition, the diesel fuel used in the research report was high cloud point material. Due to the cloud point of the base diesel material, this temperature range in the precision statement was limited.

NOTE 7—A future interlaboratory cloud study will be done to include a wider range of base biodiesel fuels with various distillate blend stocks.

10.4 *Bias for Biodiesel Products*[5]—The procedure in this test method has no bias, because the value of cloud point can be defined only in terms of a test method.

11. Keywords

11.1 cloud point; petroleum products; wax crystals

SUMMARY OF CHANGES

Subcommittee D02.07 has identified the location of selected changes to this standard since the last issue (D 2500–05) that may impact the use of this standard.

(*1*) Revised 6.7.
(*2*) Revised 7.
(*3*) Added Table 1.
(*4*) Deleted original Note 2.

APPENDIX 2

ASTM D 97-2005 Test Method for Pour Point of Petroleums

Designation: D 97 – 05

An American National Standard

Designation: 15/95

Standard Test Method for Pour Point of Petroleum Products[1]

This standard is issued under the fixed designation D 97; the number immediately following the designation indicates the year of original adoption or, in the case of revision, the year of last revision. A number in parentheses indicates the year of last reapproval. A superscript epsilon (ϵ) indicates an editorial change since the last revision or reapproval.

This standard has been approved for use by agencies of the Department of Defense.

1. Scope*

1.1 This test method is intended for use on any petroleum product.[2] A procedure suitable for black specimens, cylinder stock, and nondistillate fuel oil is described in 8.8. A procedure for testing the fluidity of a residual fuel oil at a specified temperature is described in Appendix X1.

1.2 Several ASTM test methods offering alternative procedures for determining pour points using automatic apparatus are available. None of them share the same designation number as Test Method D 97. When an automatic instrument is used, the ASTM test method designation number specific to the technique shall be reported with the results. A procedure for testing the pour point of crude oils is described in Test Method D 5853.

1.3 *This standard does not purport to address all of the safety concerns, if any, associated with its use. It is the responsibility of the user of this standard to establish appropriate safety and health practices and determine the applicability of regulatory limitations prior to use.*

2. Referenced Documents

2.1 *ASTM Standards:* [3]

D 117 Guide for Sampling, Test Methods, and Specifications for Electrical Insulating Oils of Petroleum Origin
D 396 Specification for Fuel Oils
D 1659 Test Method for Maximum Fluidity Temperature of Residual Fuel Oil[4]
D 2500 Test Method for Cloud Point of Petroleum Products
D 3245 Test Method for Pumpability of Industrial Fuel Oils
D 5853 Test Method for Pour Point of Crude Oils
E 1 Specification for ASTM Liquid-in-Glass Thermometers

2.2 *Energy Institute Standards:*
Specifications for IP Standard Thermometers [5]

3. Terminology

3.1 *Definitions:*

3.1.1 *black oil*, *n*—lubricant containing asphaltic materials. Black oils are used in heavy-duty equipment applications, such as mining and quarrying, where extra adhesiveness is desired.

3.1.2 *cylinder stock*, *n*—lubricant for independently lubricated engine cylinders, such as those of steam engines and air compressors. Cylinder stock are also used for lubrication of valves and other elements in the cylinder area.

3.1.3 *pour point*, *n—in petroleum products*, the lowest temperature at which movement of the test specimen is observed under prescribed conditions of test.

3.1.4 *residual fuel*, *n*—a liquid fuel containing bottoms remaining from crude distillation or thermal cracking; sometimes referred to as heavy fuel oil.

3.1.4.1 *Discussion*—Residual fuels comprise Grades 4, 5, and 6 fuel oils, as defined in Specification D 396.

4. Summary of Test Method

4.1 After preliminary heating, the sample is cooled at a specified rate and examined at intervals of 3°C for flow characteristics. The lowest temperature at which movement of the specimen is observed is recorded as the pour point.

---

[1] This test method is under the jurisdiction of ASTM Committee D02 on Petroleum Products and Lubricants and is the direct responsibility of Subcommittee D02.07 on Flow Properties.

Current edition approved June 1, 2005. Published July 2005. Originally approved in 1927, replacing D 47. Last previous edition approved in 2004 as D 97–04.

In the IP, this test method is under the jurisdiction of the Standardization Committee. This test method was adopted as a joint ASTM-IP Standard in 1965.

[2] Statements defining this test and its significance when applied to electrical insulating oils of mineral origin will be found in Guide D 117.

[3] *Reagent Chemicals, American Chemical Society Specifications*, American Chemical Society, Washington, DC. For suggestions on the testing of reagents not listed by the American Chemical Society, see *Annual Standards for Laboratory Chemicals,* BDH Ltd., Poole, Dorset, U.K., and the *United States Pharmacopeia and National Formulary,* U.S. Pharmacopeial Convention, Inc. (USPC), Rockville, MD.

[4] Withdrawn.

[5] Methods for Analysis and Testing, *IP Standards for Petroleum and its Products*, Part I, Vol 2.

***A Summary of Changes section appears at the end of this standard.**

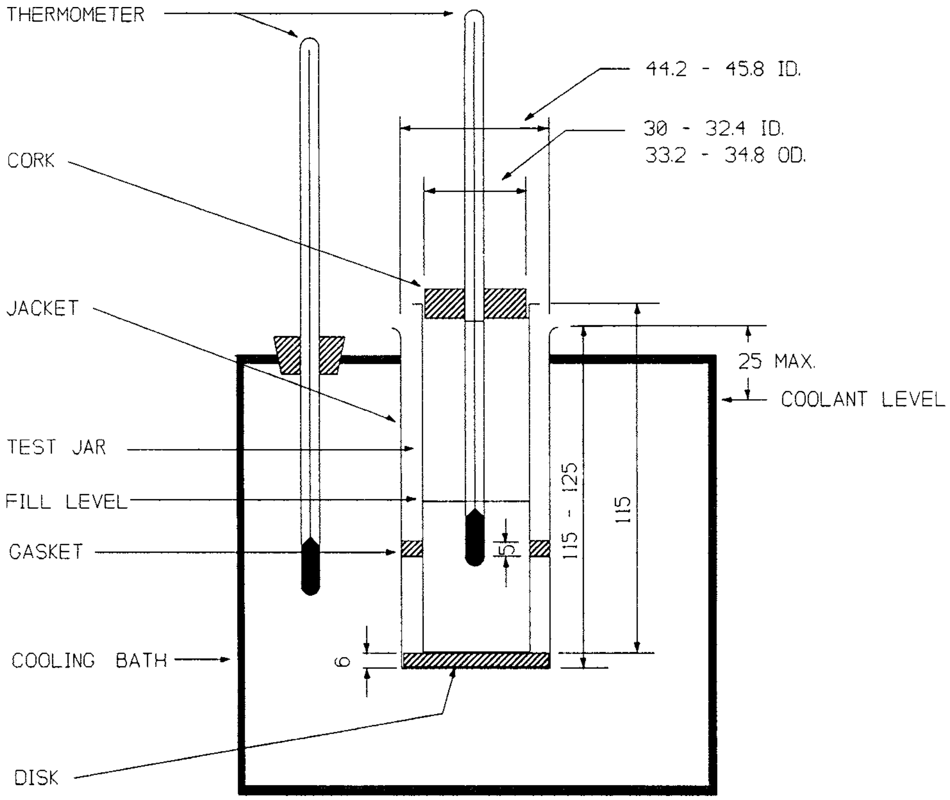

NOTE—Dimensions are in millimetres (not to scale).

FIG. 1 Apparatus for Pour Point Test

5. Significance and Use

5.1 The pour point of a petroleum specimen is an index of the lowest temperature of its utility for certain applications.

6. Apparatus

6.1 *Test Jar*, cylindrical, of clear glass, flat bottom, 33.2 to 34.8-mm outside diameter, and 115 to 125 mm in height. The inside diameter of the jar can range from 30.0 to 32.4 mm, within the constraint that the wall thickness be no greater than 1.6 mm. The jar shall have a line to indicate a sample height 54 ± 3 mm above the inside bottom. See Fig. 1.

6.2 *Thermometers*, having the following ranges and conforming to the requirements prescribed in Specification E 1 for thermometers:

	Temperature	Thermometer Number	
Thermometer	Range	ASTM	IP
High cloud and pour	−38 to +50°C	5C	1C
Low cloud and pour	−80 to +20°C	6C	2C
Melting point	+32 to +127°C	61C	63C

6.2.1 Since separation of liquid column thermometers occasionally occurs and may escape detection, thermometers should be checked immediately prior to the test and used only if they prove accurate within ±1°C (for example ice point).

6.3 *Cork*, to fit the test jar, bored centrally for the test thermometer.

6.4 *Jacket*, watertight, cylindrical, metal, flat-bottomed, 115 ± 3-mm depth, with inside diameter of 44.2 to 45.8 mm. It shall be supported in a vertical position in the cooling bath (see 6.7) so that not more than 25 mm projects out of the cooling medium, and shall be capable of being cleaned.

6.5 *Disk*, cork or felt, 6 mm thick to fit loosely inside the jacket.

6.6 *Gasket*, to fit snugly around the outside of the test jar and loosely inside the jacket. The gasket may be made of rubber, leather, or other material that is elastic enough to cling to the test jar and hard enough to hold its shape. Its purpose is to prevent the test jar from touching the jacket.

6.7 *Bath or Baths*, maintained at prescribed temperatures with a firm support to hold the jacket vertical. The required bath temperatures may be obtained by refrigeration if available, otherwise by suitable freezing mixtures. Freezing mixtures commonly used for temperatures down to those shown are as follows:

	For Temperatures Down
Ice and water	9°C
Crushed ice and sodium chloride crystals	−12°C
Crushed ice and calcium chloride crystals	−27°C
Acetone or petroleum naphtha (see Section 6) chilled in a covered metal beaker with an ice-salt mixture to −12°C then with enough solid carbon dioxide to give the desired temperature.	−57°C

7. Reagents and Materials

7.1 The following solvents of technical grade are appropriate for low-temperature bath media.

7.1.1 *Acetone*, (**Warning**—Extremely flammable).

7.1.2 *Alcohol, Ethanol* (**Warning**—Flammable).

7.1.3 *Alcohol, Methanol* (**Warning**—Flammable. Vapor harmful).

7.1.4 *Petroleum Naphtha*, (**Warning**—Combustible. Vapor harmful).

7.1.5 *Solid Carbon Dioxide*, (**Warning**—Extremely cold −78.5°C).

8. Procedure

8.1 Pour the specimen into the test jar to the level mark. When necessary, heat the specimen in a water bath until it is just sufficiently fluid to pour into the test jar.

NOTE 1—It is known that some materials, when heated to a temperature higher than 45°C during the preceding 24 h, do not yield the same pour point results as when they are kept at room temperature for 24 h prior to testing. Examples of materials which are known to show sensitivity to thermal history are residual fuels, black oils, and cylinder stocks.

8.1.1 Samples of residual fuels, black oils, and cylinder stocks which have been heated to a temperature higher than 45°C during the preceding 24 h, or when the thermal history of these sample types is not known, shall be kept at room temperature for 24 h before testing. Samples which are known by the operator not to be sensitive to thermal history need not be kept at room temperature for 24 h before testing.

8.1.2 Experimental evidence supporting elimination of the 24-h waiting period for some sample types is contained in a research report.[6]

8.2 Close the test jar with the cork carrying the high-pour thermometer (5.2). In the case of pour points above 36°C, use a higher range thermometer such as IP 63C or ASTM 61C. Adjust the position of the cork and thermometer so the cork fits tightly, the thermometer and the jar are coaxial, and the thermometer bulb is immersed so the beginning of the capillary is 3 mm below the surface of the specimen.

8.3 For the measurement of pour point, subject the specimen in the test jar to the following preliminary treatment:

8.3.1 *Specimens Having Pour Points Above −33°C*—Heat the specimen without stirring to 9°C above the expected pour point, but to at least 45°C, in a bath maintained at 12°C above the expected pour point, but at least 48°C. Transfer the test jar to a water bath maintained at 24°C and commence observations for pour point.

8.3.2 *Specimens Having Pour Points of −33°C and Below*—Heat the specimen without stirring to 45°C in a bath maintained at 48°C and cool to 15°C in a water bath maintained at 6°C. Remove the high cloud and pour thermometer, and place the low cloud and pour thermometer in position.

8.4 See that the disk, gasket, and the inside of the jacket are clean and dry. Place the disk in the bottom of the jacket. Place the gasket around the test jar, 25 mm from the bottom. Insert the test jar in the jacket. Never place a jar directly into the cooling medium.

8.5 After the specimen has cooled to allow the formation of paraffin wax crystals, take great care not to disturb the mass of specimen nor permit the thermometer to shift in the specimen; any disturbance of the spongy network of wax crystals will lead to low and erroneous results.

8.6 Pour points are expressed in integers that are positive or negative multiples of 3°C. Begin to examine the appearance of the specimen when the temperature of the specimen is 9°C above the expected pour point (estimated as a multiple of 3°C). At each test thermometer reading that is a multiple of 3°C below the starting temperature remove the test jar from the jacket. To remove condensed moisture that limits visibility wipe the surface with a clean cloth moistened in alcohol (ethanol or methanol). Tilt the jar just enough to ascertain whether there is a movement of the specimen in the test jar. The complete operation of removal, wiping, and replacement shall require not more than 3 s.

8.6.1 If the specimen has not ceased to flow when its temperature has reached 27°C, transfer the test jar to the next lower temperature bath in accordance with the following schedule:

Specimen is at +27°C, move to 0°C bath
Specimen is at +9°C, move to −18°C bath
Specimen is at −6°C, move to −33°C bath
Specimen is at −24°C, move to −51°C bath
Specimen is at −42°C, move to −69°C bath

8.6.2 As soon as the specimen in the jar does not flow when tilted, hold the jar in a horizontal position for 5 s, as noted by an accurate timing device and observe carefully. If the specimen shows any movement, replace the test jar immediately in the jacket and repeat a test for flow at the next temperature, 3°C lower.

8.7 Continue in this manner until a point is reached at which the specimen shows no movement when the test jar is held in a horizontal position for 5 s. Record the observed reading of the test thermometer.

8.8 For black specimen, cylinder stock, and nondistillate fuel specimen, the result obtained by the procedure described in 8.1 through 8.7 is the upper (maximum) pour point. If required, determine the lower (minimum) pour point by heating the sample while stirring, to 105°C, pouring it into the jar, and determining the pour point as described in 8.4 through 8.7.

8.9 Some specifications allow for a pass/fail test or have pour point limits at temperatures not divisible by 3°C. In these cases, it is acceptable practice to conduct the pour point measurement according to the following schedule: Begin to examine the appearance of the specimen when the temperature of the specimen is 9°C above the specification pour point. Continue observations at 3°C intervals as described in 8.6 and 8.7 until the specification temperature is reached. Report the sample as passing or failing the specification limit.

9. Calculation and Report

9.1 Add 3°C to the temperature recorded in 8.7 and report the result as the Pour Point, ASTM D 97. For black oil, and so forth, add 3°C to the temperature recorded in 8.7 and report the

---

[6] Supporting data have been filed at ASTM International Headquarters and may be obtained by requesting Research Report RR: D02-1377.

result as Upper Pour Point, ASTM D 97, or Lower Pour Point, ASTM D 97, as required.

10. Precision and Bias

10.1 *Lubricating Oil and Distillate and Residual Fuel Oil.*[7]

10.1.1 *Repeatability*—The difference between successive test results, obtained by the same operator using the same apparatus under constant operating conditions on identical test material, would in the long run, in the normal and correct operation of this test method, exceed 3°C only in one case in twenty. Differences greater than this should be considered suspect.

10.1.2 *Reproducibility*—The difference between two single and independent test results, obtained by different operators working in different laboratories on identical test material, would in the long run, in the normal and correct operation of this test method, exceed 6°C only in one case in twenty. Differences greater than this should be considered suspect.

10.2 *Bias*—There being no criteria for measuring bias in these test-product combinations, no statement of bias can be made.

10.3 The precision statements were prepared with data on ten new (unused) mineral oil-based lubricants and sixteen assorted fuel oils tested by twelve cooperators. The mineral oil-based lubricants had pour points ranging from −48 to −6°C while the fuel oils had pour points ranging from −33 to +51°C. The following precision data were obtained:

	Mineral Oil Lubricants	Fuel Oils
95 % Confidence		
Repeatability, °C	2.87	2.52
Reproducibility, °C	6.43	6.59

---

[7] The cloud point procedure formerly part of this test method now appears as Test Method D 2500.

APPENDIX

(Nonmandatory Information)

X1. TEST FOR FLUIDITY OF A RESIDUAL FUEL OIL AT A SPECIFIED TEMPERATURE

X1.1 General

X1.1.1 The low-temperature flow properties of a waxy fuel oil depend on handling and storage conditions. Thus, they may not be truly indicated by pour point. The pour point test does not indicate what happens when an oil has a considerable head of pressure behind it, such as when gravitating from a storage tank or being pumped along a pipeline. Failure to flow at the pour point is normally attributed to the separation of wax from the fuel; however, it can also be due to the effect of viscosity in the case of very viscous fuel oils. In addition pour points of residual fuels are influenced by the previous thermal history of the specimens. A loosely knit wax structure built up on cooling of the oil can be normally broken by the application of relatively little pressure.

X1.1.2 The usefulness of the pour point test in relation to residual fuel oils is open to question, and the tendency to regard the pour point as the limiting temperature at which a fuel will flow can be misleading. The problem of accurately specifying the handling behavior of fuel oil is important, and because of the technical limitations of the pour point test, various pumpability tests have been devised to assess the low-temperature flow characteristics of heavy residual fuel oils. Test Method D 3245 is one such method. However, most alternative methods tend to be time-consuming and as such do not find ready acceptance as routine control tests for determining low-temperature flow properties. One method which is relatively quick and easy to perform and has found limited acceptance as a "go-no-go" method is based on the appendix method to the former Test Method D 1659–65. The method is described as follows.

X1.2 Scope

X1.2.1 This method covers the determination of the fluidity of a residual fuel oil at a specified temperature in an as-received condition.

X1.3 Definition

X1.3.1 *fluidity temperature*—the sample when tested in an as-received condition is considered "fluid at the temperature of the test" if it will flow 2 mm in 1 min in a 12.5 mm U-tube under a maximum pressure of 152 mm of mercury.

X1.4 Summary of Test Method

X1.4.1 A sample of fuel in its as-received condition is cooled at the specified temperature for 30 min in the standard U-tube and is tested for movement under prescribed pressure conditions.

X1.5 Significance and Use

X1.5.1 This method may be used as a "go-no-go" procedure for operational situations where it is necessary to ascertain the fluidity of a residual oil under prescribed conditions in an as-received condition. The conditions of this method simulate those of a pumping situation where the oil is expected to flow through a 12-mm pipe under slight pressure at a specified temperature. Fluidity, like Test Method D 97, is used to define cold flow properties. It differs from D 97, however, in that (*1*) it is restricted to residual fuel oil and (*2*) a prescribed pressure is applied to the sample. The latter represents an attempt to overcome the technical limitations of the Pour Point Method where gravity-induced flow is the criterion. Test Method

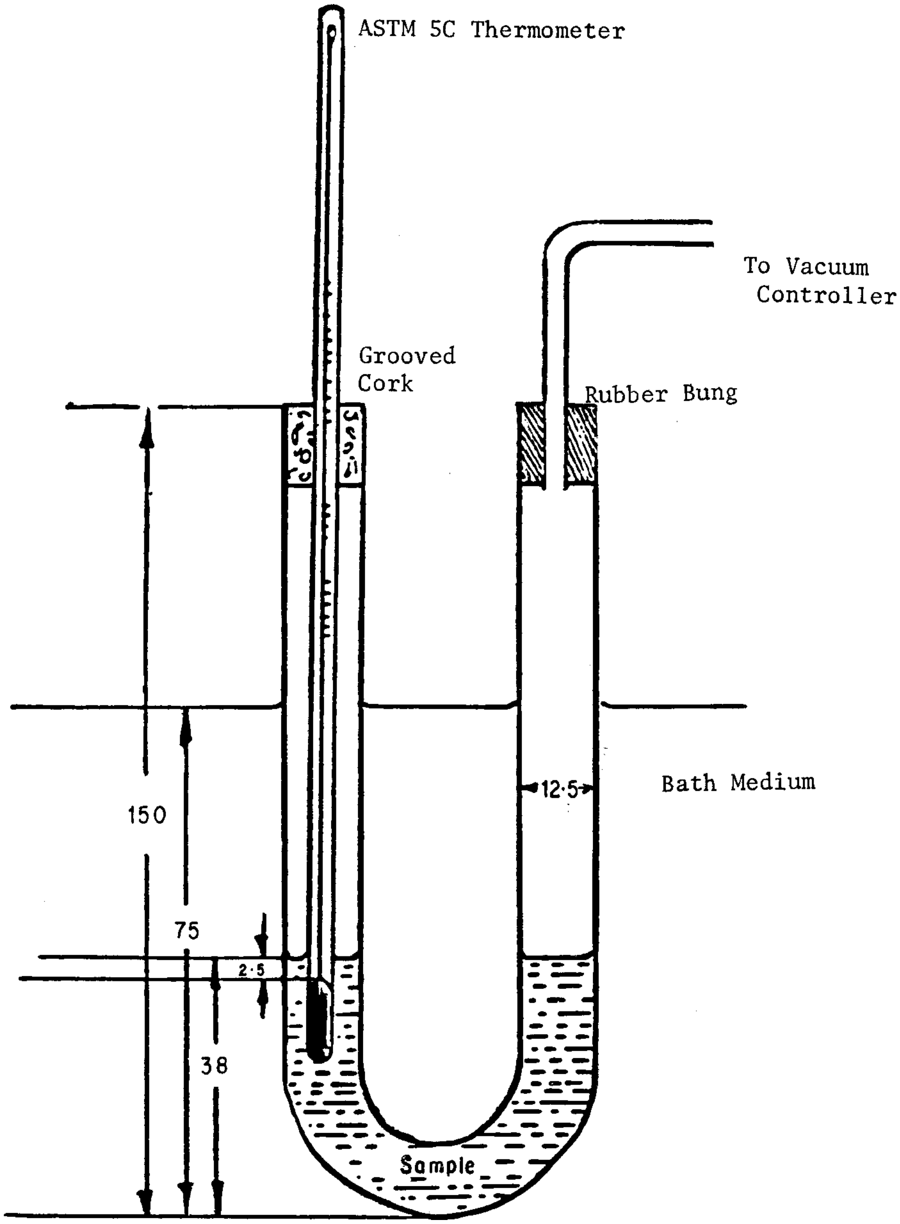

NOTE—All dimensions are in millimetres

FIG. X1.1 Disposition of U-tube in Fluidity Temperature Test Bath

D 3245, represents another method for predicting field performance in cold flow conditions. Test Method D 3245, however, does have limitations and may not be suitable for use with very waxy fuel oils which solidify so rapidly in the chilling bath that a reading cannot be obtained under the conditions of the test. It is also a time-consuming test and therefore not suitable for routine control testing.

X1.6 Apparatus

X1.6.1 *Glass U-Tubes*, 150 mm high, having a uniform internal diameter of 12.5 ± 1 mm and a radius of curvature, measured to the outside curve of the tube of 35 mm (Fig. X1.1).

X1.6.2 *Thermometers*—Thermometers having a range from −38 to +50°C and conforming to the requirements of Thermometer 5C as prescribed in Specification E 1, shall be used for insertion in the glass U-tubes and for measuring the temperatures of the baths.

X1.6.3 *Fluidity Temperature Test Bath,*[8]

consists of a reservoir, a stirrer, and a motor and pump to circulate coolant through the coils of the tubing placed in the bottom of the test bath and passing through the cold bath. The flow of coolant through these coils can be controlled by a thermostat and a solenoid valve. It is possible that, where justified by the quantity of work, more than one such bath could be utilized to permit concurrent testing at more than one temperature (Fig. X1.2).

---

[8] A kinematic viscosity bath is usually satisfactory.

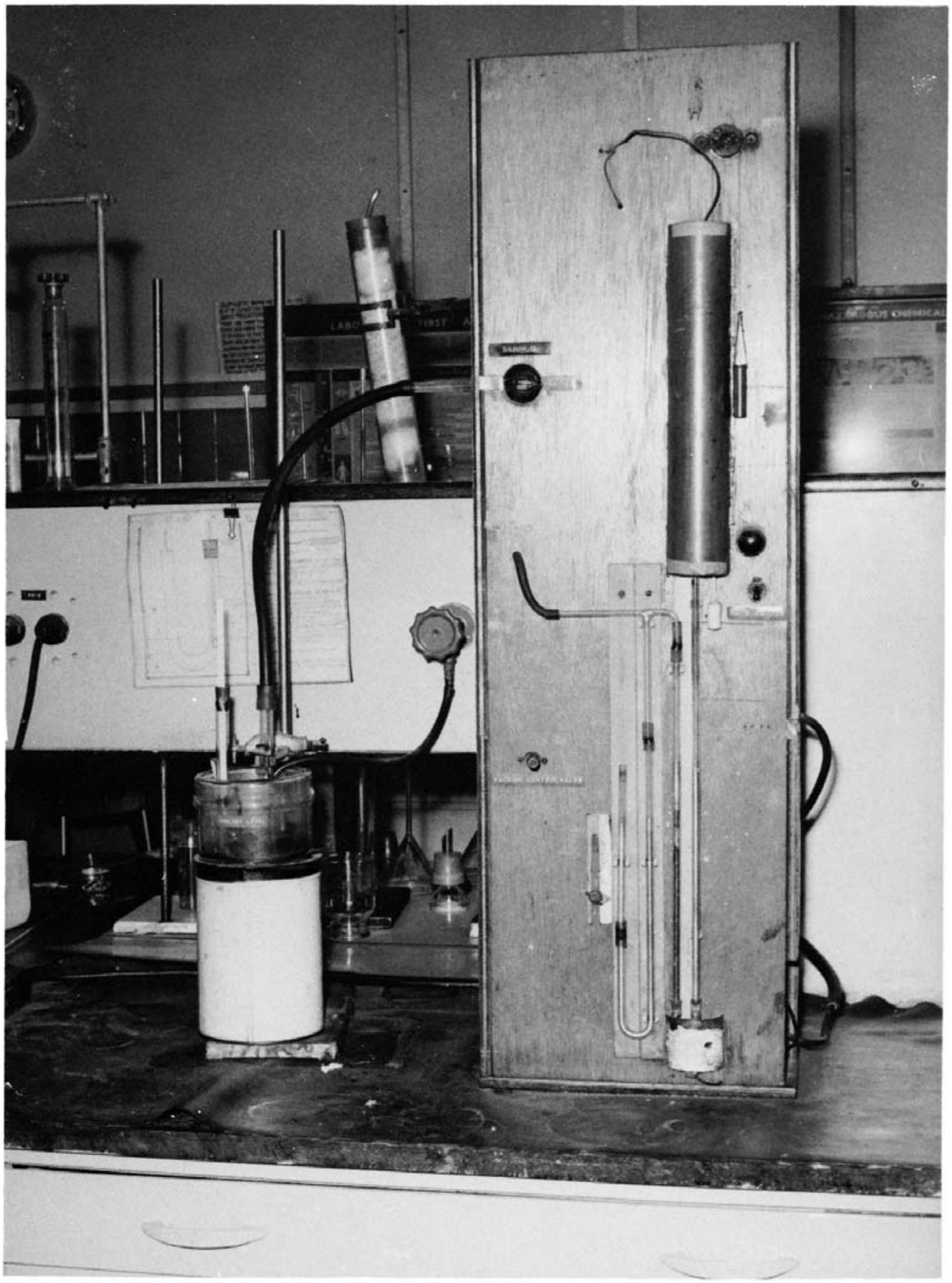

FIG. X1.2 Fluidity Temperature Apparatus

X1.6.4 *Mercury Manometer* calibrated in 10-mm divisions with a distinguishing mark at 152 mm (equivalent to 20.3 kPa).

X1.6.5 *Automatic Vacuum Controller*[9] *(as shown in Fig. X1.3 and Fig. X1.4)*—A device that gradually increased the vacuum applied to one end of the U-tube at the specified rate of 10 mm/4S.

X1.7 Preparation of Apparatus

X1.7.1 Adjust the automatic vacuum controller as follows: close the stopcock on the tube connecting the automatic vacuum controller to the fluidity tester. A pinchcock on the rubber tube will serve as well as a stopcock. Wind the thread attached to the steel rod around the pulley on the synchronous motor until the end of the rod is about 15 mm above the zero level of the mercury in the control manometer. Turn on the power switch. The thread will begin to unwind, lowering the steel rod. When the rod contacts the mercury, the relay will

---

[9] This apparatus may be shop fabricated. Details of special parts are indicated in Figs. X1.3 and X1.4. Alternatively the apparatus can be purchased.

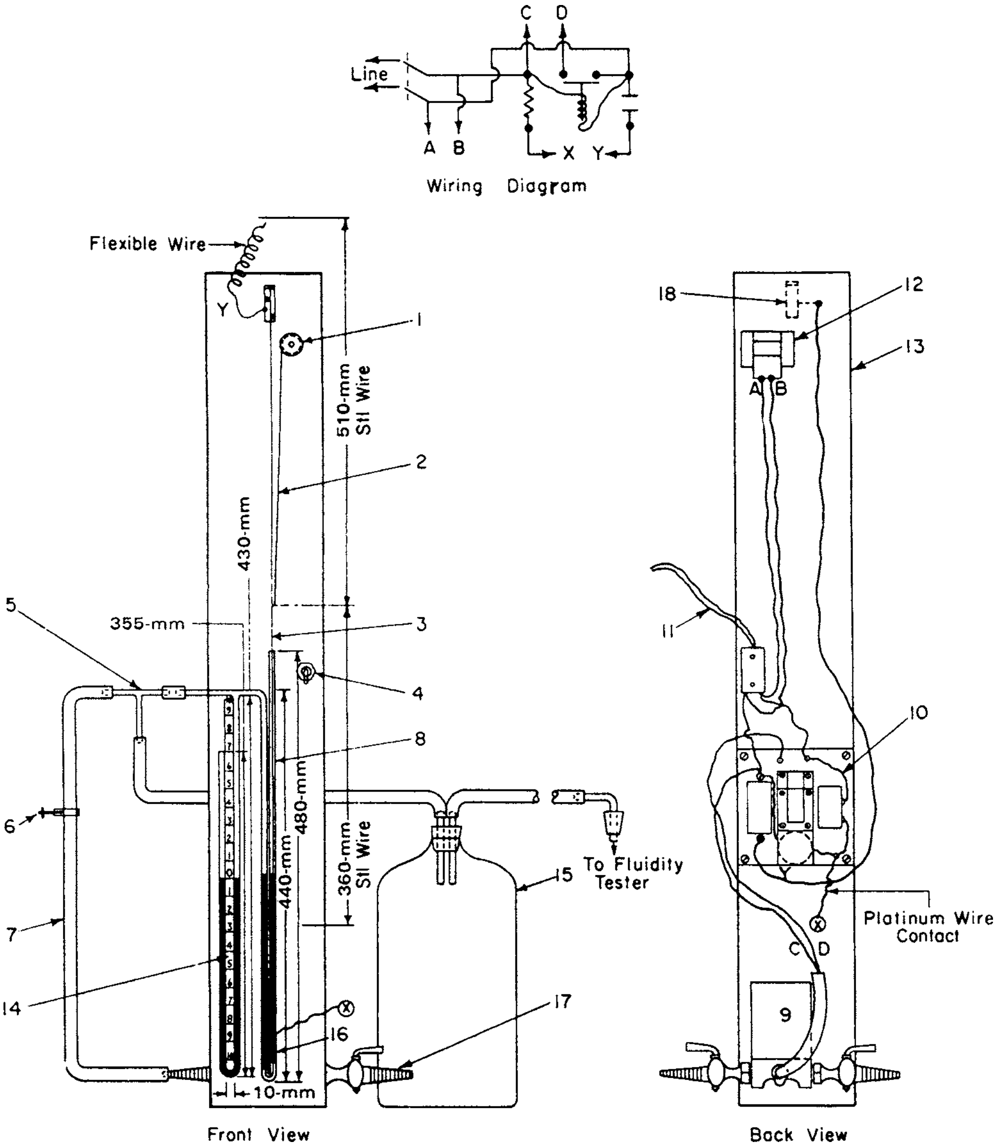

1—26-mm diameter face pulley
2—Thread
3—Steel rod
4—Switch-DPST
5—Tee, 90-mm long
6—Needle valve
7—Rubber or plastic tubing
8—6-mm heat-resistant glass tube
9—Solenoid valve
10—Electric relay
11—Electric cord to outlet
12—Synchronous motor
13—Plywood of approximately 10-mm thickness
14—Millimeter scale
15—4-L bottle
16—0.5-mm heat-resistant glass capillary
17—To vacuum line
18—Rod holder

FIG. X1.3 Assembly Automatic Vacuum Controller Apparatus

open the solenoid valve in the vacuum line and air will be pumped from the system at a rate limited by the needle valve. Adjust this needle valve until the descending mercury in the control manometer just leads the rod, reducing the relay operation to a minimum. When properly adjusted, the pulsations caused by the opening and closing of the solenoid valve should not exceed ±1 mm. In this manner the pressure in the system will be reduced gradually at a rate governed by the descent of the steel rod.

X1.8 Procedure

X1.8.1 Pour the sample as received into a thoroughly cleaned and dry standard fluidity U-tube, without contacting the upper walls of the tube, until the vertical height of the

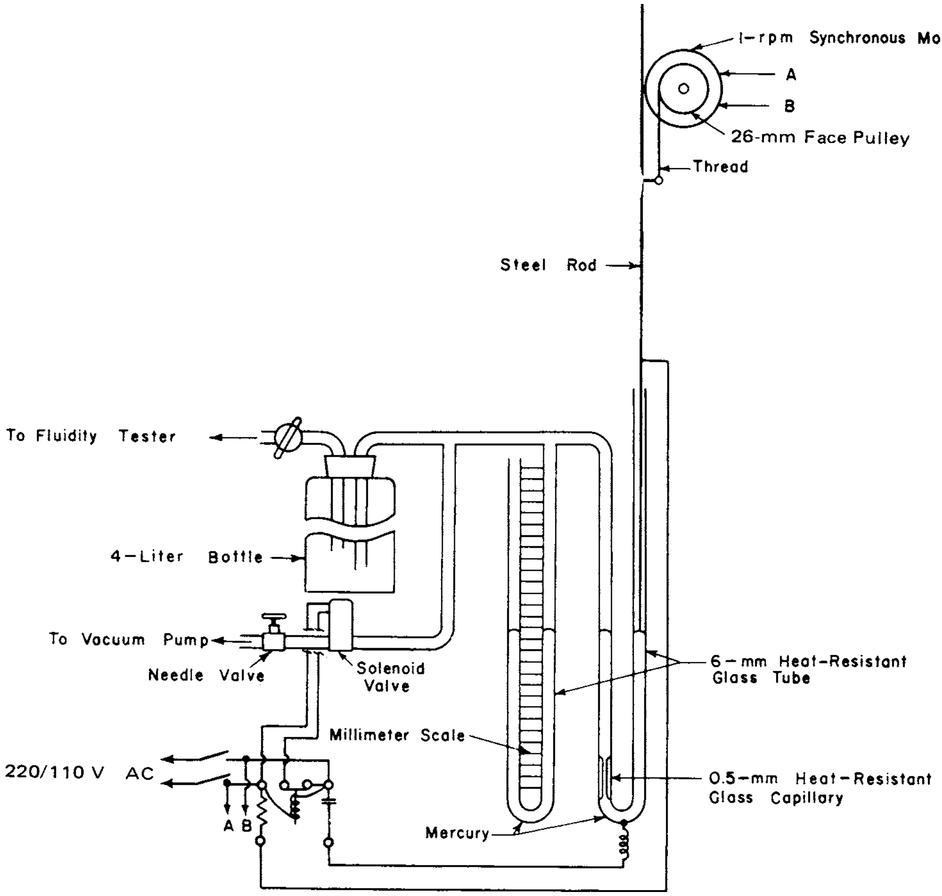

FIG. X1.4 Detail of Automatic Vacuum Controller

sample in the U-tube is 38 mm. Insert in one leg of each U-tube an ASTM Thermometer 5C in a cork that has been grooved to permit the passage of air. The thermometer must be placed in the center of the tube and its bulb immersed so that the beginning of the capillary is 3 mm below the surface of the specimen.

X1.8.2 Fix the tube in the bath set at the specific temperature, immersed to a depth of approximately 75 mm. Control the bath and sample temperatures within ±1°C and ±0.5°C, respectively, of the specified temperature of the test.

X1.8.3 Maintain the sample at the specified temperature for 30 min ± 30 s, with the U-tube connected to the automatic vacuum controller, and the stopcock or pinch-clamp open. Wind the thread on the pulley attached to the synchronous motor. Turn the power switch to the ON position. Apply suction automatically to the U-tube at the prescribed rate. Observe any movement of the specimen during a one-minute interval which is the time required to apply 152-mm Hg vacuum to the specimen in the U-tube. Immediately disconnect the U-tube from the automatic vacuum controller, turn off the power switch and rewind the thread. If the specimen has moved 2 mm or more during the time (1 min) the suction was applied, the specimen is considered fluid at the temperature of the test.

X1.9 Report

X1.9.1 Report the fluidity of the sample at a specified temperature as follows:

X1.9.1.1 If the sample fulfills the conditions of flow, as defined in X1.3.1, report fluidity: "Fluid at (temperature of test)" or fluidity at (temperature of test): "Pass."

X1.9.1.2 If the sample does not fulfill the conditions of flow, as defined in X1.3.1, report fluidity: "Not fluid at (temperature of test)" or fluidity at (temperature of test): "Fail."

X1.10 Precision and Bias

X1.10.1 As in the case of pass-fail data, no statement is made about either the precision or the bias of this method for measuring the fluidity of a residual fuel specimen since the result merely states whether there is conformance to the criteria for success specified in the procedure.

SUMMARY OF CHANGES

Subcommittee D02.07 has identified the location of selected changes to this standard since the last issue (D 97–04) that may impact the use of this standard.

(*1*) Added Test Method D 5853 to the Scope and Referenced Documents sections.

ASTM International takes no position respecting the validity of any patent rights asserted in connection with any item mentioned in this standard. Users of this standard are expressly advised that determination of the validity of any such patent rights, and the risk of infringement of such rights, are entirely their own responsibility.

This standard is subject to revision at any time by the responsible technical committee and must be reviewed every five years and if not revised, either reapproved or withdrawn. Your comments are invited either for revision of this standard or for additional standards and should be addressed to ASTM International Headquarters. Your comments will receive careful consideration at a meeting of the responsible technical committee, which you may attend. If you feel that your comments have not received a fair hearing you should make your views known to the ASTM Committee on Standards, at the address shown below.

This standard is copyrighted by ASTM International, 100 Barr Harbor Drive, PO Box C700, West Conshohocken, PA 19428-2959, United States. Individual reprints (single or multiple copies) of this standard may be obtained by contacting ASTM at the above address or at 610-832-9585 (phone), 610-832-9555 (fax), or service@astm.org (e-mail); or through the ASTM website (www.astm.org).

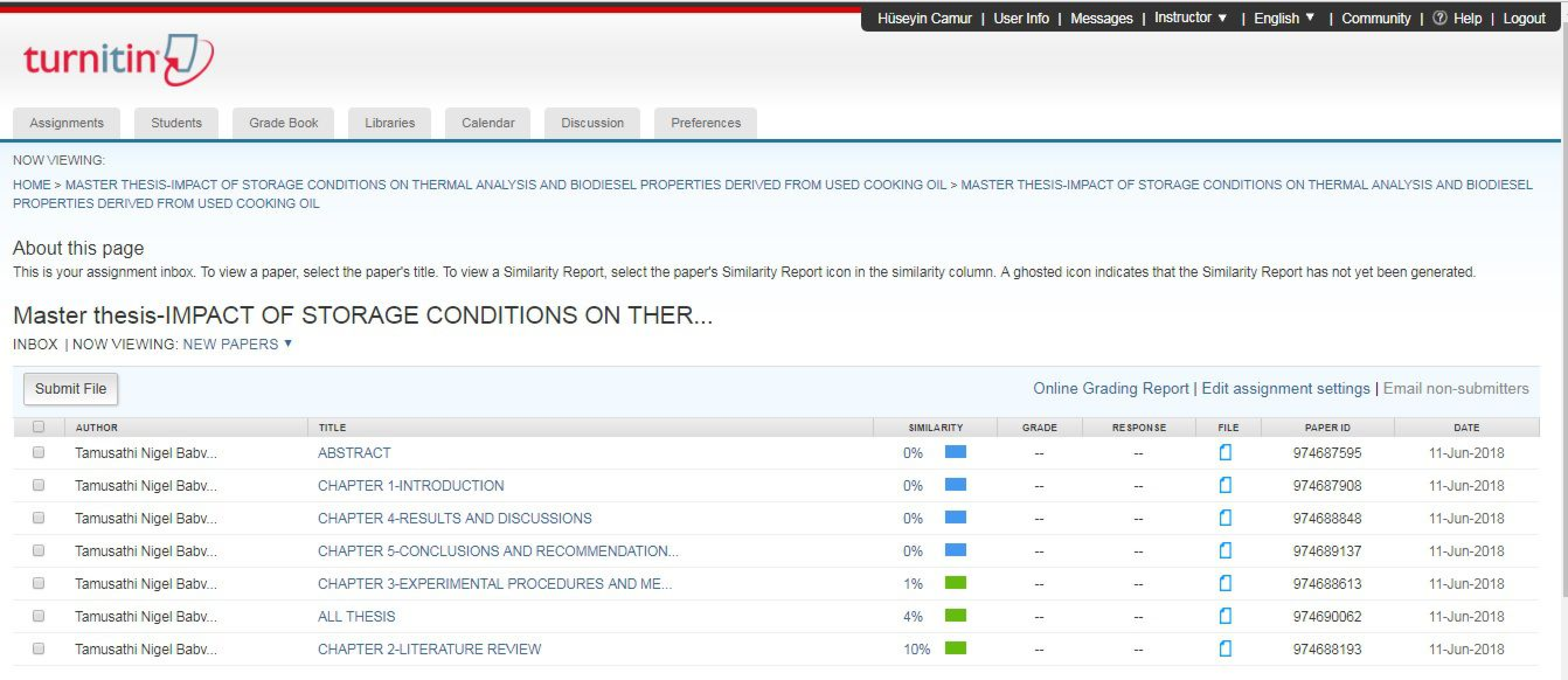

NOW VIEWING:

HOME > MASTER THESIS-IMPACT OF STORAGE CONDITIONS ON THERMAL ANALYSIS AND BIODIESEL PROPERTIES DERIVED FROM USED COOKING OIL > MASTER THESIS-IMPACT OF STORAGE CONDITIONS ON THERMAL ANALYSIS AND BIODIESEL PROPERTIES DERIVED FROM USED COOKING OIL

About this page

This is your assignment inbox. To view a paper, select the paper's title. To view a Similarity Report, select the paper's Similarity Report icon in the similarity column. A ghosted icon indicates that the Similarity Report has not yet been generated.

Master thesis-IMPACT OF STORAGE CONDITIONS ON THER...

INBOX | NOW VIEWING: NEW PAPERS ▼

☐	AUTHOR	TITLE	SIMILARITY	GRADE	RESPONSE	FILE	PAPER ID	DATE
☐	Tamusathi Nigel Babv...	ABSTRACT	0% 🟦	--	--	🗋	974687595	11-Jun-2018
☐	Tamusathi Nigel Babv...	CHAPTER 1-INTRODUCTION	0% 🟦	--	--	🗋	974687908	11-Jun-2018
☐	Tamusathi Nigel Babv...	CHAPTER 4-RESULTS AND DISCUSSIONS	0% 🟦	--	--	🗋	974688848	11-Jun-2018
☐	Tamusathi Nigel Babv...	CHAPTER 5-CONCLUSIONS AND RECOMMENDATION...	0% 🟦	--	--	🗋	974689137	11-Jun-2018
☐	Tamusathi Nigel Babv...	CHAPTER 3-EXPERIMENTAL PROCEDURES AND ME...	1% 🟩	--	--	🗋	974688613	11-Jun-2018
☐	Tamusathi Nigel Babv...	ALL THESIS	4% 🟩	--	--	🗋	974690062	11-Jun-2018
☐	Tamusathi Nigel Babv...	CHAPTER 2-LITERATURE REVIEW	10% 🟩	--	--	🗋	974688193	11-Jun-2018